JAIST Repository
https://dspace.jaist.ac.jp/

Title	有歪中継によるマルチプルアクセスリレー協調通信
Author(s)	Lu, Pen-Shun
Citation	
Issue Date	2015-06
Type	Thesis or Dissertation
Text version	ETD
URL	http://hdl.handle.net/10119/12877
Rights	
Description	Supervisor:松本　正，情報科学研究科，博士

JAIST
JAPAN
ADVANCED INSTITUTE OF
SCIENCE AND TECHNOLOGY

Japan Advanced Institute of Science and Technology

Decoding and Lossy Forwarding based Multiple Access Relaying

Pen-Shun Lu

Abstract

The goal of this thesis is to provide a unified concept of lossy-forwarding from the theoretical analysis to practical scheme design for the decode-and-forward-based multiple access relay channel (MARC) system. To improve the performance of MARC with the relay subject to resources or/and time constraints, the erroneous estimates output from simple detection schemes are used at the relay are forwarded and exploited. A correlation is then found between two sequences: one is the network-coded sequence sent from the relay, and the other is their corresponding exclusive-OR-ed information sequence. Several joint network-channel coding (JNCC) techniques are provided in which the correlation is utilized to update the log-likelihood ratio sequences during the iterative decoding process at the destination. As a result, the bit error rate (BER) and frame error rate (FER) are improved compared with those of MARC with select DF strategy (SDF-MARC). The MARC proposed above is referred to as erroneous estimates-exploiting MARC (e-MARC).

To investigate the achieved FER performance of the e-MARC system, the outage probability for e-MARC with two source nodes is theoretically derived. We re-formulate the e-MARC system and identify its admissible rate region according to the Slepian-Wolf theorem with a helper. Then, the outage probability is obtained by a set of integral over the rate region with respect to the probability density functions of all the links' instantaneous signal-to-noise power ratios. It is found through simulations that, as one of the source nodes is far away from both the relay and destination, e-MARC is superior to SDF-MARC in terms of outage performance. Furthermore, a joint adaptive network-channel coding (JANCC) technique is then proposed to support e-MARC with more source nodes. A vector is constructed at the destination in JANCC to identify the indices of the incorrectly decoded source node(s), and re-transmitted to the relay for requesting additional redundancy. The relay performs network-coding only over the estimates specified by the vector upon receiving the request. Numerical results show that JANCC-aided e-MARC is superior to e-MARC in terms of FER and goodput efficiency. In addition, compared iterative decoding is performed at relay with SDF-MARC, the use of differential detection with JANCC-aided e-MARC significantly reduces the computational complexity and latency with only a small loss in the FER.

keywords: Cooperative communication, multiple access relay channel (MARC), decode-and-forward (DF), joint network-channel coding, Slepian-Wolf theorem

Abstract

Tmn vitskirjan tarkoituksena on tuottaa yhteninen kokonaisuus hvillisest lhetyksest pura-ja-lhet (DF) -pohjaisessa monikyttrelejrjestelmss (MARC) sek teoreettisesta ett kytnnllisest nkkulmasta. Parantaakseen resurssi -tai aikarajoitetun MARC-jrjestelmn suorituskyky, vastaanotin hydynt riippuvuussuhdetta releen vlittmien informaatiosekvenssien virheellisten estimaattien ja suoraan lhteest tulevien informaatiosekvenssien vlill (e-MARC). Tyss ehdotetaan useita yhdistetyn verkko - ja kanavakoodauksen menetelmi (JNCC), joissa log-uskottavuussuhdesekvenssit iteratiivisen purkamisprosessin aikana pivitetn hydyntmll sekvenssien riippuvuussuhdetta vastaanottimessa. Tmn tuloksena sek bittivirhe- ett kehysvirhesuhdetta saadaan parannettua verrattuna selektiiviseen pura-ja-lhet menetelm kyttvn MARC-strategiaan (SDF-MARC). Kehysvirheen suorituskyvyn tarkastelua varten tyss johdetaan teoreettinen epkytettvyyden todennkisyys e-MARC-menetelmlle kahden lhettimen tapauksessa. Lisksi e-MARC-menetelmlle mritetn tiedonsiirtonopeusalue Slepian-Wolf -teoreeman mukaisesti. Tmn jlkeen saadaan epkytettvyyden todennkisyys kaikkien linkkien signaalikohinasuhteen todennkisyystiheysfunktion integraalina tiedonsiirtonopeusalueen yli. Simulointitulokset osoittavat e-MARC-menetelmn paremman epkytettvyyden todennkisyyden verrattuna SDF-MARC-menetelmn silloin kun yksi lhettimist on kaukana sek releest ett vastaanottimesta. Mahdollistaakseen useamman lhteen kytn e-MARC-menetelmss, tyss ehdotetaan lisksi adaptiivinen yhdistetyn verkko -ja kanavakoodauksen menetelm (JANCC). Siin vastaanotin mritt vrin purettujen sekvenssien lhettimet ja ilmoittaa ne vektorimuodossa takaisin releelle pyytkseen niden lhettimien informaation uudelleenlhetyst. Tmn jlkeen rele suorittaa verkkokoodauksen vain tunnistusvektorin mrittmien informaatiosekvenssien estimaatteihin perustuen. Tulokset nyttvt, ett JANCC-menetelm kyttv e-MARC saavuttaa paremman kehysvirheen ja hydyllisen lpisyn tehokkuuden verrattuna e-MARC-menetelmn.

Asiasanat: Yhteistoiminnallinen viestint, monikyttrelekanava, pura-ja-lhet (DF), yhdistetty verkko -ja kanavakoodaus, Slepian-Wolf -teoreema

Dedicated to my parents

Preface

The dissertation is made based on a curriculum that is organized by the Collaborative Education Program of the Centre for Wireless Communications (CWC), University of Oulu, and Japan Advanced Institute Science and Technology (JAIST), Japan.

First of all, I wish to express my deepest gratitude my supervisor Professor Tad Matsumoto for providing me this opportunity of becoming a doctoral student. I deeply appreciate his supervision during my doctorial research career. His creative intuition and specific ideas constantly surprise me. Furthermore, his great enthusiasm for academic research always impresses me thoroughly. This thesis would not have been completed without his ideas, advice and criticism. I would also like to sincerely thank my other supervisor Professor Markku Juntti for the valuable advice on my research. I really appreciate all of the his precious time he spent on the paper work for me for credit and system transfer and dual degree issues. His tolerance and patience always encourages me to keep going ahead and to overcome any difficulties I encounter. In fact, words are unable to convey my sincere appreciation to Professor Juntti. My gratitude gratitude also goes to Professor Lajos Hanzo and Dr. Soon Xin Ng (Michael) for their academic advice during my master's and doctorial studies.

I would like to express my gratitude to the reviewers and examiners of the thesis, Professor Alister Burr from the University of York, U.K and Professor Jan Sykora from Czech Technical University in Prague, Czech, Dr. Shinsuke Ibi from Osaka University, Japan, Dr. Brian Kurkoski and Dr. Kiyofumi Tanaka from JAIST, Japan. Many thanks for their careful reviewing for this thesis and providing constructive and insightful comments to improve the quality of the thesis significantly.

I am also very grateful to my current and previous CWC and JAIST colleagues for the discussions and inspiring working environment. In particular, I would like to thank Antti, Animesh, Attaphongse, Berhane, Carlos, Chathu, Feng Hu, Francesco, Harri, Hamidreza Bagheri, Helal, Ikram, Janne, Jarkko, Juha Karjalainen, Jussi, Kaveh, Anwar, Laiyemo, Li Wei, Marian, Markkus, Mehdi, Nuwan, Oskari, Pedro, Pekka, Petri, Qiang Xue, Ragha, Ricardo, Reza, Satya, Shen Qian, Simon Cheng, Takano, Tuomo, Uditha, Ulrico, Ume, Valtteri, Xavier, Xiaobo, Xiaojia, Xin, Zaheer, Weiwei. I would like to thank the administrative staff from the CWC and JAIST, more specifically Antero, Elina, Hanna, Jari, Juha, Kirsi, Eija, Mari, Minna Silfverhuth, Kubo, Taniguchi,

and Kimura for their patience and kindness.

The stay in Finland and Japan gave me the opportunity to make very great friends. It seems that I have no secrets from Xiaobo. The Taiko-dinner-trip with Simon is still a vivid memory for me. Valtteri constantly friendly helps me experience Finnish culture. Many thanks to Xin for inviting me to join his organization. I really appreciate the help thoughtfully provided from Ken and Xiaojia in Japan and Finland. I sincerely wish Wu recover his health. Thanks to Aleksi Kolehmainen for his hospitality, and saving my life when I fainted. Also I would like to thank all my friends in Oulu and JAIST, especially Geza & Diane, Ming-Chung & Joyce & their family, and Janne Anttila & Yuki & their family. For sure I miss you, Kisho.

Finally, my warmest thanks belongs to my parents and brother for their endless love and encouragement.

List of abbreviations

ACC	accumulator
ACC^{-1}	decoder of ACC
ACK	acknowledgement
ADD	addition
AF	amplify-and-forward
ANCC	adaptive network coded cooperation
ARQ	automatic repeat request
AWGN	additive white Gaussian noise
BC	broadcast
BCJR	Bahl-Cocke-Jelinek-Raviv
BSC	binary symmetric channel
BER	bit error rate
BPSK	binary phase-shift keying
BP	belief propagation
CCC	constellation constraint capacity
CF	compress-and-forward
COMP	comparison
CRC	cyclic redundancy check
CSIR	channel state information at the receiver
DD	differential detector
DF	decode-and-forward
DDEX	differential detector and extraction
DMT	diversity-multiplexing trade-off
DPSK	differential phase-shift keying
DTC	distributed turbo code
e-MARC	erroneous estimates-exploiting MARC
EM	electromagnetic
EXIT	extrinsic information transfer
FER	frame error rate
GANCC	generalized adaptive network coded cooperation
GF	Galois field

JANCC	joint adaptive network-and-channel coding
JNCC	joint network-and-channel coding
LAN	local area network
LDPC	low-density parity-check
LLR	log-likelihood ratio
LNC	linear network coding
LTE	long term evolution
LTE-A	long term evolution-advanced
MA	medium access
MAC	medium access control
MARC	multiple-access relay channel
MAP	maximum *a posteriori*
MI	mutual information
MIMO	multiple-input multiple-output
MRC	multi-way relay channel
MUL	multiplication
NC-MARC	network-coding-based MARC systems
PCCC	parallel concatenated convolutional code
PLNC	physical-layer network coding
pdf	probability density function
QoS	quality of service
RD	relay-destination
RSC	recursive systematic convolutional
SCCC	serially concatenated convolutional code
$SCCC^{-1}$	iterative decoding of SCCC
SISO	single input single output
SD	source-destination
SDF	select decode-and-forward
SDF-MARC	MARC systems with SDF strategy
SNCC	separated network-and-channel coding
SNR	signal to noise ratio
SR	source-relay
TDMA	time division multiple access
TMRC	two-way relay channel
WLAN	wireless local area network

WSN	wireless sensor network
XOR	exclusive-OR
2D	two-dimensional
3D	three-dimensional
3GPP	3rd generation partnership project

List of symbols

i	Source node
R	Relay
D	Destination
$\mathbf{u}_i$	information sequence of i
$\widetilde{\mathbf{u}}_i$	estimates of $\mathbf{u}_i$ received at R
$\hat{\mathbf{u}}_i$	estimates of $\mathbf{u}_i$ received at D
$\mathbf{x}_i$	coded sequences of node i
$\mathbf{y}_{iR}$	received signals at R sent from i
$\mathbf{y}_{iD}$	received signals at D sent from i
$\mathbf{y}_{RD}$	received signals at D sent from R
p_i	error probability of iR link per transmission cycle
p_R	error probability of RD link per transmission cycle
$\hat{p}_i$	theoretical limit of p_i
$\hat{p}_R$	theoretical limit of p_R
$\tilde{p}_i$	non-zero value of $\hat{p}_i$
$\tilde{p}_R$	non-zero value of $\hat{p}_R$
γ_{iR}	instantaneous SNR of iR link
γ_{iD}	instantaneous SNR of iD link
γ_{RD}	instantaneous SNR of RD link
γ_i^*	$p_i = 0$ if $\gamma_{iR} > \gamma_i^*$
γ_R^*	$p_R = 0$ if $\gamma_{RD} > \gamma_R^*$
Γ_{iR}	average SNR of iR link
Γ_{iD}	average SNR of iD link
Γ_{RD}	average SNR of RD link
$\mathcal{E}_S$	signaling scheme at i
$\mathcal{E}_R$	signaling scheme at R
$\mathcal{D}_R$	receiver at R
$\mathcal{D}_D$	receiver at D
$\mathcal{E}_S^{-1}$	decoding of $\mathcal{E}_S$ using the log-MAP algorithm
$\mathcal{E}_R^{-1}$	decoding of $\mathcal{E}_R$ using the log-MAP algorithm
$\mathcal{R}_i$	source coding rate at i

$\mathcal{R}_R$	source coding rate at R
$\mathcal{R}_{ci}$	spectrum efficiency of $\mathcal{E}_S$
$\mathcal{R}_{cR}$	spectrum efficiency of $\mathcal{E}_R$
$H(\cdot)$	entropy function
$H_b(\cdot)$	binary entropy function
$I(\mathbf{w};\mathbf{z})$	mutual information between $\mathbf{w}$ and $\mathbf{z}$
$I_a(\mathbf{w})$	mutual information between $\mathbf{w}$ and $a\ priori$ LLR of $\mathbf{w}$
$I_e(\mathbf{w})$	mutual information between $\mathbf{w}$ and $extrinsic$ LLR of $\mathbf{w}$
$\mathfrak{D}_i$	distortion over iR link transmission
P_{out}	outage probability
$\alpha * \beta$	convolution, $\alpha(1-\beta)+\beta(1-\alpha)$
δ	$H_b(p_A * p_B * p_R)$
$\hat{\delta}$	theoretical limit of δ
$\ddot{\delta}$	δ with constant p_i
p_s	source correlation
p_{nc}	network correlation; $p_{nc} = p_A * p_B$
$\mathfrak{I}[f;V]$	three-fold integral over function f with domain V
$E[\,\cdot\,]$	expectation
Δ	additional gain in dB
L	path loss in dB
$\vee$	logical '*or*'
$\wedge$	logical '*and*'
$\overline{\varepsilon}$	the complement of event ε
$f_c(\cdot)$	LLR-updating function
$\exp(\cdot)$	exponential function
var$(\cdot)$	variance function
$L(\mathbf{u})$	LLR values of sequence $\mathbf{u}$
$L_a(\mathbf{u})$	$a\ priori$ LLR values of sequence $\mathbf{u}$
$L_e(\mathbf{u})$	$extrinsic$ LLR values of sequence $\mathbf{u}$
$(x)^*$	complex conjugation of a complex number x
$\Re(x)$	taking real part of a complex number x
$\lvert x\rvert$	absolute value (magnitude) of a complex number x
$\Pi_i[\,\cdot\,]$	interleaving by Π_i
$\Pi_i^{-1}[\,\cdot\,]$	de-interleaving from Π_i
$\Pi_{ia[\cdot]}$	interleaving by Π_{ia}

$\Pi_{ia}^{-1}[\,\cdot\,]$	de-interleaving from Π_{ia}
$\Pi_R[\,\cdot\,]$	interleaving by Π_R
$\Pi_R^{-1}[\,\cdot\,]$	de-interleaving from Π_R

Contents

1 Introduction

Wireless communication systems and standards have evolved during the last decades. The main trigger for the evolution of the wireless communication systems and standards are demands for high data rate multimedia-based applications, high spectral efficiency, low power consumption and reliable services. The growth of mobile data traffic has been predicted to be more than 24-fold between 2010 and 2015, and more than 500-fold between 2010 and 2020 [1, 2]. On the other hand, many wireless mobile devices are by limited battery size, and thus the energy consumption is also critical for the design of wireless communication systems. However, achieving a high data rate usually requires high transmitting power levels; hence, there is a trade-off between communication performance and energy consumption.

Multiple-input multiple-output (MIMO) wireless technology [3, 4] is one solution for improving the data rate. However, several wireless mobile devices may not be able to deploy multiple antennas due to size, cost, or hardware limitation [5], and thus cooperative communication has emerged as a new means of emulating the strategies designed for multiple antenna systems. Wireless systems that use cooperative communication technique are also known as distributed or virtual MIMO systems [6].

1.1 Cooperative communication

Cooperative communication was initially introduced and studied by van der Meulen [7], and early formulations of general relaying problems appeared in the information theory community [8–10]. In conventional wireless transmission systems, a transmission link is built only by a source node and a destination. Hence, the successful probability of the transmission totally depends on the quality of the link. However, with using cooperative communication techniques, one or several additional nodes are introduced as relays to cooperate with the source node. Thus, multiple copies of an information sequence can be transmitted via independent fading channels, which significantly improves the probability that the information sequence is successfully received at the destination. In other words, spatial diversity gains can be exploited in cooperative communications.

In addition to the spatial diversity gains, a lot of design flexibility in the form of diversity-multiplexing trade-off (DMT), coverage extension, and multiple user quality of service (QoS) management are provided in wireless networks with cooperative com-

munications. Therefore, cooperative communication has emerged as a promising technique for improving the reliability and throughput of wireless multi-terminal networks and has attracted a lot of attention from the wireless communication research community recently. In fact, cooperative communication has been considered in several latest communication standards, for instance, in the Institute of Electrical and Electronics Engineers (IEEE) 802.16j WiMax standard [11, 12] and in the Long-Term Evolution-Advanced (LTE-A) of the Third Generation Partnership Project (3GPP) [13] multi-hop cellular networks [5, 14–17]. Nowadays cooperative communication techniques are playing an important part in modern communication systems, e.g., wireless mobile systems, device-to-device (D2D) communications, wireless sensor networks (WSNs) and ad-hoc networks.

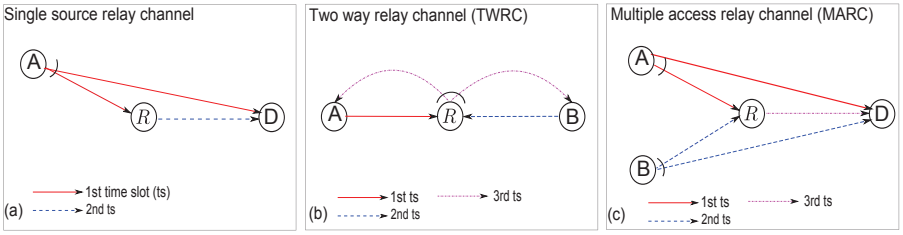

Fig 1. Basic models of cooperative communications. (a) single source relay channel, (b) two-way relay channel, (c) multiple access relay channel.

The basic model of cooperative communications is the classic single source relay channel, shown in Fig. 1(a), where there are one source node, one relay and one destination. In the first time slot, the source node broadcasts its information sequence to the relay and destination. The relay processes the received signal vector sent via the source-relay (SR) link, and forwards the processed signal to the destination in the second time slot. Another two popular models of cooperative communications were extended based on the classic single source relay channel: two-way relay channel (TWRC) [18] and multiple access relay channel (MARC) [19].

The system model of a TWRC is shown in Fig. 1(b), where two sources nodes communicate with each other through a relay, but there is no direct link between source nodes. In the first two time slots (the multiple access (MA) phase), each source node individually transmits its information sequence to the relay, and the relay can separately transmit the estimated sequence intended to the other source node in the last two time

slots, or performs network-coding on both estimates and broadcasts the network-coded sequence to the source nodes only in one time slot (the broadcast (BC) phase). The TWRC can be further extended to the multi-way relay channel where more than two source nodes communicate with each other through a relay. The MARC system model, on the other hand, is shown in Fig. 1(c), which consists of two source nodes, one relay and one common destination; the role of the relay is to assist the source nodes in improving the probability of successful transmission to the destination.

Multi-way relay channel systems can represent various practical communication scenarios. For example, in LTE networks, a set of mobile stations can form a group of users (i.e., source nodes) that multicast the information through the base station in a multi-way fashion. Another example can be found in satellite communication, where several ground stations can exchange information via the satellite which acts as a relay. In ad hoc networks, several users can contribute in building a distributed file sharing database via a central access point. In a WSN, sensor nodes can cooperatively pass their information to a fusion center. Similarly, the MARC system also can represent several scenarios and applications. For instance, in WSNs, the sensors are too weak to cooperative but they can send their information to the fusion center with the help of more powerful nodes. In data gathering networks, a larger cache is provided by the relay and thus more compressed data can be forwarded to the destination.

Designing energy-efficient functions for the relay for signal processing and relaying protocols is one of the important issues for cooperative communications, especially for cooperative communications in resource-constrained wireless networks. For example, it is difficult to replace or recharge the batteries for sensor nodes in WSN in some scenarios [20]. In addition, as the basic models exemplified above are expanded to form a larger network, multiple cooperative relays may be employed in cooperative communications. Hence, the choice of a relay node (i.e., relay selection [21–25]) plays a significant role in cooperative communications.

1.2 Relaying strategy

The design of relaying protocols and strategies has attracted considerable attention for almost the entire last decade. Various protocols and strategies have been developed for cooperative communications to increase throughput or reduce energy consumption. We briefly introduce the relaying protocols and strategies in this section.

1.2.1 Relaying protocols

Relaying protocols in cooperative communications are mainly involved with the scheduling of the transmission. Diversity protocols were introduced by Laneman *et al.* [5, 26], and classified into the following categories:

Static protocols

The transmission from the source node and the relay follows a fixed pattern, in which the source node transmits an information sequence in the first time slot and the relay repeats the obtained estimates in the second time slot. Static protocols are simple and easy for implementation. However, if the information sequence is correctly received at the destination in the first time slot, the transmission for the second time slot becomes redundant. Besides, if the information sequence is incorrectly received at the relay in the first time slot, the transmission of the second time slot is wasted. Hence, to improve the efficiency of static protocols, adaptive protocols, such as selection relaying and incremental relaying, were proposed [5].

Adaptive protocols

To avoid the waste of the transmission in the second time slot, in selection relaying, the relay remains silent if the information sequence is incorrectly received at the relay in the first time slot. Instead, the source node re-transmits a copy of the original information sequence directly to the destination in the second phase [5]. On the other hand, in incremental relaying, the destination is assumed to be able to give feedback to the source and the relay nodes after each transmission. With this assumption, the transmission in the second time slot is not necessarily required if the transmission from the source to the destination was successful in the first time slot. Thus, incremental relaying has the best performance among the proposed protocols in terms of spectral efficiency [5].

1.2.2 Forwarding behavior

According to forwarding behaviors, relay strategies can be mainly classified into following categories:

Amplify and Forward

In the amplify-and-forward (AF) strategy, the received signal vector sent via SR link is simply amplified by a relay, and forwarded to the destination [27]. No decoding and re-encoding is performed on the received signal vector at the relay. In the AF strategy, in addition to amplification, several practical issues such as sampling, and retransmitting analog values have to be taken into account. Furthermore, any noise is also amplified with the received signal vector and retransmitted, which degrades the performance of the system.

Decode and Forward

In the decode-and-forward (DF) strategy, the received signal vector sent via SR link is decoded at the relay [27]. After that, error detection, such as a cyclic redundancy check (CRC) [28], is used to check whether the estimated sequence contains error(s) or not. The correctly decoded estimates are re-encoded at the relay and forwarded to the destination, while the estimates decoded in error are discarded by the relay to avoid error propagation [29, 30]. In the scenario where multiple source nodes are served by a common relay, the DF strategy may be modified to the select DF (SDF) strategy [29, 31–34], in which a header has to be added to identify the correctly decoded source node(s).

Compress and Forward

In the compress-and-forward (CF) strategy, the received signal vector sent via SR link is quantized and compressed at a relay before being forwarded to the destination [35]. The CF strategy is sometimes referred to as estimate-and-forward [36]. In fact, the received signals at the relay and the destination are correlated due to the nature of broadcasting. Hence, the correlation is utilized by the relay to compress the received signal vector, and the compressed version of the received signals is forwarded to the destination. Compressing the received signal vector at the relay may be computationally expensive and thus adaptive protocols are suitable for the CF strategy.

1.3 Network coding

In a multicast network, an information sequence is transmitted from a source node to the destination via several intermediate nodes. To improve the throughput efficiency and multicast capacity of a network, Ahlswede *et al.* introduced a network coding technique by which the intermediate nodes in networks can can encode the received information sequences sent from its neighboring nodes [37]. Assuming an error-free point-to-point network, Ahlswede *et al.* [37] proved that a source node is able to multicast k information sequences to several destinations if the min-cut between the source node and each destination has the capacity of k per unit time. [38, 39] have demonstrated that the bandwidth efficiency for a wireless mesh is significantly improved with network coding. In 2003, Li *et al.* explicitly constructed a linear network code (LNC) [40] and demonstrated that the min-cut capacity for the multicast problem can always be achieved. The network coding for LNC is assumed to be operated at a higher layer protocol. In 2006, physical-layer network coding (PLNC) was proposed where network coding is operated at the physical layer by superimposing electromagnetic (EM) waves which carry the information sequences transmitted from source nodes. The concepts of LNC and PLNC are briefly described in the following sections.

1.3.1 Linear network coding

In LNC, each intermediate node in the network randomly generates its encoding vector [41], and uses the encoding vector to encode the previously received information sequences in a linear combination. Then, the encoded sequence with the corresponding encoding vector is forwarded to the next routing node. To be able to recover the original information sequences, as many encoded sequences as possible should be received at the destination, and the encoding vectors associated with the received sequences have to be linearly independent. Thus, by solving a system of linear equations with Gaussian elimination, the original information sequences can be obtained at the destination. A detailed discussion with respect to LNC or random network coding are available in [42, 43].

It should be noticed that the exclusive-OR (XOR) network-coding is a special case of LNC [40]. The coded sequences that are transmitted in the network are elements in the Galois field (GF) $\mathbb{F}_q$ with $q = 2$ (i.e., GF(2)), and bit-wise XOR in GF(2) is used as an operation.

1.3.2 Physical-layer network coding

Unlike LNC operating at a higher layer, PLNC directly superimposes the EM waves which carry the information sequences in the physical layer. For example, assuming source nodes A and B attempt to exchange their complex information symbols $u_A = a_A + jb_A$ and $u_B = a_B + jb_B$ with each other via a relay R in a TWRC system. In the first time slot, nodes A and B simultaneously broadcast their symbols modulated on the same radio frequency ω to the relay R. The combined bandpass signal y_R received at R during one symbol period t is

$$\begin{aligned} y_R(t) &= \Re\left\{u_A e^{j\omega t} + u_B e^{j\omega t}\right\} \\ &= \Re\left\{(a_A + jb_A)e^{j\omega t} + (a_B + jb_B)e^{j\omega t}\right\} \\ &= (a_A + a_B)\cos(\omega t) - (b_A + b_B)\sin(\omega t) \end{aligned} \tag{1}$$

where $\Re\{\cdot\}$ denotes a function that takes the real part of its argument. Hence, the baseband in-phase and quadrature components of y_R are $y_R^I = a_A + a_B$ and $y_R^Q = b_A + b_B$, respectively. Suppose u_A and u_B are QPSK symbols, the arithmetic sum in y_R^I and y_R^Q is equivalent to the bit-wise XOR operation; in other words, the network coding is performed by nature. Hence, as several source nodes transmit simultaneously, the transmission efficiency can be significantly improved using PLNC. Several critical issues for PLNC, such as synchronization and channel estimation, are studied in [44–46].

1.3.3 Network and channel coding

We have briefly reviewed network coding for multi-casting in error-free networks in the previous subsection. Nevertheless, error-free networks may be less practical in real scenarios. Several reasons such as link outage, collision or buffer overflow may cause errors to occur in the links of the network. Hence, channel coding is in general combined with network coding to eliminate errors occurring in the links of the network. Existing research on unifying channel and network coding can be roughly classified into the following two categories

Separated network-and-channel coding (SNCC)

Network coding and channel coding are separately designed and the redundant information is not jointly exploited. More specifically, received sequences are firstly channel decoded in the physical layer to obtain the estimates of information sequences. After that, the estimates are directly passed to the network layer to be network-coded. The output from the network coding operation is directly delivered back to the physical layer for channel encoding again. Thus, in the design of SNCC, the overall problems are separated into two independent problems and thus researchers can focus on one of these two independent problems. For example, Larsson *et al.* [47] introduced an automatic repeat request (ARQ) scheme for multiple unicast flows in a multi-user system. Berger *et al.* theoretically analyzed the optimization problem in joint erasure-correction and error-correction coding schemes [48].

Joint network-and-channel coding (JNCC)

Network coding and channel coding are merged in such a way that the network coding is able to contribute to error protection. Instead of guaranteeing the error-free transmission for each point-to-point link, the aim is to guarantee error-free decoding at the destination. Hence, in the design of JNCC, the network-coded sequence is designed to carry the additional redundancy to help decode the received sequences at the destination. Many studies jointly design network-channel codes to exploit the redundancy in both channel and network codes. For example, Bao *et al.* proposed adaptive network coded cooperation (ANCC) [49] and generalized adaptive network coded cooperation (GANCC) [50] where channel coding and network coding are unified in a general framework. Hausl *et al.* introduced iterative network and channel decoding on a Tanner graph [51], and also proposed joint network-channel coding [52, 53] for both MARC and TWRC based on distributed turbo code (DTC) [54, 55]. Besides, Duyck *et al.* proposed a structured full-diversity joint network-channel code in [56] and applied it in large networks [57]. Zhang *et al.* uses low-density parity-check (LDPC) codes [58] and network coding to approach the capacity of TWRC [59].

1.4 Motivation

Cooperative communications have attracted a lot of attention from the wireless communication research community, since spatial diversity gain is provided. In cooperative communications, one or several nodes may act as relays to help other nodes forward their data to a common destination. Typically, the relay performs the decoding of powerful codes, such as turbo codes [60] and LDPC codes to ensure that the received estimates are correctly decoded with a high probability.

However, in practice, the source nodes are not geographically always close enough to the relay in cooperative communications, and the average received signal-to-noise power ratio (SNR) is determined by the pathloss. Furthermore, the signal/signals received by the nodes may suffer from deep fade, depending on their locations. Errors occurring in the SR links may well be eliminated by using powerful codes in the signaling scheme. Nevertheless, in many scenarios, the use of powerful codes per link does not always provide a reasonable solution, especially for scenarios where the relay may operate with resources or/and time constraints.

For example, the sensor nodes in WSN are typically with a finite energy and data buffer (memory) [20], and replacing or recharging the batteries is difficult in some scenarios. Additionally, exhaustive energy and memory are required to perform complicated decoding algorithms, such as the maximum *a posteriori* (MAP) [61] or belief propagation (BP) [62] algorithms. Also, several real-time systems operate with tight time constraints, which may prevented powerful codes from being used in real-time systems due to their large latency resulting from the iterative decoding process.

In above exemplifying situations, the relay may be only allowed to use simple detection schemes. However, when using low computational complexity detection, there is a high probability of receiving erroneous estimates at the relay, and forwarding these erroneous estimates will result in error propagation in the decoding process at the destination. As mentioned in [29, 30], performance and diversity gain are dramatically degraded due to the error propagation. Therefore, utilizing the forwarded erroneous estimates and mitigating error propagation caused by the estimates has been gaining more and more attention recently.

DF (or SDF) is one the most simple and popular relaying strategies used in cooperative communications to avoid the error propagation, and many excellent DF-based JNCC techniques for TWRC/MARC systems have been developed [52, 63–69] and [70–73], respectively. Most DF strategies used at the relay discard estimated sequence(s)

containing errors, and thus, either perfectly decoding or CRC is assumed in [52, 63–67]. However, CRC-based selection relaying/combining are not bandwidth efficient and would incur decoding delays, even though they are effective in controlling error propagation. Furthermore, much power is wasted on decoding unreliable received signals especially when the quality of SR links is low.

On the other hand, erroneous estimates still contain a lot of useful information, which is helpful in reconstructing the transmitted signals from the source nodes at the destination. Hence, several emerging design schemes have been proposed for preserving the information of the erroneous estimates at the relay, and forwarding the estimates in an analog form or their quantized versions. For example, in [30, 74–78], the relay forwards the log likelihood ratio (LLR) values of the network-coded sequence to the destination in case of erroneous SR links. The soft-DF technique was introduced in [79–81] where the relay performs a soft decoding of the received signal and re-encodes it softly. However, relaying the signals in an analog form requires more bandwidth for the representation of the soft bits, and thus applying the above techniques at the relay may not be suitable for the resource-constrained wireless networks. Motivated by this, a simple DF-based MARC system with the concept of lossy-forwarding is proposed and studied in this thesis.

1.5 Objectives and outline for the thesis

The target of this thesis is to provide a unified concept of lossy-forwarding from the theoretical analysis to practical scheme design for the DF-based MARC system where the relay is assumed to be subject to resources or/and time constraints. Due to the fact that source-channel separation theorem does not hold in general for sending correlated sources over multiuser networks [82], to facilitate the theoretical analysis, time-division multiple-access (TDMA) is used for the transmission of each node and thus the MARC system is orthogonal (i.e., the orthogonal MARC system). The time allocation parameters are assumed to be fixed and the relay and every source node have their own transmission interval. The channels of the MARC system are assumed to suffer from additive white Gaussian noise (AWGN) and block Rayleigh fading, respectively. The relay is assumed to operate in a half-duplex mode [83]. Channel state information at the receiver (CSIR) is assumed to be available at the destination, but not necessarily required at the relay if non-coherent differential detection is performed on the received signal vector sent via the SR link.

In Chapter 2 [84, 85], a simple DF-based lossy-forwarding MARC system, referred to as an erroneous estimates-exploiting MARC (e-MARC) system, is proposed. The aim of the e-MARC system is to exploit the erroneous estimates resulting from a low computational complexity detection scheme applied at the relay. Both estimates, regardless of whether or not they are correctly received at the relay, are always XOR-coded and forwarded to the destination. Due to performing the XOR coding at the relay, a correlation is found between the two sequences: one is the XOR-coded sequence sent from the relay, and the other is their corresponding XOR-ed information sequence. The correlation is referred to as network correlation in this thesis. Then, several JNCC and corresponding decoding schemes are developed for the practical realization of the e-MARC system, in which the knowledge of the network correlation is exploited at the destination by using a log-likelihood ratio (LLR)-updating function [86] in the iterative JNCC decoding process. Furthermore, extrinsic information transfer (EXIT) analysis [87, 88] is used to verify the simulated bit error rate (BER) results of the JNCC scheme used in the e-MARC system. It is found that, even though a very simple detection scheme is used at the relay, the BER and frame error rate (FER) performances of the e-MARC system are superior to those of MARC systems with the SDF strategy (SDF-MARC) [33].[1]

Chapter 3 [89] theoretically derives the outage probability for the e-MARC system with two source nodes proposed in Chapter 2. The theoretical analyses are based on the techniques presented in [90, 91]. We re-formulate the e-MARC system according to the Slepian-Wolf theorem [92] for correlated source coding with a helper, and analyze the e-MARC system's admissible rate region according to the re-formulation. After that, we derive the outage probability of the e-MARC system where all five links in the system (two SD links, two SR links and one relay-destination (RD) link) suffer from statistically independent block Rayleigh fading.

The probability distribution of the SR links' error probabilities in practice depends on the signaling scheme applied at the source and relay nodes. Nevertheless, to be able to make comparisons of the outage performances with other relaying strategies used in the MARC system, it is necessary for the theoretical outage probability of the e-MARC to be independent of any signaling scheme. Therefore, in this chapter, we also derive the theoretical limit of the SR links' error probabilities by using rate distortion and inverse entropy functions [93]. Following this, it is shown that the outage probability of the e-MARC system, independent of signaling schemes, can be theoretically derived by

[1] Any MARC system with the SDF strategy is viewed as the SDF-MARC system in this thesis.

a fivefold-integral over the admissible rate region with respect to the probability density functions (pdfs) of the five links' instantaneous SNRs.

The process for deriving the probability is then applied to the following two special cases: 1) Two SR links are assumed to be binary symmetric channels (BSCs), and 2) The e-MARC system with a practical signaling scheme [85] presented in Chapter 2. Then the fivefold-integral needed to obtain the outage probability can be reduced to simpler expressions, corresponding to their error probabilities of SR links. Numerical results show that theoretical outage probabilities of the e-MARC applying differential detection at the relay are roughly 3.5 and 4.5 dB away from the probabilities of the e-MARC system independent of signaling schemes in the Symmetric and Asymmetric scenarios, respectively. This performance loss is because we aim at reducing the computational complexity. Finally, we investigate the impact of the correlation between the two source nodes on the outage probability of the e-MARC system. It is found that for the case two source nodes are highly correlated, the outage performance can still be improved as long as one of the SD links is reliable. However, to improve the outage performance by exploiting the network correlation, the RD link and at least one of the SD links needs to be reliable.

Chapter 4 [94] proposes a novel joint adaptive network-channel coding (JANCC) technique to aid the e-MARC system with more than two source nodes. As the number of the source nodes in the orthogonal MARC system is increased, unnecessary erroneous estimates may be included in the XOR coding process at the relay, which leads to low network correlation and degrades the decoding performance of the JNCC schemes for e-MARC. Hence, to efficiently exploit the network correlation, in the proposed JANCC technique, the destination constructs a vector identifying the indices of the incorrectly decoded source nodes, and sends it to the relay to request a re-transmission. Upon receiving the request, the relay performs network-coding only over the stored estimates specified by the identifier vector, rather than over all estimates as the e-MARC. In addition, an algorithm is proposed to estimate the knowledge of the network correlation during the iterative decoding process of JANCC, by which the destination is able to exploit the knowledge of the network correlation without the aid of a higher layer protocol. Compared to the e-MARC in terms of FER and goodput efficiency, it has been observed that the performance of a JANCC-aided e-MARC is improved with three source nodes. In addition, compared with the SDF-MARC system where the iterative decoding is performed at the relay, the use of differential detection with a JANCC-aided e-MARC significantly reduces the computational complexity and latency with only a small loss

in the FER performance.

Chapter 5 concludes the thesis and summarizes the main results. The open issues and suggestions for future research are presented.

1.6 Author's contribution

This thesis is based on two journal papers [89, 94], and two published conference papers [84, 85]. The first journal paper [94] has already been published and the second one [89] is under revision. The author has had the main responsibility for performing the analysis, programming the simulation, generating the numerical results, and writing all the papers [84, 85, 89, 94]. Other authors provided ideas, help, comments and criticism during the writing process.

In summary, the main contributions of the thesis are summarized in the following,

– The e-MARC system is proposed for low computational complexity detection schemes applied at the relay. In the proposed system, the received erroneous estimates, instead of being discarded by the relay with the SDF strategy, are forwarded to the destination to help the recovery of the information sequences sent via the SR links. As a result, by using very simple detection at the relay, it is found that roughly $0.2 - 0.4$ dB and $0.7 - 2.2$ dB gain can be obtained from the forwarded erroneous estimates received at relay in AWGN and fading scenarios, respectively.

– The theoretical outage probability of the e-MARC system, independent of signaling schemes, is derived to investigate the achieved FER performance of the e-MARC system. It is found through simulations that lossy-forwarding improves the outage performance in the case that the sources are far away from both the relay and the destination.

– The JANCC and its decoding techniques are proposed to improve the e-MARC system, especially when the number of the source node increases. Compared with the SDF-MARC system where fully-iterative decoding is performed at the relay, the utilization of differential detection with JANCC-aided e-MARC at least reduces the computational complexity to 1/200, which leads to meaningful power savings with only a $0.5 - 1.5$ dB loss in the FER performance

2 Erroneous estimates-exploiting MARC

This chapter concentrates on the performances of e-MARC in AWGN and fading channels when very simple detection schemes are applied at the relay to obtain estimates sent from source nodes. The chapter is organized as follows. The assumptions and the proposed e-MARC system model are described in Section 2.1. The exploitation of erroneous estimates received at the relay in the proposed e-MARC system is introduced in Section 2.2. In addition, for the practical realization of the e-MARC system, a JNCC framework and its corresponding decoding scheme are developed in Section 2.2 to support the relay using very simple detection. Section 2.3 provides an EXIT analysis for the convergence property evaluation of the decoder of the JNCC in terms of the $extrinsic$ information exchange. Section 2.4 shows the BER performance of the e-MARC system with JNCC schemes based on the EXIT analysis; furthermore, we compare the BER and FER of the proposed e-MARC system with those of the SDF-MARC system. Finally, Section 2.5 concludes the chapter.

2.1 System model

Fig. 2 illustrates a basic model of the orthogonal e-MARC system assumed in this thesis, where there are two source nodes A and B, one common relay R, and one common destination D. The K-bit length independent identically distributed (i.i.d.) binary information sequences generated from nodes A and B are denoted as $\mathbf{u}_A = \{u_A(k)\}_{k=1}^{K}$ and $\mathbf{u}_B = \{u_B(k)\}_{k=1}^{K}$, respectively. The signaling scheme used at the source node is denoted as $\mathcal{E}_S(\cdot)$, which consists of a serial concatenation of encoding and modulation. There are three time slots in one transmission cycle. In the first two

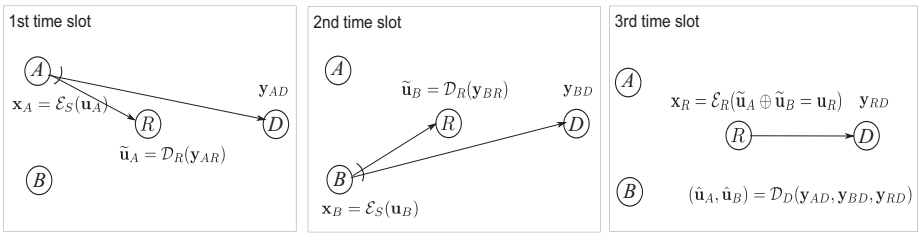

Fig 2. Orthogonal e-MARC system model, where there are three time slots in a transmission cycle, [89] (© 2015 IEEE).

time slots, nodes A and B respectively broadcast their M-bit length symbol sequences $\mathbf{x}_A = \mathcal{E}_S(\mathbf{u}_A) = \{x_A(m)\}_{m=1}^{M}$ and $\mathbf{x}_B = \mathcal{E}_S(\mathbf{u}_B) = \{x_B(m)\}_{m=1}^{M}$ to the relay R and destination D, and their corresponding received signals obtained at R and D are respectively written as

$$\begin{aligned} \mathbf{y}_{iR} &= h_{iR} \cdot \mathbf{x}_i + \mathbf{n}_{iR} \\ \mathbf{y}_{iD} &= h_{iD} \cdot \mathbf{x}_i + \mathbf{n}_{iD}, \qquad i \in \{A, B\} \end{aligned} \tag{2}$$

where h_{iR} and h_{iD} indicate the channel coefficients of iR and iD links with the source node i, respectively. $\mathbf{n}_{iR}$ and $\mathbf{n}_{iD}$ indicate the vectors of independent zero-mean complex AWGN of the iR and iD links, respectively, with variance $\sigma_{iR}^2 = \sigma_{iD}^2 = \sigma^2$ per dimension. The iR and iD links are also referred to as the intra and direct links, respectively, in this thesis.

The receiver applied at the relay R is denoted as $\mathcal{D}_R(\cdot)$, composed of demodulation and signal detection/decoding, which corresponds to the inverse structure of $\mathcal{E}_S(\cdot)$. The estimates $\widetilde{\mathbf{u}}_i = \mathcal{D}_R(\mathbf{y}_{iR})$ of $\mathbf{u}_i$ obtained at R may contain errors due to the variation of the iR link. The error probability of the iR link is represented by

$$p_i = \mathfrak{B}(\mathbf{u}_i, \widetilde{\mathbf{u}}_i) = \frac{\sum_{k=1}^{K} |u_i(k) - \widetilde{u}_i(k)|}{K}, \quad i \in \{A, B\}. \tag{3}$$

If the estimates $\widetilde{\mathbf{u}}_i$ is found to contain errors, it will be discarded at the relay in the SDF-MARC system. However, in the e-MARC system, the estimates $\widetilde{\mathbf{u}}_A$ and $\widetilde{\mathbf{u}}_B$, are always joint network-channel coded at the relay R regardless of whether they are correct or not, as

$$\mathbf{x}_R = \mathcal{E}_R(\mathbf{u}_R) = \mathcal{E}_R(\widetilde{\mathbf{u}}_A \oplus \widetilde{\mathbf{u}}_B) = \{x_R(m)\}_{m=1}^{M}, \tag{4}$$

where the notation $\oplus$ denotes bit-wise XOR operation and $\mathcal{E}_R(\cdot)$ represents the signaling scheme applied at R, including channel encoding and modulation. The destination D obtains the signal vector $\mathbf{y}_{RD}$ of $\mathbf{x}_R$ sent via the RD link as

$$\mathbf{y}_{RD} = h_{RD} \cdot \mathbf{x}_R + \mathbf{n}_{RD}, \tag{5}$$

where h_{RD} and $\mathbf{n}_{RD}$ indicate the channel coefficient and AWGN vector of the RD link with variance $\sigma_{RD}^2 = \sigma^2$, respectively. The estimated sequence of $\mathbf{u}_R$ obtained at the

destination is denoted as $\hat{\mathbf{u}}_R$, and the error rate of the RD link is $p_R = \mathfrak{B}(\mathbf{u}_R, \hat{\mathbf{u}}_R)$. Finally, to obtain the estimated sequences $\hat{\mathbf{u}}_A$ and $\hat{\mathbf{u}}_B$ of the information sequences $\mathbf{u}_A$ and $\mathbf{u}_B$, respectively, at the destination, decoding of JNCC is performed on the received signal vectors $\mathbf{y}_{AD}$ and $\mathbf{y}_{BD}$ with the help of the signal vector $\mathbf{y}_{RD}$.

If all the links are assumed to suffer from block Rayleigh fading, h_{iR}, h_{iD} and h_{RD} are assumed to be constant over one symbol sequence but vary independently transmission-by-transmission and link-by-link. Without loss of generality, we assume that $E[|h_{iR}|^2] = E[|h_{iD}|^2] = E[|h_{RD}|^2] = 1$. The error probabilities p_i and p_R, thus, vary in each transmission cycle. The instantaneous SNRs γ_{iR}, γ_{iD} and γ_{RD} of the links are then given by

$$\begin{aligned} \gamma_{iR} &= |h_{iR}|^2 \cdot \Gamma_{iR} \\ \gamma_{iD} &= |h_{iD}|^2 \cdot \Gamma_{iD} \\ \gamma_{RD} &= |h_{RD}|^2 \cdot \Gamma_{RD} \end{aligned} \tag{6}$$

where Γ_{iR}, Γ_{iD} and Γ_{RD} represent the average SNRs of the intra, direct and RD links, respectively.

2.2 AWGN MARC

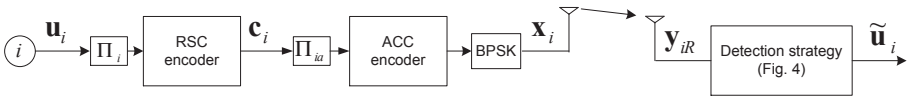

Fig 3. Block diagram of signaling schemes applied in the SR link.

To better understand the fundamental idea of the e-MARC system, all the links in e-MARC are assumed to be AWGN (i.e., $h_{iR} = h_{iD} = h_{RD} = 1$) in this section. With this assumption, the average value of the probability p_i in (3) is equivalent to a bit-flipping model [95, 96]. In addition, the average value of p_i depends on the signaling and detection scheme applied at the source node and relay, respectively. For the purpose of reducing the computational complexity in the encoding process, the source node in this thesis employs a serially concatenated convolutional code (SCCC), composed of a rate-$1/2$ recursive systematic convolutional (RSC) code and a rate-1, memory-1

accumulator (ACC) [97]. The generator polynomials of the RSC and ACC encoder are $(1, 5/7)_8$ and $(2/3)_8$, respectively, where the notation $(\cdot)_8$ represents the argument is an octal number.

As shown in Fig. 3, the interleaved version of the information sequence $\mathbf{u}_i$ is first encoded by the RSC code to produce the coded sequence $\mathbf{c}_i$, and the interleaved version of the sequence $\mathbf{c}_i$ is further encoded by the ACC and modulated using binary phase-shift keying (BPSK) to produce the symbol sequence $\mathbf{x}_i$. The use of the ACC aims to ensure that the EXIT convergence tunnel is open until a point very close to the (1.0, 1.0) mutual information (MI) point [98]. The notations $\Pi_i[\,\cdot\,]$ and $\Pi_{ia}[\,\cdot\,]$ shown in Fig. 3 denote interleaving by Π_i and by Π_{ia}, respectively.

According to the encoder structure applied at the source node, several detection strategies are able to be used at the relay:

– IR: the relay obtains the estimated sequence $\widetilde{\mathbf{u}}_i$ by performing iterative decoding between the decoders of the ACC and RSC code with the log-MAP algorithm on vector $\mathbf{y}_{iR}$, as shown in Fig. 4(a). Here the notations $\Pi_i^{-1}[\,\cdot\,]$ and $\Pi_{ia}^{-1}[\,\cdot\,]$ denote de-interleaving by Π_i and by Π_{ia}, and 10 iterations are set for the decoding.

– DACC: to eliminated heavy computational complexity caused by iterative decoding, the relay only performs the decoding of the ACC using the log-MAP algorithm, and extracts the systematic part output from the ACC decoder to obtain $\widetilde{\mathbf{u}}_i$ as the decoding of the ACC is completed. The detection scheme of DACC is depicted in Fig. 4(b)

– DDEX: the relay simply extracts the systematic part output from the differential detector (DD), as shown in Fig. 4(c). Hence, the computational complexity of detection is further reduced.

Note that the bits in sequence $\mathbf{u}_i$ may be correlated caused by the shift registers of the signaling chain. To eliminate the correlation, the information sequence $\mathbf{u}_i$ is interleaved by Π_i before the encoding process at the source node, and the estimated sequence $\widetilde{\mathbf{u}}_i$ is the de-interleaved output after detection, by which the relationship between $\mathbf{u}_i$ and $\widetilde{\mathbf{u}}_i$ is guarantied to be equivalent to an equivalent bit-flipping model.

The error probability p_i of the three detection strategies are demonstrated in Fig. 5, where 100 information sequences are used in the simulation, and the length of the information sequence is 10000 bits. It can be observed in Fig. 5 that, even in the relatively low SNR regime, the IR strategy can recover the sequence $\mathbf{u}_i$ at the relay with a high

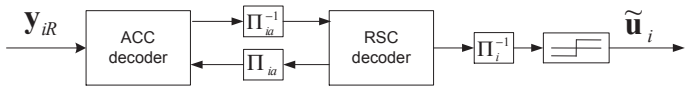

(a) IR

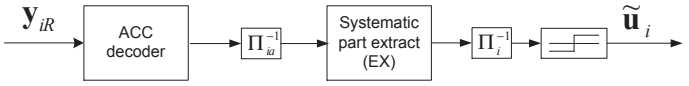

(b) DACC

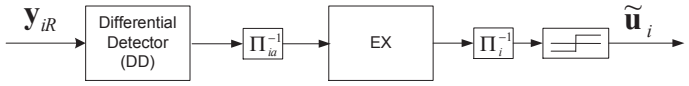

(c) DDEX, [85] (© 2011 IEEE).

Fig 4. Detection strategies used at the relay.

probability, this is because powerful decoding is performed at the relay. On the contrary, the DACC and DDEX strategies obtain the estimated sequence $\widetilde{\mathbf{u}}_i$ containing errors with a high probability although heavy computational complexity is eliminated. Hence, in the following subsection, a technique is proposed to exploit the erroneous estimates.

2.2.1 Network correlation

As mentioned above, the average value of the SR link's error probability p_i is equivalent to the bit-flipping model. Then, since bitwise XOR coding is always performed at the relay in the proposed e-MARC system, we found a new bit-flipping probability p_{nc} between the two sequences: one is the forwarded XOR-coded sequence generated by the relay by performing bitwise XOR coding on $\widetilde{\mathbf{u}}_A$ and $\widetilde{\mathbf{u}}_B$, and the other is their corresponding XOR-ed information sequences $\mathbf{u}_{\oplus}$ (i.e., $\mathbf{u}_{\oplus} = \mathbf{u}_A \oplus \mathbf{u}_B$). Hence, by utilizing p_A and p_B, the probability p_{nc} between sequences $\mathbf{u}_{\oplus}$ and $\mathbf{u}_R$ can be calculated as

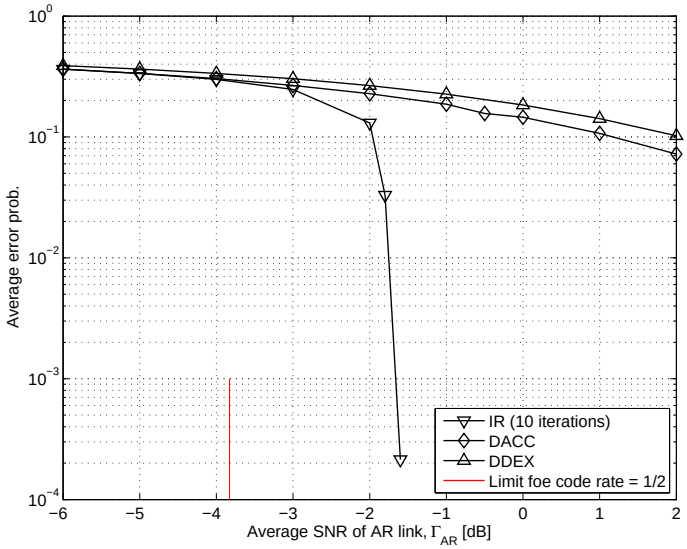

Fig 5. Average value of probabilities p_i of detection strategies listed in Fig. 4, [84] (© 2011 IEEE).

$$\begin{aligned} p_{nc} &= \Pr(u_R(k) \neq u_{\oplus}(k)) \\ &= \Pr((\widetilde{u}_A(k) \oplus \widetilde{u}_B(k)) \neq (u_A(k) \oplus u_B(k))) \\ &= 1 - (1 - p_A)(1 - p_B) - p_A p_B \\ &= p_A + p_B - 2 \cdot p_A p_B, \qquad k = 1, 2, ..., K \end{aligned} \tag{7}$$

We refer the probability p_{nc} as a network correlation in this thesis. Note that in this chapter, the values of p_A and p_B are assumed to be known to the relay, and the knowledge of p_{nc} is available at the destination with the aid of higher layer protocol setting. In fact, p_{nc} can be directly estimated at the destination during the iterative JNCC decoding process, which will be introduced in Chapter 4.

To exploit the erroneous estimates $\widetilde{\mathbf{u}}_i$, in the following subsection, a JNCC framework and its corresponding decoding scheme are developed to support the relay using very simple detection, such as DACC and DDEX, in which the knowledge of the network correlation p_{nc} is utilized at the destination to help recover the information sequences sent via iD links.

2.2.2 e-MARC scheme

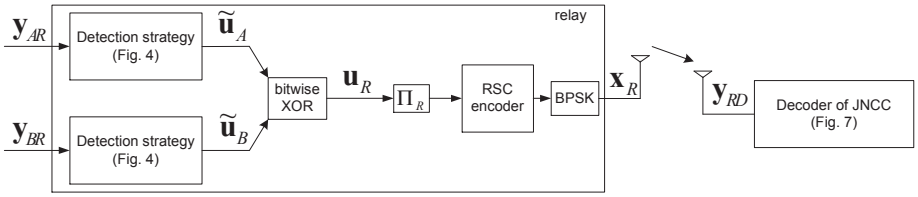

Fig 6. JNCC framework in proposed e-MARC scheme.

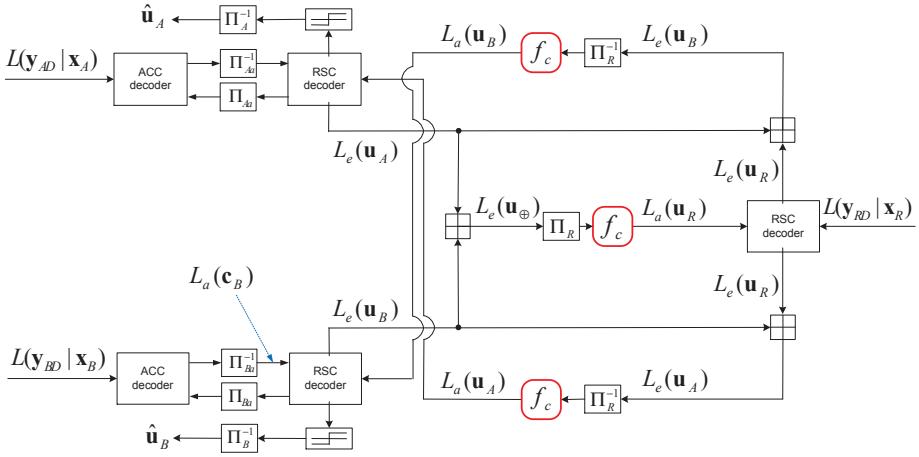

Fig 7. Decoder of JNCC applied at destination in proposed e-MARC scheme, [84] (© 2011 IEEE).

Fig. 6 shows the JNCC framework developed for the e-MARC system, where the relay first performs bit-wise XOR coding on both the estimates $\widetilde{\mathbf{u}}_A$ and $\widetilde{\mathbf{u}}_B$, and the interleavered version of $\mathbf{u}_R$ is encoded by a RSC code, and modulated using BPSK. Here $\Pi_R[\,\cdot\,]$ denotes interleaving by Π_R.

The corresponding decoder of the JNCC coding scheme is shown in Fig. 7. To exploit the erroneous estimated sequence $\widetilde{\mathbf{u}}_i$ obtained at the relay, the LLR-updating function $f_c(\cdot)$ [86] is used in the JNCC decoding scheme, where the knowledge of

network correlation p_{nc} is exploited by the function $f_c(\cdot)$ to avoid the error propagation if the XOR-coded sequence $\mathbf{u}_R$ is erroneous. The function $f_c(\cdot)$ is defined as follow

$$\begin{aligned}\mathfrak{L}' &= f_c(\mathfrak{L},\, p_{nc}) \\ &= \ln \frac{(1-p_{nc})\cdot e^{\mathfrak{L}} + p_{nc}}{(1-p_{nc}) + p_{nc}\cdot e^{\mathfrak{L}}},\end{aligned} \tag{8}$$

where $\mathfrak{L}$ represents the input LLR sequence to be updated by the bit-wise function $f_c(\cdot)$, and $\mathfrak{L}'$ is the updated LLR sequence output from $f_c(\cdot)$.

The received signal vectors $\mathbf{y}_{iD}$ sent from the two source nodes are respectively demodulated bit-wisely at D to obtain the corresponding soft channel values, as

$$L(\mathbf{y}_{iD}|\mathbf{x}_i) = 2\cdot\Re\left(\frac{\mathbf{y}_{iD}h_{iD}^*}{\sigma^2}\right), \quad i\in\{A,B\}, \tag{9}$$

where the notations $L(\cdot)$ and $\Re(\cdot)$ denote the LLR[2] and a function that takes the real part of its argument, respectively, and $*$ indicates complex conjugation.[3] The computation from the received vector $\mathbf{y}_{RD}$ to $L(\mathbf{y}_{RD}|\mathbf{x}_R)$ also applies (9).

As shown in Fig. 7, given the soft channel values, the soft-in-soft-out (SISO) SCCC and RSC decoders compute the $extrinsic$ LLR values $L_e(\mathbf{u}_i)$ and $L_e(\mathbf{u}_R)$, respectively, using the log-MAP algorithm. Then, since XOR coding is performed at the relay, the $extrinsic$ LLR sequence $L_e(\mathbf{u}_\oplus)$ is obtained by performing the bit-wisely "box-plus" operation [99] on $L_e(\mathbf{u}_A)$ and $L_e(\mathbf{u}_B)$, as

$$\begin{aligned}L_e(\mathbf{u}_\oplus) &= L_e(\mathbf{u}_A)\boxplus L_e(\mathbf{u}_B) \\ &= \ln\frac{\exp(L_e(\mathbf{u}_A))+\exp(L_e(\mathbf{u}_B))}{1+\exp(L_e(\mathbf{u}_A)+L_e(\mathbf{u}_B))}\end{aligned} \tag{10}$$

Since the correlation between bits $u_\oplus(k)$ and $u_R(k)$ is p_{nc}, the $a\ priori$ LLR values for $\mathbf{u}_R$ can be obtained by using $f_c(\cdot)$ to bit-wisely modify $L_e(\mathbf{u}_\oplus)$, as

$$L_a(\mathbf{u}_R) = f_c\left(\Pi_R\left[L_e(\mathbf{u}_\oplus)\right],\, p_{nc}\right) \tag{11}$$

Similarly, with using the bit-wise "box-plus" operation, $L_e(\mathbf{u}_A)$ and $L_e(\mathbf{u}_B)$ can be

[2] $L(x) = \ln\frac{\Pr(x=1)}{\Pr(x=0)}$, where $\Pr(\cdot)$ denotes the probability of its argument.

[3] Please refer Appendix 1 for the derivation of (9).

extracted from $L_e(\mathbf{u}_R)$ computed by the RSC decoder, and be modified by function $f_c(\cdot)$ to become $a\ priori$ LLR values for $\mathbf{u}_A$ and $\mathbf{u}_B$, as

$$L_a(\mathbf{u}_A) = \Pi_R^{-1}\left[f_c(L_e(\mathbf{u}_R),\ p_{nc}) \boxplus L_e(\mathbf{u}_B)\right] \tag{12}$$

and

$$L_a(\mathbf{u}_B) = \Pi_R^{-1}\left[f_c(L_e(\mathbf{u}_R),\ p_{nc}) \boxplus L_e(\mathbf{u}_A)\right], \tag{13}$$

where $\Pi_R^{-1}[\,\cdot\,]$ indicates de-interleaving from Π_R. For the sake of simplicity, the combination of the JNCC and its decoding scheme developed for the e-MARC system is referred to as an e-MARC scheme. It should be emphasized that the proposed e-MARC scheme is not a unique practical realization for the e-MARC system. It is possible to exploit the network correlation with more sophisticated coding and modulation schemes.

2.2.3 SDF-MARC scheme

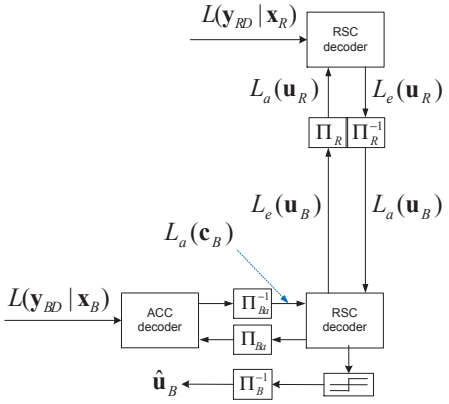

Fig 8. Decoder of SDF-MARC scheme as only one correct estimated sequence is forwarded. Here $\widetilde{\mathbf{u}}_B = \mathbf{u}_B$ and $\widetilde{\mathbf{u}}_A \neq \mathbf{u}_A$ for example.

For the purpose of fair comparison, the JNCC and its decoding schemes, respectively shown in Fig. 6 and Fig. 7, are also used for the SDF-MARC system with simple modifications. Unlike e-MARC, the relay discards the erroneous received estimates in the SDF-MARC system. Therefore, in the case that both estimates are correctly de-

coded, the encoding and decoding processes of JNCC is same as that of the proposed e-MARC scheme. As one of the estimates is decoded in error, instead of performing JNCC encoding, the relay simply encodes the interleaved version of the correct estimated sequences using RSC code, and the JNCC decoder shown in Fig. 7 is reduced to a parallel concatenated convolutional code (PCCC) decoder, as shown in Fig. 8. The relay remains silent as both estimated sequences are incorrect. For consistency, the modified JNCC and its decoding scheme described above is referred to as a SDF-MARC scheme.

2.3 EXIT analysis

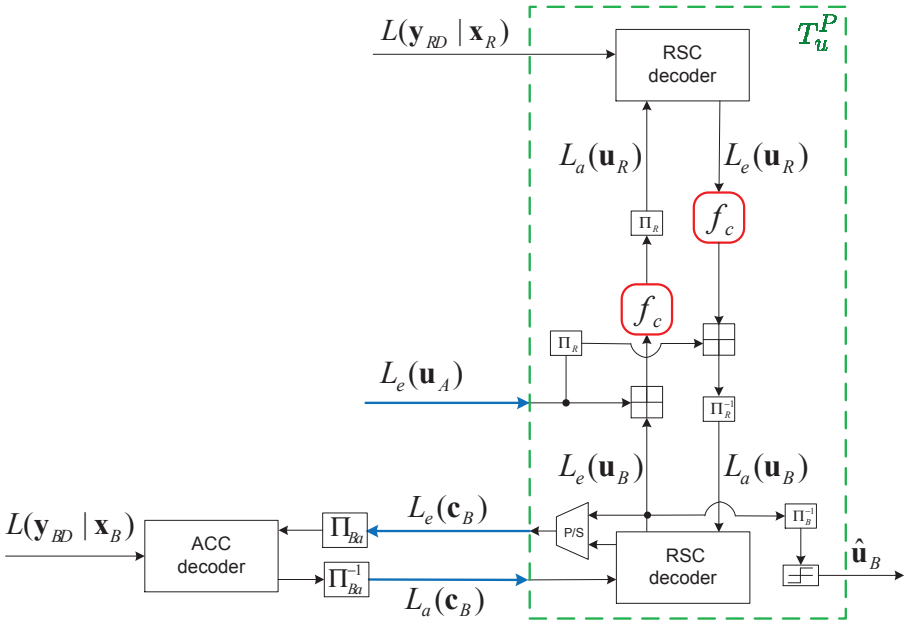

Fig 9. Detailed flows of LLR values for 3D EXIT analysis, [84] (© 2011 IEEE).

In this section, we analyze the JNCC decoder of the proposed e-MARC scheme illustrated in Fig. 7 by utilizing a three-dimensional (3D) EXIT chart for tracking the convergence property of the information estimates while the two SCCC decoders simultaneously exchange the message in the from of LLR values with the RSC decoder. The

analysis focuses on the both SCCC decoders since our aim is to perfectly retrieve the information estimates $\hat{\mathbf{u}}_A$ and $\hat{\mathbf{u}}_B$. In Fig. 9, we temporarily remove one of the SCCC decoders from the JNCC decoder to compute the mutual information of the $extrinsic$ bit probabilities $I_e(\mathbf{u}_B)$; since the JNCC decoder is symmetric in structure, the computation for $I_e(\mathbf{u}_A)$ is same as for $I_e(\mathbf{u}_B)$. As shown in Fig. 9, the EXIT function $T_u^P(\cdot)$ composed of the two RSC decoders can be characterized as follows

$$I_e(\mathbf{u}_B) = T_u^P(I_a(\mathbf{c}_B), I_e(\mathbf{u}_A)|p_{nc}, \Gamma_{RD}) \tag{14}$$

in which

$$I_e(\mathbf{u}_B) = I(\mathbf{u}_B; L_e(\mathbf{u}_B)) \tag{15}$$

$$I_a(\mathbf{c}_B) = I(\mathbf{c}_B; L_a(\mathbf{c}_B)) \tag{16}$$

$$I_e(\mathbf{u}_A) = I(\mathbf{u}_A; L_e(\mathbf{u}_A)) \tag{17}$$

As shown in (14), the function $T_u^P(\cdot)$ has two input parameters $I_a(\mathbf{c}_B)$ and $I_e(\mathbf{u}_A)$, and thus we use a 3D EXIT chart to draw the output mutual information $I_e(\mathbf{u}_B)$ given the SNR of the RD link and the value of p_{nc}.

2.3.1 Consistency condition

As mentioned in [87], the Gaussian distributed LLR sequence with symmetric and consistency conditions are fundamental requirements for a tight EXIT chat analysis. In general, the LLR values output from the decoder using Bahl-Cocke-Jelinek-Raviv (BCJR) decoding algorithm are Gaussian distributed. However, the LLR values updated by the function $f_c(\cdot)$ are not; moreover, the consistency condition does not hold for the distribution of the updated LLR values. Hence, we numerically measure the distribution of $L_e(\mathbf{u}_B)$ (and $L_e(\mathbf{c}_B)$) output from the function $T_u^P(\cdot)$ to verify the robustness of the function $f_c(\cdot)$ to EXIT analysis.

As shown in Fig. 9, the two inputs $L_a(\mathbf{c}_B)$ and $L_e(\mathbf{u}_A)$ come from the ACC and RSC decoders, respectively, and thus, it is reasonable to artificially generate the values of $L_a(\mathbf{c}_B)$ and $L_e(\mathbf{u}_A)$ with Gaussian distribution. The distribution of $L_e(\mathbf{u}_B)$ given

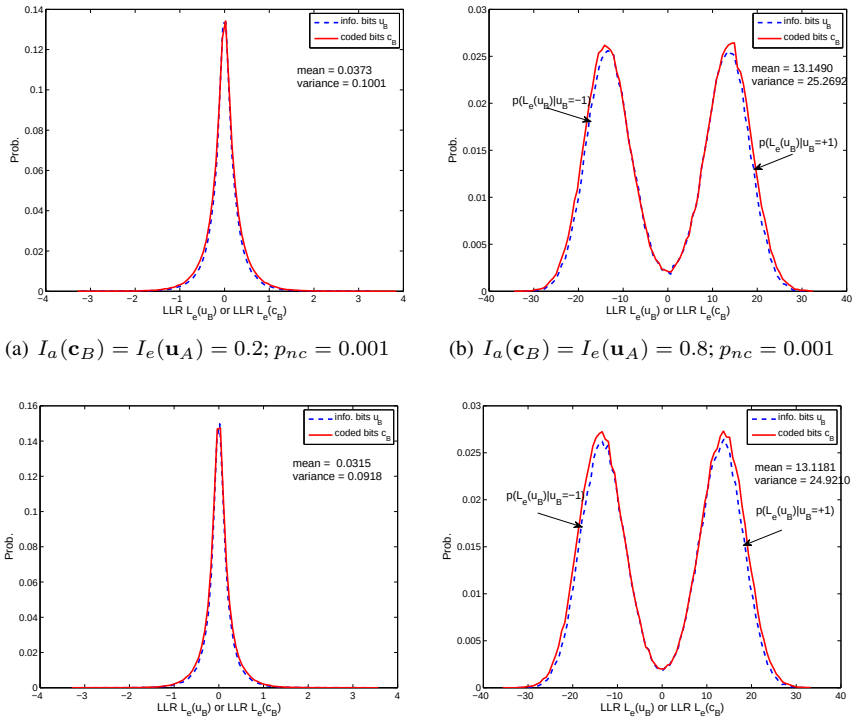

(a) $I_a(\mathbf{c}_B) = I_e(\mathbf{u}_A) = 0.2; p_{nc} = 0.001$ (b) $I_a(\mathbf{c}_B) = I_e(\mathbf{u}_A) = 0.8; p_{nc} = 0.001$

(c) $I_a(\mathbf{c}_B) = I_e(\mathbf{u}_A) = 0.2; p_{nc} = 0.25$ (d) $I_a(\mathbf{c}_B) = I_e(\mathbf{u}_A) = 0.8; p_{nc} = 0.25$

Fig 10. Density evolution of extrinsic LLR $L_e(\mathbf{u}_B)$ with different values of $I_a(\mathbf{c}_B)$, $I_e(\mathbf{u}_A)$ and p_{nc}, given Γ_{RD} = 0 dB

$u_B = 1$ and $u_B = -1$ (or, the distribution of $L_e(\mathbf{c}_B)$ given $c_B = 1$ and $c_B = -1$) are measured after completing 40 iterations for the information exchange between the two RSC decoders of $T_u^P(\cdot)$. Figs. 10(a)-10(d) show the conditional distributions of $L_e(\mathbf{u}_B)$ and $L_e(\mathbf{c}_B)$ with different input parameters. It can be observed that the conditional distribution of $L_e(\mathbf{u}_B)$ output from the $T_u^P(\cdot)$ is approximated to Gaussian; furthermore, for the conditional distribution of $L_e(\mathbf{u}_B)$, the variance is nearly two times that of the mean. This states that the consistency condition is still maintained even though the function $f_c(\cdot)$ is embedded in the function $T_u^P(\cdot)$.

2.3.2 Impact of p_{nc}

Figs. 11(a) and 11(b) show the EXIT planes of $T_u^P(\cdot)$ with small and large p_{nc} values, respectively, where Γ_{RD} = 0 dB. It can be seen from Fig. 11(a) that when p_{nc} is small

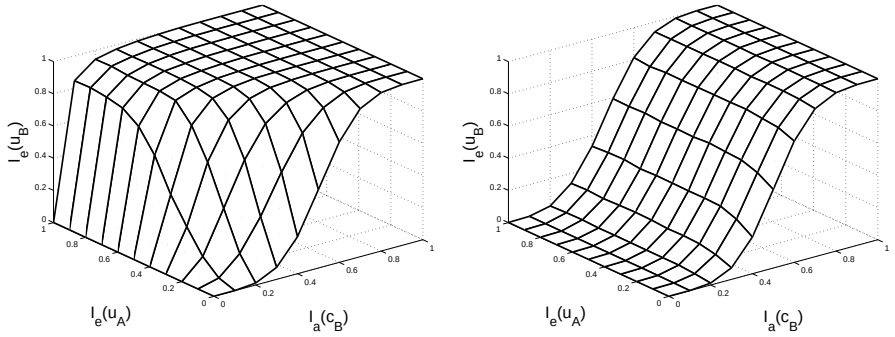

(a) $p_{nc} = 0.001$ (b) $p_{nc} = 0.25$

Fig 11. EXIT plane of function $T_u^P(\cdot)$ with different p_{nc} values, given Γ_{RD} = 0 dB. Generator polynomials of RSC codes are $(1, 5/7)_8$, [84] (© 2011 IEEE).

(i.e., $\mathbf{u}_R$ and $\mathbf{u}_\oplus$ are highly correlated), the $extrinsic$ information provided from the other SCCC decoder, $I_e(\mathbf{u}_A)$, has a significantly effect on $T_u^P(\cdot)$; however, when p_{nc} is large, as indicated by Fig. 11(b), that $I_e(\mathbf{u}_B)$ is nearly a constant value over the entire range of $I_e(\mathbf{u}_A)$. Therefore, when p_{nc} is small, we have to consider the impact of the other SCCC decoder when performing an EXIT analysis for the JNCC decoder; on the contrary, when p_{nc} is large, the 3D EXIT analysis for the JNCC decoder can be simplified to a two-dimensional (2D) EXIT analysis.

2.4 Numerical results

Table 1. Parameters for BER simulations.

Parameter	Value
Length of information sequence (K)	10000 bits
Generator polynomial of RSC code	$(1, 5/7)_8$
Generator polynomial of ACC	$(2/3)_8$
Spectrum efficiency of $\mathcal{E}_S$ (K/M)	$1/2$
Spectrum efficiency of $\mathcal{E}_R$ (K/M)	$1/2$
Signaling scheme $\mathcal{E}_R$	RSC code
Receiver $\mathcal{D}_D$	Fig. 7
Global iteration (GI)	40 iterations
Local iteration (LI)	6 iterations
Loops between GI and LI	3
Decoding algorithm	log-MAP
Interleavers	Random

In this section, we apply the analytical method presented in Sec. 2.3 to identify the

SNR values required for the AD and BD links to be able to retrieve the information estimates $\hat{\mathbf{u}}_A$ and $\hat{\mathbf{u}}_B$ successfully given Γ_{iR} and Γ_{RD}. All the detection strategies numerated in Section 2.2 use the same iterative decoder illustrated in Fig. 7, since the same structure in signaling scheme is applied at the source node. The procedure of the decoding process is described as follows

– (Step1) $L_e(\mathbf{u}_j)$ for $j \in \{A, B, R\}$ is computed from $L(\mathbf{y}_{jD}|\mathbf{x}_j)$. No iterative decoding is performed between the ACC and RSC decoders for the computation of $L_e(\mathbf{u}_A)$ and $L_e(\mathbf{u}_B)$.

– (Step2) The two SCCC decoders simultaneously exchange the message in the from of LLR values with the RSC decoder. The behavior is denoted as a global iteration (GI). The number of global iterations is set to 40.

– (Step3) The RSC decoder of the two SCCC obtains the $apriori$ $L_a(\mathbf{u}_i)$ for $i \in \{A, B\}$ after completing Step2. Then, iterative decoding is performed between the ACC and RSC decoders, which is referred to as a local iteration (LI). The number of local iterations is set to 6. Go back to Step2 when Step3 is finished, and the number of loops between Step2 and Step3 is set to 3.

The BER here is defined as follows: total number of errors $\hat{\mathbf{u}}_A$ and $\hat{\mathbf{u}}_B$ contain, divided by the total number of transmission bits. The main parameters are listed in Table 1.

2.4.1 AWGN links

With the assumption of relatively high SNR intra links, Γ_{AR} = Γ_{BR} = 2 dB and Γ_{RD} = 0 dB were assumed. The 3D EXIT chart analysis for the JNCC decoder with the DACC strategy is shown in Fig. 12, where the 3D EXIT planes of the function $T_u^P(\cdot)$ and ACC decoder are demonstrated. Note that the same structure of the SCCC is used for the decoding of the signal vectors sent from A and B, and thereby, we use the same EXIT analysis to trace the decoding trajectories of the both information estimates $\hat{\mathbf{u}}_A$, $\hat{\mathbf{u}}_B$, and placed them together in Fig. 12.

Given Γ_{AR}, Γ_{BR} and Γ_{RD}, we simultaneously change the values of Γ_{AD} and Γ_{BD} and draw the corresponding decoding trajectories. It can be observed in Fig. 12 that as Γ_{AD} and Γ_{BD} achieve -2.3 dB, the convergence tunnel, seen in the 2D EXIT chart

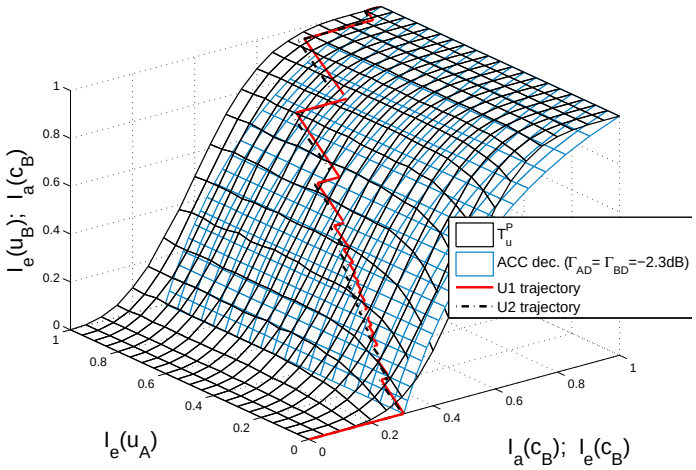

Fig 12. The 3D EXIT chart analysis for JNCC decoder of proposed e-MARC scheme, where DACC strategy is used, [84] (© 2011 IEEE).

when $I_e(\mathbf{u}_A) = 0$, is closed, but the 3D tunnel ($0 \leq I_e(\mathbf{u}_A) \leq 1$) is slightly open; moreover, the trajectories for the $\hat{\mathbf{u}}_A$ and $\hat{\mathbf{u}}_B$ match the EXIT planes and both reach the (1, 1, 1) mutual information point. Therefore, the turbo cliff of the DACC strategy with the proposed e-MARC scheme is expected to occur when Γ_{AD} and Γ_{BD} achieve around -2.3 dB.

Fig. 13 shows the BER performances of all the strategies listed in Fig. 4 with the proposed e-MARC scheme. The turbo cliff of the DACC strategy happens when Γ_{AD} and Γ_{BD} are around at -2.3 dB. The BER curve of the IR strategy is provided as a limit for those of the DACC and DDEX strategies, since both the SR links with using the IR strategy are nearly error-free as Γ_{AR} = Γ_{BR} = 2 dB. As shown in Fig. 13, there is a 0.55-dB gap between the IR and DACC/DDEX strategies; however, it should be noticed that even when Γ_{AR} = Γ_{BR} = 2 dB, as shown in Fig. 5, the estimates $\widetilde{\mathbf{u}}_i$ received at the relay still contain errors with a very high probability with using the DACC and DDEX strategies; furthermore, to achieve nearly error-free SR links as Γ_{AR} = Γ_{BR} = 2 dB, iterative decoding requiring heavy computational complexity has to be performed at the relay. Such a high complexity requirement can be eliminated with the DACC/DDEX detection strategy, since only ACC decoding/differential detection has to be performed at the relay, for which computational complexity is very low. In summary, compared to a high complexity decoding strategy at the relay, the DACC/DDEX strategies combined with the proposed e-MARC scheme significantly reduces the relay complexity, which

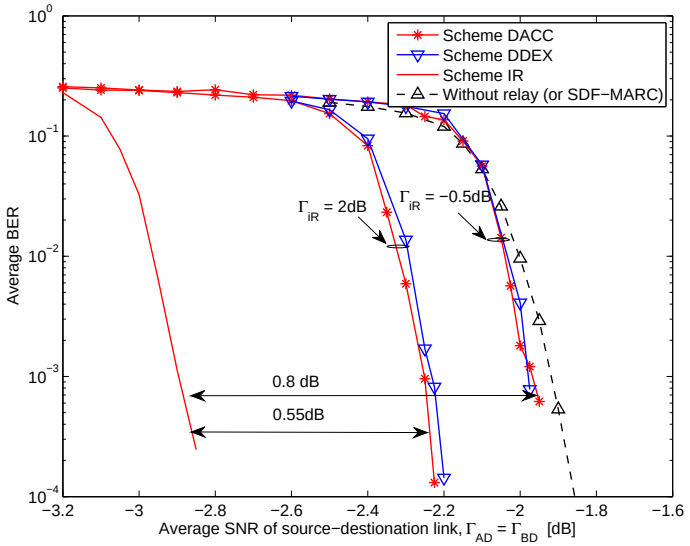

Fig 13. BER performances of all strategies with e-MARC and SDF-MARC schemes. All links in MARC are AWGN. Γ_{RD} is fixed to 0 dB, [84] (© 2011 IEEE).

is in exchange for a 0.55 dB loss in the BER performance from the case of nearly error-free SR links.

With the assumption of relatively low SNR intra links, Γ_{AR} = Γ_{BR} = -0.5 dB and Γ_{RD} = 0 dB. In this case the quality of the intra links is worse (i.e., $p_i \simeq 0.1564, 0.2015$ for DACC and DDEX, respectively); therefore, the performance of the two strategies with the proposed e-MARC scheme are, as shown in Fig. 13, worse than the case of relatively high SNR intra links. Moreover, It can be observed in Fig. 13 that, compared with no cooperation, forwarding erroneous estimates achieves only a slightly better performance, but requires higher power consumption. This implies a trade-off between the performance and energy efficiency when the e-MARC scheme is used in the poor quality of both intra links.

2.4.2 SR links with constant error probability

In this subsection, comparisons of the BER performances are made between the e-MARC and SDF-MARC schemes[4] when the SR links are modeled by BSCs[5] while the

[4]The code used at the sources is shown in Fig. 3.
[5]The detection strategy needs not to be taken into account since the SR links are modeled by BSCs.

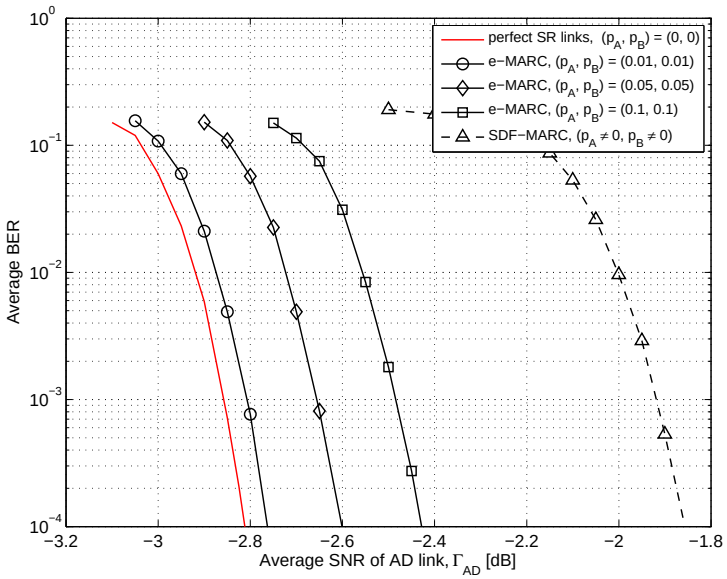

Fig 14. BER performances of e-MARC and SDF-MARC, where SR links are modeled by BSCs while SD and RD links are AWGN.

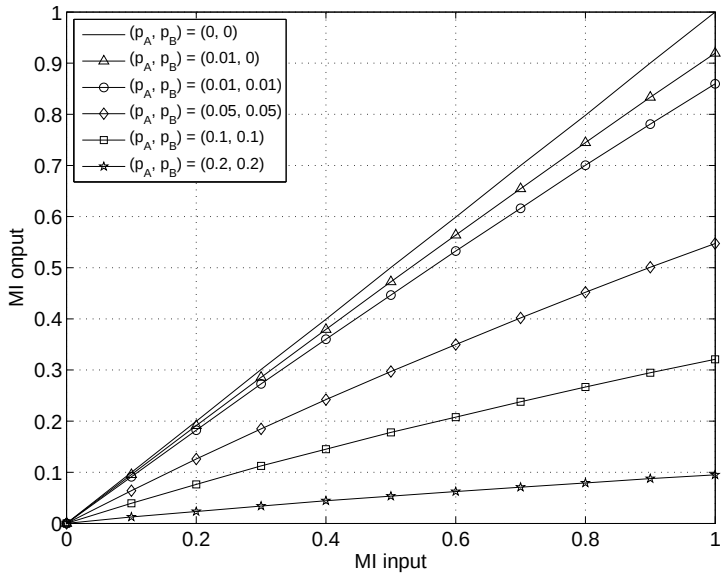

Fig 15. EXIT analysis of LLR-updating function $f_c(\cdot)$.

other links are assumed to be AWGN. It is found in Fig. 14 that e-MARC is superior to SDF-MARC except for the case that $(p_A, p_B) = (0, 0)$. This is because with applying the SDF relay strategy, the recovery of the information sequences totally depends on the error correction capability of the schemes applied in the direct link (i.e, SCCC), and according to [100], the minimum SNR for the SCCC, composed of a $(1, 5/7)_8$ RSC code and a $(2/3)_8$ ACC, to achieve convergence after performing 40 iterations is -1.8 dB.

Nevertheless, the BER performance is significantly improved with the proposed e-MARC scheme due to the exploitation of the erroneous estimates $\widetilde{\mathbf{u}}_i$. Furthermore, it can be observed in Fig. 14 that the fewer number of errors $\widetilde{\mathbf{u}}_A$ and $\widetilde{\mathbf{u}}_B$ contain, the better BER performance can be achieved. This is because the large value of p_{nc} degrades the output amount of mutual information from the LLR-updating function $f_c(\cdot)$, as shown in Fig. 15.

2.4.3 Fading channels

Table 2. Settings of Symmetric and Asymmetric scenarios, [89] (© 2015 IEEE).

Scenario	Γ_{AD}	Γ_{BD}	Γ_{AR}	Γ_{BR}	Γ_{RD}
Symmetric	X	X	X+Δ	X+Δ	X+Δ
Asymmetric	X	X-L	X+Δ	X+Δ-L	X+Δ

Table 3. Parameters for BER/FER simulations in fading channels, [89] (© 2015 IEEE).

Variable	Value
Length of information sequence (K)	2048 bits
Generator polynomial of RSC code	$(1, 5/7)_8$
Generator polynomial of ACC	$(2/3)_8$
Spectrum efficiency of $\mathcal{E}_S$ (K/M)	$1/2$
Spectrum efficiency of $\mathcal{E}_R$ (K/M)	$1/2$
Signaling scheme $\mathcal{E}_R$	SCCC
Receiver $\mathcal{D}_R$	DDEX
Receiver $\mathcal{D}_D$	[85, Fig. 4]
Global iteration (GI)	1 iteration
Local iteration (LI)	10 iterations
Loops between GI and LI	10
Decoding algorithm	log-MAP
Interleavers	Random

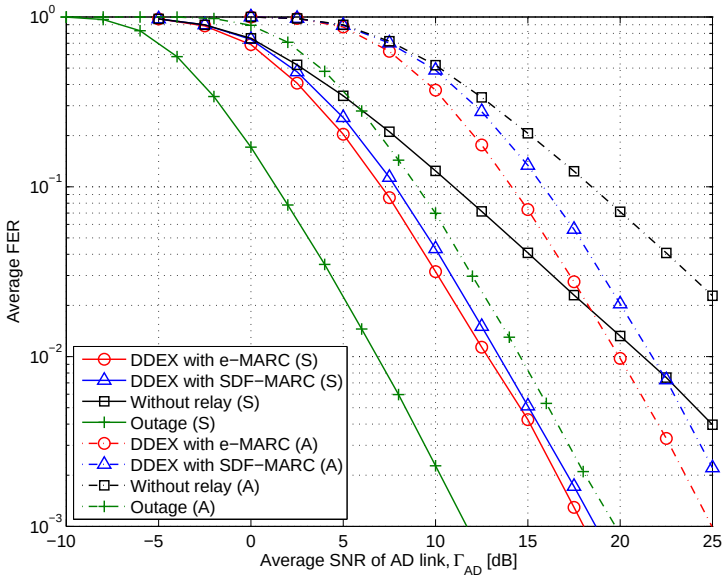

Fig 16. FER performances of DDEX with e-MARC and with SDF-MARC, where all links in MARC suffer from block Rayleigh fading. Notations (S) and (A) denote the Symmetric and Asymmetric scenarios listed in Table 2, respectively, [89] (© 2015 IEEE).

The SR links are assumed to be AWGN and BSCs in subsections 2.4.1 and 2.4.2, respectively. To be more practical for the real scenarios, in this subsection, all the links in MARC are assumed to suffer from block Rayleigh fading. We compare the e-MARC and SDF-MARC schemes in terms of the FER and BER performances, where DDEX is used as an example. The aim of utilizing the low-complexity and non-coherent DDEX is to reduce the power consumption and large latency caused by complicated decoding algorithms. The settings of the both scenarios are summarized in Table 2 for testing, where X represents the average SNR of the AD link in dB; Δ and L denoting additional gain and loss due to the shorter and longer distance, respectively, and are set to 3 dB and 10 dB in this subsection. The main parameters are listed in Table 3.

Results of the FER performances in the Symmetric and Asymmetric scenarios are demonstrated in Fig. 16 for comparison. Here FER is defined as follows: the number of the transmission cycles where either one or both of the information sequences sent from the nodes A and B cannot successfully recovered at D even with the help of R, divided by the total number of transmission cycles.

It can be observed in Fig. 16 that in the Symmetric and Asymmetric scenarios, using DDEX, e-MARC respectively obtains 0.7 dB and 2.2 dB gain from SDF-MARC.

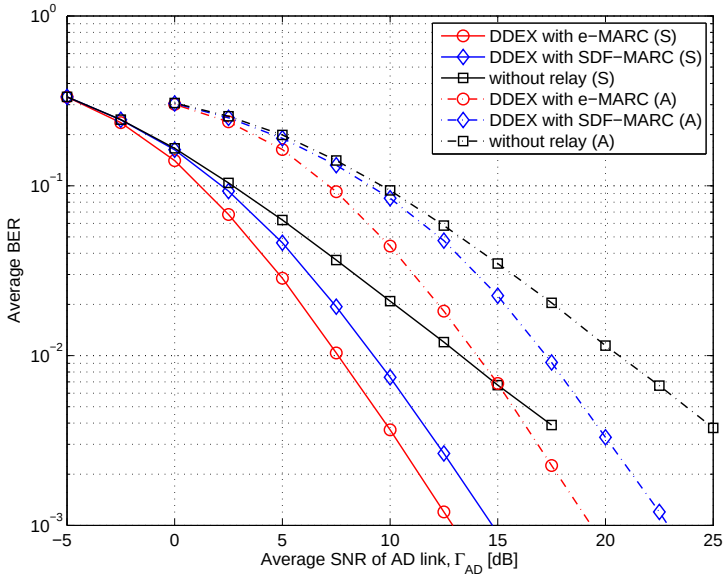

Fig 17. BER performances of DDEX with e-MARC and with SDF-MARC, where all links in MARC suffer from block Rayleigh fading. Notations (S) and (A) denote the Symmetric and Asymmetric scenarios listed in Table 2, respectively.

This indicates that even though the estimates $\widetilde{\mathbf{u}}_i$ contain errors with a high probability due to the use of DDEX, the erroneous estimates received at the relay, instead of being discarded, can still be effectively exploited in the proposed e-MARC system for reconstructing the information sequences $\mathbf{u}_i$, sent via the iD link, at the destination.

The theoretical outage probabilities of SDF-MARC in both scenarios are also included in Fig. 16 as the limits, and obtained using the results of [33, eqs. (4)-(6)] with a modification of [101, eq. (12)]. Here the outage probabilities are assumed to use Gaussian codebook with an infinite sequence length. It can be observed from Fig. 16 that the FER performances of the proposed e-MARC with DDEX are roughly 6 dB and 5 dB away from the outage of SDF-MARC in the Symmetric and Asymmetric scenarios, respectively. The loss is due to several reasons, such as the very short sequence length used in the simulation, and very simple DDEX; furthermore, optimal code design is not taken into account here.

The BER performances of DDEX with e-MARC and with SDF-MARC schemes are also demonstrated in Fig. 17. Compared to the FER performance shown in Fig. 16, the e-MARC is more advantageous in the BER performance, and provides roughly 2.3 dB and 3.8 dB gain over SDF-MARC at BER = 10^{-3} in the Symmetric and Asymmetric

scenarios, respectively. This is because the lower amount of mutual information, caused by the larger value of p_{nc}, is still helpful in correcting several error bits, even though it is not enough to correct all the error bits.

2.5 Conclusions

The e-MARC system has been proposed to improve the BER/FER performances by exploiting the erroneous information estimates received at the relay, especially for the case where low-computational complexity detection strategies are applied at the relay due to several constraints, such as the large latency induced by the iterative decoding process and/or the battery and memory resources of the relay may be limited to perform complicated decoding algorithms. The key factors of the e-MARC system are: I) the relay always performs network-coding on both estimates and forwards the coded sequence, and II) the knowledge of the network correlation p_{nc} is utilized by using the LLR-updating function in the JNCC iterative decoding process at the destination. According to the simulated results, the BER and FER performances are apparently improved in the proposed e-MARC system. A significant improvement has been observed for the cases: 1) where two SR links are assumed to be BSCs with constant small crossover probabilities while other links are assumed to be AWGN, and 2) where one source node is far away from both the relay and destination when all links suffer from block Rayleigh fading.

The knowledge of the network correlation p_{nc} is assumed to be known in the destination, which may be less practical in the real scenario. In addition, the limit of the proposed e-MARC system has not been explored. We will demonstrate these in the later chapters of this thesis.

3 Outage probabilities of erroneous estimates-exploiting MARC

In this chapter, we derive the outage probability of the proposed e-MARC system where all five links in the system (two SD links, two SR links and one RD link) suffer from statistically independent block Rayleigh fading. A theoretical limit of the SD link's error probability is first found by utilizing the rate-distortion and inverse capacity functions. After that, we identify the e-MARC system's admissible rate region according to the Slepian-Wolf theorem [92] for correlated source coding with a helper. Then, the outage probability of the proposed e-MARC system, independent of signaling schemes, can be theoretically derived by a fivefold-integral over the admissible rate region with respect to the pdfs of the five links' instantaneous SNRs.

This chapter is organized as follows: The outage probability for the proposed e-MARC system is theoretically derived in Section 3.1. Numerical results of the outage probabilities for the universal case and two special cases are presented in Section 3.2. Furthermore, the results of simulations are presented to evaluate the performance of the DDEX with the proposed e-MARC scheme introduced in Chapter 2 in terms of FER in Section 3.2. Also, the theoretical outage probabilities of network-coding-based MARC systems (NC-MARC) [29] and that of SDF-MARC are included in Section 3.2 for comparison. The impact of the source correlation and network correlation on the outage probability is discussed in Section 3.3. Finally, Section 3.4 concludes the chapter.

3.1 Derivation for outage probability of e-MARC

For the e-MARC system depicted in Fig. 2, the two source nodes aim to be losslessly recovered given the side information provided by the relay. Furthermore, the information sequences $\mathbf{u}_A$, $\mathbf{u}_B$ and relay sequence $\mathbf{u}_R$ are correlated. Therefore, the e-MARC system model can be viewed as correlated source coding with a helper [82, Section 10.4], where the relay helps reduce the source coding rate. In the following, we establish the admissible rate region for the e-MARC system, and define the outage event according to the region.

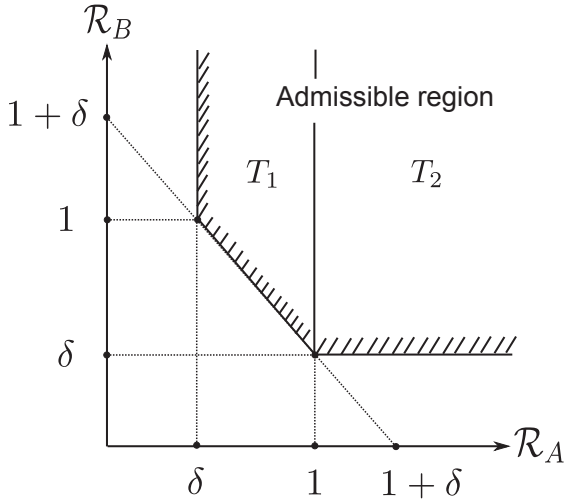

Fig 18. Admissible rate region of rate pair $(\mathcal{R}_A, \mathcal{R}_B)$ given $\mathcal{R}_R \geq I(\mathbf{u}_R; \hat{\mathbf{u}}_R)$ for lossless compression, where $\delta = H_b(p_A * p_B * p_R)$, [89] (© 2015 IEEE).

3.1.1 Outage event for each transmission cycle

The proposed e-MARC system model shown in Fig. 2 can be viewed as a system having two source nodes A and B, and one helper R. Letting $\mathcal{R}_A$ and $\mathcal{R}_B$ be the source coding rate of A and B, respectively. To investigate the admissible rate region for the two independent source nodes with one helper, we thus invoke the theorem [82, Theorem 10.4.], according to which the information sequences $\mathbf{u}_A$ and $\mathbf{u}_B$ can be successfully recovered at the destination if

$$\begin{aligned} \mathcal{R}_A &\geq H(\mathbf{u}_A|\mathbf{u}_B, \hat{\mathbf{u}}_R), \\ \mathcal{R}_B &\geq H(\mathbf{u}_B|\mathbf{u}_A, \hat{\mathbf{u}}_R), \\ \mathcal{R}_A + \mathcal{R}_B &\geq H(\mathbf{u}_A, \mathbf{u}_B|\hat{\mathbf{u}}_R), \\ \mathcal{R}_R &\geq I(\mathbf{u}_R; \hat{\mathbf{u}}_R), \end{aligned} \tag{18}$$

where $\mathcal{R}_R$ represents the source coding rate at R, and the coded side information provided by the relay R (helper) helps reduce the rate $\mathcal{R}_A$ and $\mathcal{R}_B$. Then, by using the

chain rule, (18) can be re-formulated (see Appendix 2) as follows

$$\mathcal{R}_A \geq \delta, \tag{19a}$$

$$\mathcal{R}_B \geq \delta, \tag{19b}$$

$$\mathcal{R}_A + \mathcal{R}_B \geq \delta + 1, \tag{19c}$$

$$\mathcal{R}_R \geq 1 - H_b(p_R), \tag{19d}$$

where

$$\delta = H_b(p_A * p_B * p_R). \tag{20}$$

The operation $\alpha * \beta$ is defined as $\alpha(1-\beta) + \beta(1-\alpha)$, and $H_b(\cdot)$ denotes the binary entropy function [102]. To simplify the derivation, we assume that the inequality (19d) is satisfied. With a given $\mathcal{R}_R$, the admissible rate region of $(\mathcal{R}_A, \mathcal{R}_B)$ for each transmission cycle is obtained, as shown in Fig. 18.

For a transmission cycle, the outage event is defined as: one or both of the information sequences $\mathbf{u}_A$ and $\mathbf{u}_B$ cannot be successfully recovered at the destination. Therefore, given a value of $\mathcal{R}_R$, the outage event happens when the pair $(\mathcal{R}_A, \mathcal{R}_B)$ falls outside the admissible rate region. As shown in Fig. 18, the entire admissible rate region can be divided into two parts T_1 and T_2. ε_1 and ε_2 denote the events that the rate pair $(\mathcal{R}_A, \mathcal{R}_B)$ falls into T_1 and T_2, respectively, as

$$\begin{aligned} \varepsilon_1 &= \{(\mathcal{R}_A, \mathcal{R}_B) \in T_1\} = \{\delta \leq \mathcal{R}_A \leq 1\} \wedge \{\mathcal{R}_A + \mathcal{R}_B \geq \delta + 1\} \\ \varepsilon_2 &= \{(\mathcal{R}_A, \mathcal{R}_B) \in T_2\} = \{\mathcal{R}_A \geq 1\} \wedge \{\mathcal{R}_B \geq \delta\}. \end{aligned} \tag{21}$$

where the symbols '$\vee$' and '$\wedge$' denote as the logical '*or*' and '*and*' operators, respectively. Therefore, with the assumption that (19d) is satisfied, the outage event of the e-MARC system for each transmission cycle is obtained, as

$$\text{OUT} = \overline{\{\varepsilon_1 \vee \varepsilon_2\}}. \tag{22}$$

where the $\overline{\{\varepsilon_1 \vee \varepsilon_2\}}$ denotes the complement of event $\{\varepsilon_1 \vee \varepsilon_2\}$.

According to Shannon's source-channel separation theorem, the relationship be-

tween the instantaneous SNR γ_{iD} and its corresponding source coding rate $\mathcal{R}_i$ is given by [96]

$$\mathcal{R}_i = \frac{C(\gamma_{iD})}{\mathcal{R}_{ci}} = f_{_i}(\gamma_{iD}), \qquad i \in \{A, B\} \tag{23}$$

where it is assumed that a capacity-achieving channel code is used in the iD link (see Appendix 3). Here $\mathcal{R}_{ci}$ represents the spectrum efficiency of the signaling scheme $\mathcal{E}_S(\cdot)$, including the coding rate and bit-per-symbol modulation, and $C(\alpha) = \log_2(1 + \alpha)$. It should be emphasized that the optimality of source-channel separation holds for Rayleigh fading MARC systems where all the links are orthogonal [103, 104].

Since the function $f_{_i}(\cdot)$ is one-to-one mapping, the events ε_1 and ε_2 can be, respectively, expressed as

$$\begin{aligned} \varepsilon_1 &= \{f_{_A}^{-1}(\delta) \leq \gamma_{_{AD}} \leq f_{_A}^{-1}(1)\} \wedge \{f_{_B}^{-1}(\omega) \leq \gamma_{_{BD}}\} \\ \varepsilon_2 &= \{f_{_A}^{-1}(1) \leq \gamma_{_{AD}}\} \wedge \{f_{_B}^{-1}(\delta) \leq \gamma_{_{BD}}\}, \end{aligned} \tag{24}$$

where

$$\omega = \delta + 1 - f_{_A}(\gamma_{_{AD}}). \tag{25}$$

3.1.2 Theoretical limits of p_A and p_B

The boundaries of the events ε_1 and ε_2 in (24) are involved with the iR link error probability[6] p_i, and the value of the p_i is a function of $\gamma_{_{iR}}$. However, the relationship between p_i and $\gamma_{_{iR}}$ depends on the signaling schemes employed in the iR link, as shown in Fig. 5. Furthermore, it is quite common that p_i cannot be explicitly expressed as a function of $\gamma_{_{iR}}$, if specific channel coding or modulation schemes are used. Therefore, instead, we aim to derive a theoretical limit for the value of p_i, given a $\gamma_{_{iR}}$ value in the following.

According to Shannon's lossy source-channel separation theorem [105], the infor-

[6]The length of information sequence K is assumed to be infinite for deriving the fully theoretical outage probability.

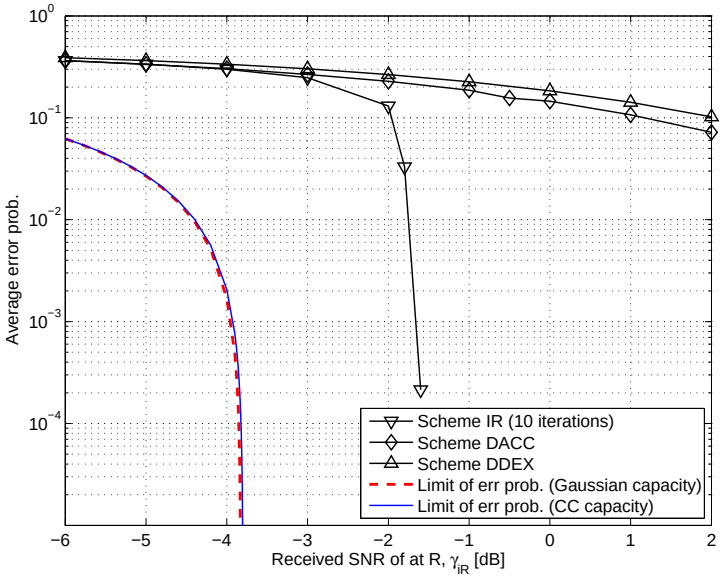

Fig 19. Theoretical limit $\hat{p}_i$ of p_i for given γ_{iR}. CC is the abbreviation of constellation constraint.

mation sequence $\mathbf{u}_i$ can be transmitted over the iR link with a distortion level $\mathfrak{D}_i$ if

$$\mathcal{R}_i(\mathfrak{D}_i)\mathcal{R}_{ci} \leq C(\gamma_{iR}), \qquad i \in \{A, B\}. \tag{26}$$

With the Hamming distortion measure, the distortion $\mathfrak{D}_i$ is equivalent to the error probability p_i, and thus according to [102], the rate-distortion function $\mathcal{R}_i(\mathfrak{D}_i)$ is represented as

$$\mathcal{R}_i(\mathfrak{D}_i) = 1 - H_b(p_i). \tag{27}$$

By assuming that a capacity-achieving channel code is applied at the iR link, the equality in (26) holds, yielding the theoretical limit $\hat{p}_i$ of p_i for any given γ_{iR}, as

$$\hat{p}_i(\gamma_{iR}) = \begin{cases} H_b^{-1}(1 - f_i(\gamma_{iR})) = \tilde{p}_i(\gamma_{iR}), & 0 \leq \gamma_{iR} < \gamma_i^* \\ 0, & \gamma_{iR} \geq \gamma_i^* \end{cases} \tag{28}$$

where $H_b^{-1}(\cdot)$ denotes the inverse function of $H_b(\cdot)$, and γ_i^* is a threshold value of the

instantaneous SNR γ_{iR} such that $f_i(\gamma_i^*) = 1$. Fig. 19 shows the result of the theoretical limit $\hat{p}_i$ of p_i derived by (28).

3.1.3 Theoretical limit of p_R

In this subsection, the assumption that the inequality (19d) holds in (24) is eliminated, such that the variation of the rate $\mathcal{R}_R$ can be taken into account when deriving the outage probability in the next subsection. In the same way as deriving (23), the relationship between the instantaneous SNR γ_{RD} and rate $\mathcal{R}_R$ can be expressed, as

$$\mathcal{R}_R = \frac{C(\gamma_{RD})}{\mathcal{R}_{cR}} = f_R(\gamma_{RD}) \geq 1 - H_b(p_R) \tag{29}$$

where $\mathcal{R}_{cR}$ represents the spectrum efficiency of the signaling scheme $\mathcal{E}_R(\cdot)$. Considering the constraint imposed on $\mathcal{R}_R$ (i.e., $\mathcal{R}_R \geq 1 - H_b(p_R)$), it is found from (29) that, although the variation range of the rate $\mathcal{R}_R$ is $[0, \infty)$, p_R is reduced to zero when the value of γ_{RD} is larger than $f_R^{-1}(1)$. Therefore, by (29), the theoretical limit $\hat{p}_R$ of p_R for any given instantaneous SNR value γ_{RD}, is

$$\hat{p}_R(\gamma_{RD}) = \begin{cases} H_b^{-1}(1 - f_R(\gamma_{RD})) = \tilde{p}_R(\gamma_{RD}), & 0 \leq \gamma_{RD} < \gamma_R^* \\ 0, & \gamma_{RD} \geq \gamma_R^*, \end{cases} \tag{30}$$

where $\gamma_R^* = f_R^{-1}(1)$.

By replacing p_i and p_R with $\hat{p}_i(\gamma_{iR})$ and $\hat{p}_R(\gamma_{RD})$ in (24), respectively, the boundaries of events ε_1 and ε_2 in (24) are converted to the domains of instantaneous SNR, as

$$\begin{aligned} \varepsilon_1 =& \{f_A^{-1}(\hat{\delta}) \leq \gamma_{AD} \leq f_A^{-1}(1)\} \wedge \{f_B^{-1}(\hat{\omega}) \leq \gamma_{BD}\} \\ \varepsilon_2 =& \{f_A^{-1}(1) \leq \gamma_{AD}\} \wedge \{f_B^{-1}(\hat{\delta}) \leq \gamma_{BD}\}, \end{aligned} \tag{31}$$

where

$$\hat{\delta} = H_b(\hat{p}_A(\gamma_{AR}) * \hat{p}_B(\gamma_{BR}) * \hat{p}_R(\gamma_{RD}))$$
$$\hat{\omega} = \hat{\delta} + 1 - f_A(\gamma_{AD}). \tag{32}$$

3.1.4 Outage probability of e-MARC

Recall that in this chapter all the links are assumed to be statistically independent and their corresponding instantaneous SNRs are Rayleigh distributed,[7] transmission-by-transmission and link-by-link. Hence, the probabilities of ε_1 and ε_2 are calculated, as

$$\begin{aligned}
\Pr(\varepsilon_1) &= \Pr\left(\{f_A^{-1}(\hat{\delta}) \le \gamma_{AD} \le f_A^{-1}(1)\} \wedge \{f_B^{-1}(\hat{\omega}) \le \gamma_{BD}\}\right) \\
&= \iiint_V \underbrace{\int_{f_A^{-1}(\hat{\delta})}^{f_A^{-1}(1)} p(\gamma_{AD})d\gamma_{AD} \int_{f_B^{-1}(\hat{\omega})}^{\infty} p(\gamma_{BD})d\gamma_{BD}}_{g_1} \cdot p(\gamma_{AR}, \gamma_{BR}, \gamma_{RD})d\gamma_{AR}d\gamma_{BR}d\gamma_{RD} \\
&= \iiint_V \underbrace{\frac{1}{\Gamma_{AD}} \int_{f_A^{-1}(\hat{\delta})}^{f_A^{-1}(1)} \exp\left(\frac{-f_B^{-1}(\hat{\omega})}{\Gamma_{BD}} - \frac{\gamma_{AD}}{\Gamma_{AD}}\right) d\gamma_{AD}}_{g_1} \cdot p(\gamma_{AR})p(\gamma_{BR})p(\gamma_{RD})d\gamma_{AR}d\gamma_{BR}d\gamma_{RD} \\
&= \Im[g_1; V]
\end{aligned} \tag{33}$$

[7] $p(\gamma_q) = \frac{1}{\Gamma_q} \exp\left(-\frac{\gamma_q}{\Gamma_q}\right), \quad q \in \{AR, BR, AD, BD, RD\}$

and

$$\begin{aligned}\Pr(\varepsilon_2) &= \Pr\left(\{f_{_A}^{-1}(1) \le \gamma_{_{AD}}\} \wedge \{f_{_B}^{-1}(\hat{\delta}) \le \gamma_{_{BD}}\}\right) \\ &= \iiint\limits_{V} \underbrace{\int_{f_{_A}^{-1}(1)}^{\infty} p(\gamma_{_{AD}})d\gamma_{_{AD}} \int_{f_{_B}^{-1}(\hat{\delta})}^{\infty} p(\gamma_{_{BD}})d\gamma_{_{BD}}}_{g_2} \cdot p(\gamma_{_{AR}}, \gamma_{_{BR}}, \gamma_{_{RD}})d\gamma_{_{AR}}d\gamma_{_{BR}}d\gamma_{_{RD}} \\ &= \iiint\limits_{V} \underbrace{\exp\left(\frac{-f_{_A}^{-1}(1)}{\Gamma_{AD}} - \frac{f_{_B}^{-1}(\hat{\delta})}{\Gamma_{BD}}\right)}_{g_2} \cdot p(\gamma_{_{AR}})p(\gamma_{_{BR}})p(\gamma_{_{RD}})d\gamma_{_{AR}}d\gamma_{_{BR}}d\gamma_{_{RD}} \\ &= \Im[g_2; V], \end{aligned} \tag{34}$$

where the domain of the threefold integral is

$$\begin{aligned} &V = \{(\gamma_{_{AR}}, \gamma_{_{BR}}, \gamma_{_{RD}}) \colon \gamma_{_{AR}} \in \mathbb{R}^+, \gamma_{_{BR}} \in \mathbb{R}^+, \gamma_{_{RD}} \in \mathbb{R}^+\}, \\ &\mathbb{R}^+ = [0, \infty). \end{aligned} \tag{35}$$

Finally, the outage probability of the e-MARC system can be obtained, as

$$P_{\text{out}} = 1 - (\Pr(\varepsilon_1) + \Pr(\varepsilon_2)). \tag{36}$$

It may be difficult to calculate the integrals shown in (33) and (34) in closed form. Hence, the results of (33) and (34) in this thesis are numerically obtained by using functions provided in [106]. Moreover, (33) and (34) can be respectively divided into eight sub-integrals according to different domains, which makes the numerical calculation of (33) and (34) tractable. The divisions of (33) and (34) are listed in Appendix 4.

3.2 Numerical results

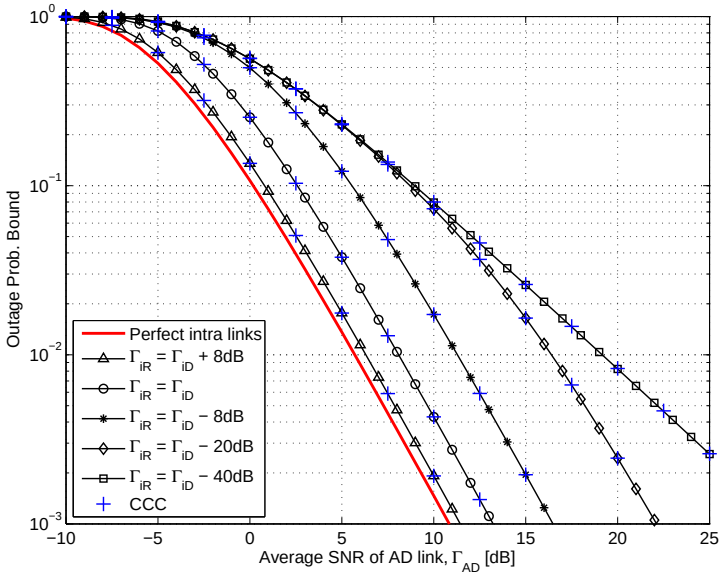

Fig 20. Outage probabilities of e-MARC that are independent of signaling schemes, where $\Gamma_{AD} = \Gamma_{BD}$ and $\Gamma_{RD} = \Gamma_{AD} + 3$ dB is assumed, and $\mathcal{R}_{ci} = \mathcal{R}_{cR} = 1/2$, [89] (© 2015 IEEE).

3.2.1 Outage probability of e-MARC

Fig. 20 shows the numerical results of the outage probability for the e-MARC system that are independent of signaling schemes, obtained by calculating from (36) with (33) and (34) shown in Section 3.1, where $\Gamma_{AD} = \Gamma_{BD}$ and $\Gamma_{RD} = \Gamma_{AD} + 3$ dB is assumed. The values of $\mathcal{R}_{ci}$ and $\mathcal{R}_{cR}$ are set to $1/2$. The curve of the probability with perfect (i.e., error-free) intra links is obtained from [91]. It is found that as the quality of the intra links degrades, the gap increases between the probabilities with perfect and imperfect intra links.

The curves of the outage probabilities with constellation constraint capacity (CCC) are also provided in Fig. 20, where the capacity function $C(\alpha) = \log_2(1+\alpha)$ is replaced with $C(\alpha) = 2J(\sqrt{4\alpha})$. Here the J function can be closely approximated by

$$J(\alpha) \approx (1 - 2^{-H_1 \alpha^{2 \cdot H_2}})^{H_3}, \tag{37}$$

where $H_1 = 0.3073$, $H_2 = 0.8935$ and $H_3 = 1.1064$ [88].

As shown in Fig. 19, the theoretical limit of p_i obtained by using CCC function is slightly different with that obtained by using Gaussian capacity function. Furthermore, as the average SNRs of the iR links increase, the probability that the instantaneous SNR is less than the threshold γ_i^* is significantly reduced. Hence, it can be observed in Fig. 20 that there is only a slight difference in the low SNR regime between the curves with Gaussian capacity and with CCC, while in the high SNR regime the curves overlap.

3.2.2 Outage performance comparisons

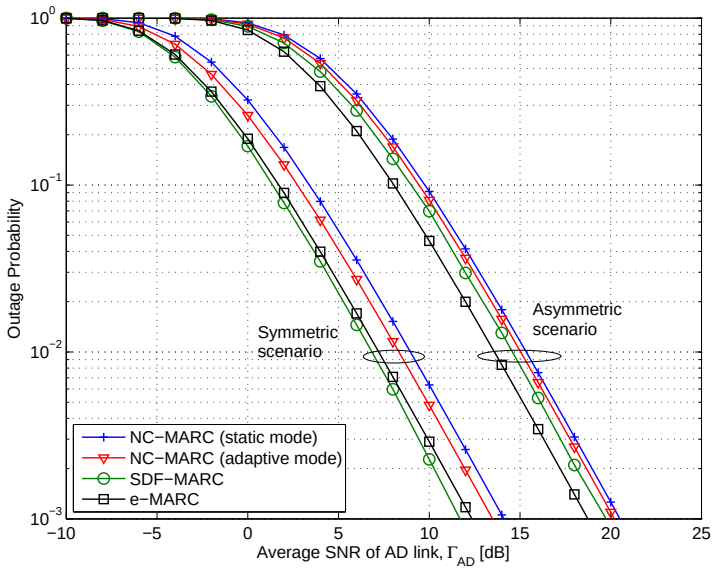

Fig 21. Outage probabilities of e-MARC in comparisons with those with NC-MARC [29], and with SDF-MARC [33]. $\mathcal{R}_{ci} = \mathcal{R}_{cR} = 1/2$**, [89] (© 2015 IEEE).**

To evaluate the impact of the utilization of the erroneous estimates received at the re-

Table 4. Relaying behavior.

System	Estimates obtained at R			
	$\widetilde{\mathbf{u}}_A = \mathbf{u}_A$ $\widetilde{\mathbf{u}}_B = \mathbf{u}_B$	$\widetilde{\mathbf{u}}_A = \mathbf{u}_A$ $\widetilde{\mathbf{u}}_B \neq \mathbf{u}_B$	$\widetilde{\mathbf{u}}_A \neq \mathbf{u}_A$ $\widetilde{\mathbf{u}}_B = \mathbf{u}_B$	$\widetilde{\mathbf{u}}_A \neq \mathbf{u}_A$ $\widetilde{\mathbf{u}}_B \neq \mathbf{u}_B$
e-MARC	$\widetilde{\mathbf{u}}_A \oplus \widetilde{\mathbf{u}}_B$	$\widetilde{\mathbf{u}}_A \oplus \widetilde{\mathbf{u}}_B$	$\widetilde{\mathbf{u}}_A \oplus \widetilde{\mathbf{u}}_B$	$\widetilde{\mathbf{u}}_A \oplus \widetilde{\mathbf{u}}_B$
NC-MARC (static mode) [29]	$\widetilde{\mathbf{u}}_A \oplus \widetilde{\mathbf{u}}_B$	silent	silent	silent
NC-MARC (adaptive mode) [29]	$\widetilde{\mathbf{u}}_A \oplus \widetilde{\mathbf{u}}_B$	$\widetilde{\mathbf{u}}_A$	$\widetilde{\mathbf{u}}_B$	silent
SDF-MARC [33]	$\widetilde{\mathbf{u}}_A \oplus \widetilde{\mathbf{u}}_B$	$\widetilde{\mathbf{u}}_A$	$\widetilde{\mathbf{u}}_B$	silent

lay, we also compare the outage probability of the e-MARC system with the theoretical outage probabilities with NC-MARC [29] and SDF-MARC [33]. Results of the outage probability analysis in the Symmetric and Asymmetric scenarios are demonstrated in Fig. 21 for comparison. The scenarios settings exemplifying the symmetric and asymmetric cases are summarized in Table 2, where X represents the average SNR of the AD link in dB; Δ and L denoting additional gain and loss due to the shorter and longer distance, respectively, and are set to 3 dB and 10 dB in this subsection.

NC-MARC is a special case of the SDF-MARC system where a maximal ratio combining (MRC) technique is used at the destination. Furthermore, according to [29], the NC-MARC system is able to operate in static and adaptive modes. In the static mode, the relay forwards the sequence only when both the estimates sent from the two sources are decoded correctly at the relay. On the other hand, in the adaptive mode, except for the case that the estimates sent from the two sources are decoded correctly, the relay also forwards the correct estimate if only one source node is correctly decoded at the relay. The relaying behaviors of e-MARC, SDF-MARC and NC-MARC are summarized in Table 4.

The theoretical outage probabilities of NC-MARC, analyzed in a SNCC framework, were included in Fig. 21. The outage probabilities[8] in static and adaptive modes are obtained by [29, eqs. (4)-(5)] and [29, eqs. (4),(8)-(9),(11)], respectively. It is found that the e-MARC system outperforms NC-MARC in terms of outage performance.

In principle, as stated in [33], a header (i.e., flag) is used at the relay in SDF-MARC to identify the correctly decoded source nodes, and furthermore, the header has to be protected with a very powerful error correction code. On the contrary, the relay in e-MARC always performs network-coding and does not add a header to the forwarded XOR-ed sequence. Therefore, it is not reasonable to make comparisons between SDF-MARC and e-MARC, because SDF-MARC and e-MARC belong to different categories of MARC (i.e., SDF-MARC is "address-based", while e-MARC is

[8]The probabilities are computed at a system level [29].

"non-address-based").

To the best of our knowledge, there is no explicit mathematical expression to calculate the theoretical outage probability of SDF-MARC. Nevertheless, it is still meaningful to include SDF-MARC performance curves as a reference. The performance results with SDF-MARC, shown in Fig. 21, are all based on the Monte-Carlo method according to [33, eqs. (4)-(6)] with a modification of [101, eq. (12)], while all the curves for e-MARC are the theoretical results.

Deriving an explicit mathematical expression of the outage probability with SDF-MARC is an open future problem and out of the scope of this thesis; hence, we emphasize again that the conclusions for the superiority/inferiority of e-MARC related to SDF-MARC in the Asymmetric/Symmetric scenarios are based on simulations[9]. Rigorous mathematical analysis for the results shown in Fig. 21 are left as future study.

3.2.3 Special cases

Static intra links

In the case that intra links are static (not suffering from fading), AR and BR links can be modeled as BSCs with constant crossover probabilities p_A and p_B, respectively. This scenario may be exemplified by sensor networks where only the destination moves. In that case, averaging the AR and BR intra link variations over their pdfs can be eliminated from (33) and (34). Accordingly, the derivations of $\Pr(\varepsilon_1)$ and $\Pr(\varepsilon_2)$ can be reduced to

$$\Pr(\varepsilon_1) = \frac{1}{\Gamma_{AD}} \int_0^{\infty} \int_{f_A^{-1}(\ddot{\delta})}^{f_A^{-1}(1)} \exp\left(\frac{-f_B^{-1}(\ddot{\omega})}{\Gamma_{BD}} - \frac{\gamma_{AD}}{\Gamma_{AD}} \right) d\gamma_{AD} p(\gamma_{RD}) d\gamma_{RD}$$

$$\Pr(\varepsilon_2) = \int_0^{\infty} \exp\left(\frac{-f_A^{-1}(1)}{\Gamma_{AD}} - \frac{f_B^{-1}(\ddot{\delta})}{\Gamma_{BD}} \right) p(\gamma_{RD}) d\gamma_{RD}, \tag{38}$$

[9]Text-based explanation for the superiority/inferiority of e-MARC related to SDF-MARC in the Asymmetric/Symmetric scenarios is provided in Appendix 5

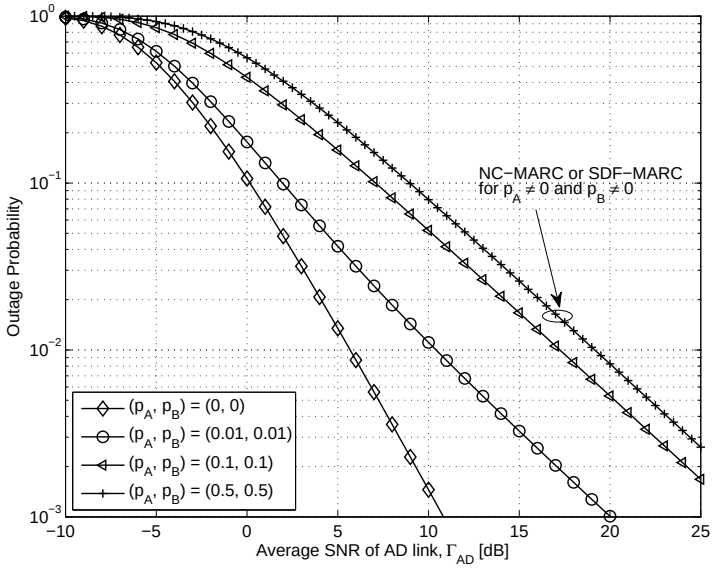

Fig 22. Theoretical outage probabilities of e-MARC with static intra links, where $\Gamma_{AD} = \Gamma_{BD}$ and $\Gamma_{RD} = \Gamma_{AD} + 3$ dB. $\mathcal{R}_{ci} = \mathcal{R}_{cR} = 1/2$, [89] (© 2015 IEEE).

where

$$\ddot{\delta} = H_b(p_A * p_B * \hat{p}_R(\gamma_{RD}))$$
$$\ddot{\omega} = \ddot{\delta} + 1 - f_A(\gamma_{AD}). \tag{39}$$

The results of the theoretical outage probabilities calculated in this special case are shown in Fig. 22. It can be clearly observed in Fig. 22 that the outage probability achieves second-order diversity when $p_A = p_B = 0$, and matches the probability curve with perfect intra links in Fig. 20. When both intra links are imperfect but with relatively small crossover probabilities (e.g. when $p_A = p_B = 0.01$), it is found that the decay of the outage probability follows the second order diversity in the low Γ_{iD} regime. However, the diversity order asymptotically converges to the first order as Γ_{iD} increases. It should be noticed that for the case that $p_A \neq 0$ and $p_B \neq 0$, the relay remains silent with SDF-MARC or NC-MARC; however, with e-MARC, the erroneous estimates forwarded from the relay still contribute to reducing the outage probability.

In the case that one of the intra links is perfect but the other one is imperfect, the helper's contribution, provided by the relay, depends on the quality of the imperfect

link. This is because in (19a)-(19d) provided in Section 3.1, the value of $p_A * p_B$ is a dominating factor that determines the size of the admissible rate region of $(\mathcal{R}_A, \mathcal{R}_B)$. Hence, p_A dominates the value of $p_A * p_B$ if $p_B = 0$, and vice versa.

DDEX strategy with e-MARC

The derivation for the outage probability of the e-MARC system shown in Section 3.1 can further be used to evaluate the efficiency of the DDEX strategy with the proposed e-MARC scheme [85] where the erroneous estimates are also utilized. As mentioned in Chapter 2, with using DDEX, the information sequences $\mathbf{u}_i$ for $i \in \{A, B\}$ are first encoded using RSC codes, and then broadcasted from the source nodes using binary differential phase-shift keying (DPSK) modulation.[10] To achieve low computational complexity and a small degree of latency, instead of performing fully-iterative decoding between the decoders of the ACC and RSC code, the relay R obtains the estimates $\widetilde{\mathbf{u}}_i$ of $\mathbf{u}_i$ by employing the DDEX detection strategy, where the relay simply extracts the systematic part output from the differential detector. The estimates $\widetilde{\mathbf{u}}_i$ for $i \in \{A, B\}$ are detected in error with a high probability because no error correction is performed at R, in exchange for saving battery and memory resources due to low computational complexity. The obtained estimates are XOR-coded at R and forwarded to the destination D for improving the FER performance.

As shown in [85], DPSK modulation and differential detection are used at the source node and relay, respectively, and hence according to [107], the error probability of the *extracted* estimates of the information sequence is expressed as

$$p_i(\gamma_{iR}) = \frac{1}{2}\exp(-\gamma_{iR}), \qquad i \in \{A, B\}. \tag{40}$$

The theoretical outage probability (i.e., the theoretical achievable FER performance) for the DDEX with the proposed e-MARC scheme is obtained by replacing (28) with (40) in (36). Results of outage probabilities in the Symmetric and Asymmetric scenarios are demonstrated in Fig. 23 for comparison. The settings of both scenarios are same as those in Section 3.2.2.

In the Symmetric scenario, as shown in Fig. 23, the outage probability of the DDEX e-MARC scheme is roughly 3.5 dB away from the outage probability of e-MARC that is independent of the signaling scheme. The gap is due to the relatively high p_i value

[10]The ACC followed by coherent PSK is equivalent to DPSK.

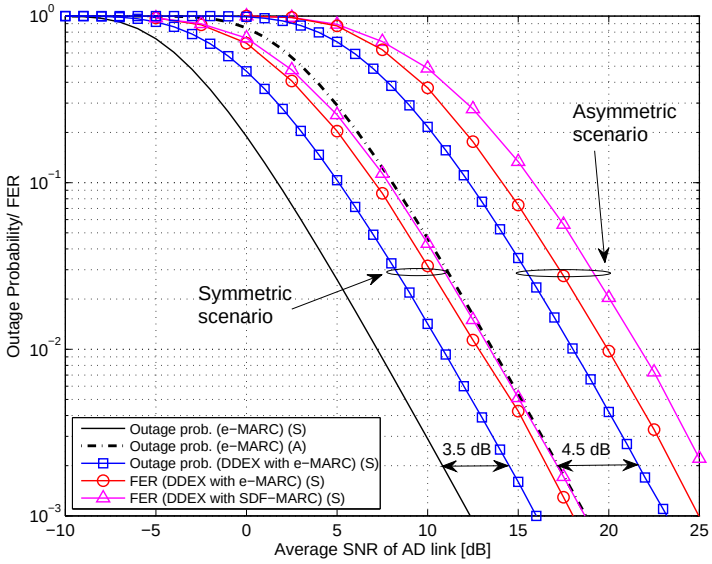

Fig 23. Theoretical outage probabilities of DDEX with e-MARC system. Notations (S) and (A) denote the Symmetric and Asymmetric scenarios listed in Table 2, respectively, [89] (© 2015 IEEE).

with the DDEX strategy. In the Asymmetric scenario, the gap is further increased by 1 dB, resulting in a 4.5-dB gap from the outage probability of e-MARC. However, a large number of addition, multiplication and comparison operations can be eliminated on obtaining the estimates $\widetilde{\mathbf{u}}_i$, according to [108, Section 4.1].

The FER performance results of the DDEX e-MARC scheme obtained through simulations are also included in Fig. 23. Here FER is defined as follows: the number of the transmission cycles where either one or both of the information sequences sent from the nodes A and B cannot successfully recovered at D even with the help of R, divided by the total number of transmission cycles. The parameters used in the simulations are summarized in Tables 2 and 3. It is found from Fig. 23 that both in the Symmetric and Asymmetric scenarios, there is a roughly 1.8-dB loss with the practical FER performance from the corresponding theoretical outage probabilities. The loss is because the theoretical outage probabilities are derived assuming the use of capacity-achieving codes in the iD and RD links.

3.3 Impact of correlation

In some scenarios, for example in WSNs, an object could be observed by several source nodes, which causes the correlation among the observations of these nodes. Hence, in this subsection, we further extended our analysis to the e-MARC system where the correlation between two source nodes is taken into account. The correlation of source nodes is modeled by random bit-flipping with the flipping probability $p_s = \mathfrak{B}(\mathbf{u}_A, \mathbf{u}_B)$. The admissible rate region for the e-MARC system with the correlation p_s between source nodes is analyzed in (67) in Appendix 2. To investigate the impact of the source correlation p_s and the network correlation $p_{nc} = p_A * p_B = \mathfrak{B}(\mathbf{u}_R, \mathbf{u}_\oplus)$, three extreme scenarios: $(\Gamma_{AD}, \Gamma_{BD}, p_R) = (30$ dB, -30 dB, $0)$, $(30$ dB, -30 dB, $0.5)$ and (-30 dB, -30 dB, $0.5)$ are investigated, respectively. The values of $\mathcal{R}_{ci}$ and $\mathcal{R}_{cR}$ are set to $1/2$.

3.3.1 Source correlation p_s

We first focus on the impact of source correlation p_s on the e-MARC outage probability. For the scenarios $(\Gamma_{AD}, \Gamma_{BD}, p_R) = (30$ dB, -30 dB, $0)$ and $(30$ dB, -30 dB, $0.5)$, the soft channel values of the received signal vector $\mathbf{y}_{AD}$ are reliable while the values of $\mathbf{y}_{BD}$ are unreliable at the destination D. Even in this case, the information sequence $\mathbf{u}_B$ can still be recovered with a high probability if two source nodes are highly correlated. This is because when $\mathbf{u}_A$ and $\mathbf{u}_B$ are highly correlated, reliable $a\ priori$ information for the recovery of $\mathbf{u}_B$ can be directly acquired from $extrinsic$ information related to $\mathbf{u}_A$ during the decoding process. Hence, it can be concluded that, with or without the relay, when at least one of the direct links is reliable and the two source nodes are highly correlated, a very low probability can be achieved. This situation is demonstrated in Figs. 24(a) and 24(b), where the probability is shown as a function of p_s and p_{nc}.

3.3.2 Network correlation p_{nc}

Next, let us focus on the impact of the network correlation p_{nc}. Assuming $\mathbf{u}_A$ and $\mathbf{u}_B$ are uncorrelated, but $\mathbf{u}_R$ and $\mathbf{u}_\oplus$ are fully correlated (i.e., $\mathbf{u}_R = \mathbf{u}_\oplus$ and $p_{nc} = 0$). For the scenario $(\Gamma_{AD}, \Gamma_{BD}, p_R) = (30$ dB, -30 dB, $0)$, the soft channel values of $\mathbf{y}_{AD}$ and $\mathbf{y}_{RD}$ at the destination are reliable while the values of $\mathbf{y}_{BD}$ are unreliable. In this scenario, $\mathbf{u}_A$ and $\mathbf{u}_R$ can be recovered with a high probability after the decoding of $\mathbf{y}_{AD}$ and $\mathbf{y}_{RD}$, respectively. $\mathbf{u}_B$ can also be recovered with the aid of reliable $a\ priori$

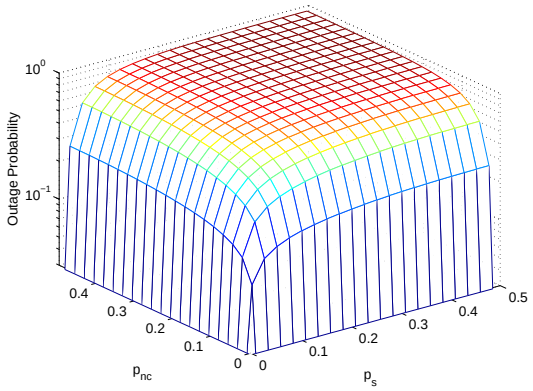

(a) Γ_{AD} = 30 dB, Γ_{BD} = -30 dB, $p_R = 0$

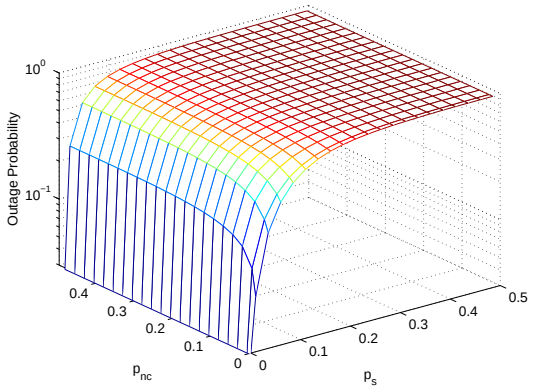

(b) Γ_{AD} = 30 dB, Γ_{BD} = -30 dB, $p_R = 0.5$

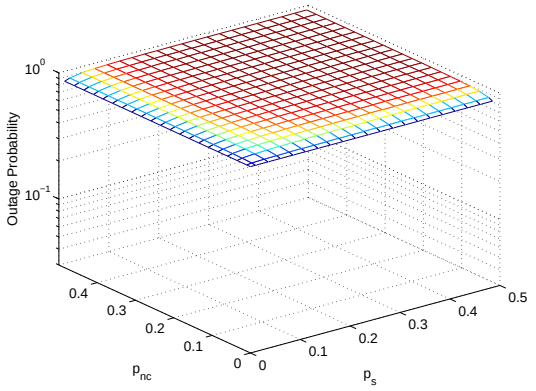

(c) Γ_{AD} = -30 dB, Γ_{BD} = -30 dB, $p_R = 0$

Fig 24. Impacts of source correlation p_s and network correlation p_{nc} on outage probability of e-MARC. Here $\mathcal{R}_{ci} = \mathcal{R}_{cR} = 1/2$, [89] (© 2015 IEEE).

information using boxplus operation [99] on both $extrinsic$ information corresponded to $\mathbf{u}_A$ and $\mathbf{u}_R$. However, for the scenario $(\Gamma_{AD}, \Gamma_{BD}, p_R) =$ (-30 dB, -30 dB, 0) with the same assumption, only the soft channel values of $\mathbf{y}_{RD}$ are reliable, and thus the recoveries of $\mathbf{u}_A$ and $\mathbf{u}_B$ require $apriori$ information output from the boxplus operation. Nevertheless, the $extrinsic$ information related to $\mathbf{u}_A$ and $\mathbf{u}_B$ is unreliable with high probabilities, and hence, the output from the boxplus operation is still unreliable for the decoding of $\mathbf{y}_{iD}$ for $i \in \{A, B\}$. Therefore, as shown in Fig. 24(c), the value of the probability cannot be reduced to a very small value, although both intra links and the RD link are perfect (i.e., $p_A = p_B = p_R = 0$).

3.4 Conclusion

We have derived the outage probability for the e-MARC system. The theoretical outage probabilities of NC-MARC [29] and SDF-MARC [33] were also included for comparison in the Symmetric/Asymmetric scenarios listed in Table 2. It has been observed through simulations that the outage probability of NC-MARC is inferior to that of e-MARC. Moreover, it has been found through simulations that in the Asymmetric scenario where one of the source nodes is far away from both the relay and the destination, e-MARC performs better than SDF-MARC. However, in the Symmetric scenario, e-MARC is inferior to SDF-MARC.

We have further applied the derivation process of the outage probabilities to two special cases: 1) static intra links and 2) the DDEX with the proposed e-MARC scheme. According to the numerical results shown in case 1), we verified that erroneous estimates received at the relay are useful for the recovery of the information sequences at the destination. To evaluate the DDEX with the proposed e-MARC scheme, comparisons are provided between the e-MARC outage probability and the outage probability of the DDEX with e-MARC in case 2). It was found that a 3.5 to 4.5-dB loss occurs in exchange for a significant reduction in computational complexity. Finally, we recognized that for the case where two source nodes are highly correlated, the source correlation can be exploited to improve the e-MARC outage performance as long as one of the direct links is reliable. However, the RD link and at least one of the direct links have to be reliable for the exploitation of the network correlation p_{nc}.

4 Joint adaptive network-channel coding

This chapter aims to further improve our previously proposed e-MARC scheme in Chapter 2. The system model described in Chapter 2 is first generalized with an arbitrary number of source nodes. We then propose a novel joint adaptive network-channel coding (JANCC) technique to avoid unnecessary erroneous estimates being network-coded at the relay. In the proposed JANCC technique, after completing the decoding of all the information sequences transmitted from the source nodes, the destination constructs a vector identifying the indices of the incorrectly decoded source nodes. The identifier vector is then sent to the relay via a feedback channel to request a re-transmission. Upon receiving the request, the relay performs network-coding by taking the XOR-operation *only* over its received estimates of the information sequences specified by the identifier vector. The decoding of JANCC is performed at the destination, where the knowledge of network correlation p_{nc} is directly estimated by using the proposed algorithm and effectively utilized in the decoding process.

This chapter is organized as follows. Section 4.1 introduces the system model. A detailed description of the proposed JANCC and its corresponding decoding techniques are presented in Section 4.2. Section 4.3 presents simulation results to demonstrate the performance of JANCC-aided e-MARC, in terms of average FER and the computational complexity. The average goodput evaluation results are also provided in Section 4.3. Finally, Section 4.4 concludes this chapter.

4.1 System model

Fig. 25 shows a block diagram of the generalized e-MARC scheme assumed in this chapter, where there are N source nodes, one common relay node R, and one common destination node D. Each node is equipped with a single antenna, and R is assumed to be connected to D via a half-duplex link. As shown in Fig. 25, each source node S_i, $i = 1, 2, ..., N$ generates its binary and CRC encoded information sequence $\mathbf{u}_i = \{u_i(k)\}_{k=1}^{K}$. All the information sequences are assumed to be statistically independent.

Each sequence $\mathbf{u}_i$ is interleaved and encoded by an SCCC where the SCCC is composed of a rate-K/M RSC encoder C_S and rate-1 ACC. The corresponding coded bit sequence $\mathbf{x}_i = \{x_i(m)\}_{m=1}^{M}$ is modulated by BPSK and broadcasted to R and D at the each source node's dedicated independent time slot.

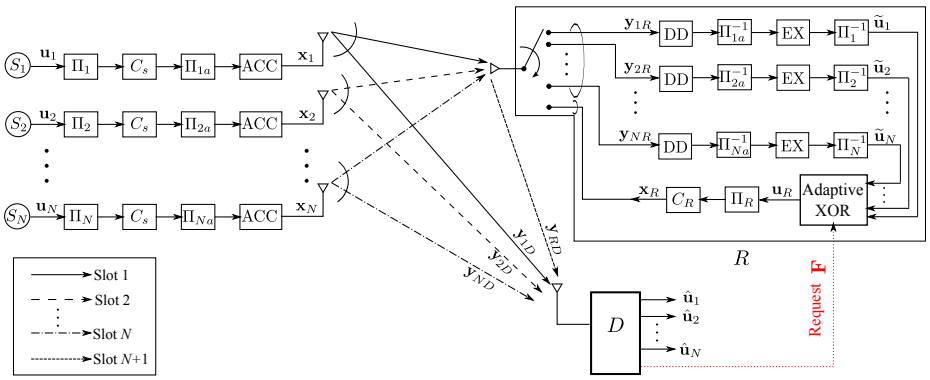

Fig 25. Orthogonal Multiple Access Relay Channel model with N source nodes combined with ARQ, [94] (© 2014 IEEE).

Without loss of generality, all transmitted signals have unit power. All the links are assumed to suffer from block Rayleigh fading, and thus the signal vectors received at R and D are

$$\begin{aligned} \mathbf{y}_{iR} &= h_{iR} \cdot \mathbf{x}_i + \mathbf{n}_{iR} \\ \mathbf{y}_{iD} &= h_{iD} \cdot \mathbf{x}_i + \mathbf{n}_{iD} \end{aligned} \tag{41}$$

with $i = 1, 2, ..., N$, where h_{iR} and h_{iD} indicate the channel coefficients of SR and SD links with the source node S_i. $\mathbf{n}_{iR}$ and $\mathbf{n}_{iD}$ indicate the vectors of the independent zero-mean complex AWGN at R and D with the source node S_i, respectively, with variance $\sigma_{iR}^2 = \sigma_{iD}^2 = \sigma^2$ per dimension. Block Rayleigh fading is assumed with which h_{iR} and h_{iD}, and assumed to be constant over one coded sequence, but to vary independently transmission-by-transmission and link-by-link.

Unlike the previously proposed e-MARC scheme, the re-transmission technique is utilized in the new system model shown in Fig. 25. Hence, the forwarding behavior of the relay R depends on the decoding status of the destination D. If the destination D identifies that all the users' information sequences are successfully decoded by the CRC error detection, acknowledgement (ACK) is broadcasted back to the source nodes and relay, and the source nodes broadcast their following information sequences in their dedicated time slots. Otherwise D sends to the relay R a redundancy re-transmission request via the feedback channel,[11] and once receiving the re-transmission request, the

[11]The feedback channel is assumed to be error-free. This assumption is reasonable because the re-

relay R transmits BPSK-modulated symbol sequence $\mathbf{x}_R = \{x_R(m)\}_{m=1}^{M}$ to the destination D via RD link, as

$$\mathbf{y}_{RD} = h_{RD} \cdot \mathbf{x}_R + \mathbf{n}_{RD} \tag{42}$$

where h_{RD} and $\mathbf{n}_{RD}$ indicate the channel coefficient and AWGN vector of the RD link with variance $\sigma_{RD}^2 = \sigma^2$, respectively. In this chapter, it is assumed that $E[|h_{iR}|^2] = E[|h_{iD}|^2] = E[|h_{RD}|^2] = 1$, with $i = 1, 2, ..., N$. The instantaneous SNR γ_{iR}, γ_{iD} and γ_{RD} of the links are then given by

$$\begin{aligned} \gamma_{iR} &= |h_{iR}|^2 \cdot \Gamma_{iR} \\ \gamma_{iD} &= |h_{iD}|^2 \cdot \Gamma_{iD} \\ \gamma_{RD} &= |h_{RD}|^2 \cdot \Gamma_{RD} \end{aligned} \tag{43}$$

where Γ_{iR} and Γ_{iD} represent the average SNRs of the SR and SD links connected to the source node S_i, respectively. Γ_{RD} is the average SNR of the RD link.

Instead of performing the iterative decoding of the SCCC, the relay R utilizes very simple DDEX strategy to detect the received signal vector $\mathbf{y}_{iR}$ transmitted from the source node S_i. The aim of utilizing DDEX has been addressed.

With the process for estimating the information sequences at the relay R, it is highly probable that the sequences $\widetilde{\mathbf{u}}_i$ obtained at R contain errors by using DDEX detection strategy because the decoding of C_S is not performed. The average FER performance of the SR link with using DDEX and with performing the iterative decoding of the SCCC were evaluated by [109], respectively. It can be observed in Fig. 26 that when R performs the iterative decoding of the SCCC, the FER performance of the SR link is very close to the outage probability, however, it is about 12 dB away from the outage when using the DDEX strategy although the decoding complexity of the SCCC is eliminated.

4.2 Proposed techniques

The drawback of the DDEX detection strategy is that the estimates of the information sequences $\widetilde{\mathbf{u}}_i$ obtained at R contain errors with a high probability. Therefore, a JANCC

transmission request can be represented by N bits, as detailed in Section 4.2, which is protected by using a powerful channel coding.

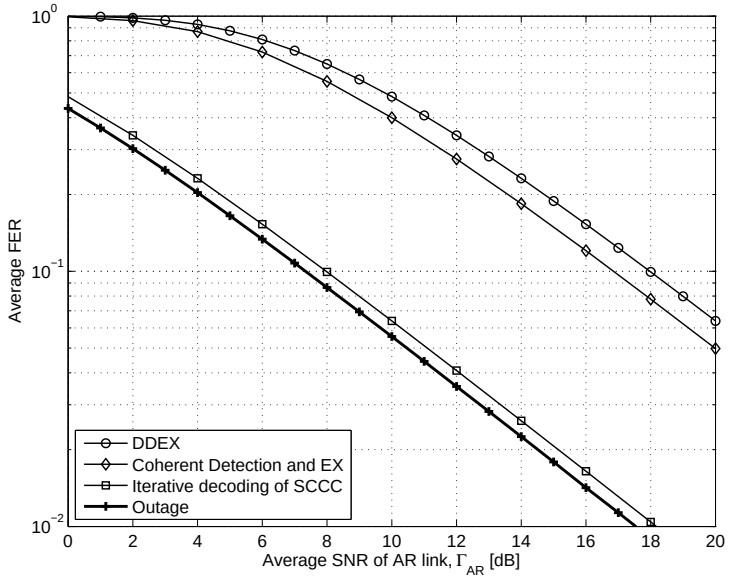

Fig 26. Average FER of iterative decoding, DDEX, and coherent detection with EX.

and its corresponding decoding techniques are proposed here, where the erroneous estimates obtained at R after the DDEX strategy are further efficiently exploited to help recover the information sequences decoded in error at D.

4.2.1 JANCC

The received signal vector $\mathbf{y}_{iD} = \{y_{iD}(m)\}_{m=1}^{M}$ of the ith slot at D is demodulated to the corresponding soft channel values $L(\mathbf{y}_{iD}|\mathbf{x}_i) = \{L(y_{iD}(m)|x_i(m))\}_{m=1}^{M}$ by (9). The values $L(\mathbf{y}_{iD}|\mathbf{x}_i)$ for the ith slot, are iteratively decoded by the decoder of SCCC with the log-MAP [108] algorithm at the destination D. The estimated sequence $\hat{\mathbf{u}}_i$ of $\mathbf{u}_i$ is obtained by making a binary hard decision on the $a\ posteriori$ LLR $\{L(u_i(k)|\mathbf{y}_{iD})\}_{k=1}^{K}$ output from the decoder of C_S, when no relevant increase in LLR is obtained by the iterations.

The sequences $\hat{\mathbf{u}}_i$ are CRC decoded for error detection after completing the iterative decoding of the SCCC, and the decoding results for each user are stored in an N-bit

identifier vector $\mathbf{F} = \{f(i)\}_{i=1}^{N}$, where

$$f(i) = \begin{cases} 0, & \hat{\mathbf{u}}_i = \mathbf{u}_i \\ 1, & \hat{\mathbf{u}}_i \neq \mathbf{u}_i \end{cases} \tag{44}$$

and a set $\mathcal{F}$ is defined as

$$\mathcal{F} = \{i : f(i) = 1\}. \tag{45}$$

If $\mathcal{F} \neq \phi$, the destination D sends to the relay R a redundancy-retransmission request with the vector $\mathbf{F}$ via the feedback channel and attempts to recover the information sequences decoded in error with additional redundancy forwarded from R.

As shown in Fig. 25, upon receiving the re-transmission request, the relay R performs network-coding by taking a sequence-by-sequence XOR-operation, notated as $\bigoplus$, only over the received estimates of the information sequences specified by $\mathbf{F}$, not over all the estimates as e-MARC, although the specified estimates may contain errors, as

$$\mathbf{u}_R = \bigoplus_{\forall_j \in \mathcal{F}} \widetilde{\mathbf{u}}_j. \tag{46}$$

The relay node R then re-encodes the interleaved version of the network-coded bit sequence $\mathbf{u}_R = \{u_R(k)\}_{k=1}^{K}$ by using a rate-K/M RSC encoder C_R, and finally, the corresponding symbol sequence $\mathbf{x}_R = \{x_R(m)\}_{m=1}^{M}$ is forwarded to D using BPSK modulation as additional redundancy.

4.2.2 Decoding scheme and algorithm of JANCC

Fig. 27 shows a factor graph representation of the proposed JANCC decoding scheme, where C_S^{-1} and C_R^{-1}, respectively, indicate the RSC decoders corresponding to C_S and C_R used in the source nodes and relay R. The notations L_a and L_e shown in Fig. 27 denote $a\ priori$ and $extrinsic$ LLR of their argument variables, respectively. Once D receives additional redundancy forwarded from R, the decoding of JANCC is initiated to recover the information sequences decoded in error at D via the SD links.

As shown in Fig. 27, the LLR-updating function $f_c(\cdot)$ is utilized in the proposed JANCC decoding scheme with the knowledge of the network correlation p_{nc}, where

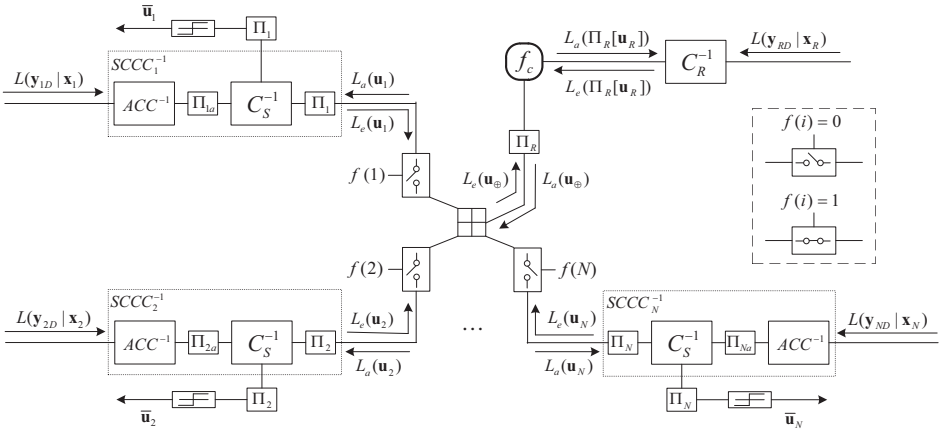

Fig 27. Proposed JANCC decoding scheme represented by a factor graph, where ACC^{-1} and $SCCC_i^{-1}$ denote the ACC decoder and the decoder of the SCCC applied by S_i, respectively, [94] (© 2014 IEEE).

p_{nc} is defined as

$$p_{nc} = \frac{\sum_{k=1}^{K} |u_R(k) - u_\oplus(k)|}{K} \tag{47}$$

where the sequence $\mathbf{u}_\oplus$ is generated by the source nodes specified by $\mathbf{F}$ as

$$\mathbf{u}_\oplus = \bigoplus_{\forall_j \in \mathcal{F}} \mathbf{u}_j. \tag{48}$$

Knowledge of correlation p_{nc} is exploited during the JANCC decoding process in the LLR-updating function $f_c(\cdot)$ to avoid error propagation if one/some of the sequences $\widetilde{\mathbf{u}}_j$ obtained at R is/are erroneous. It should be emphasized that correlation p_{nc} can be directly estimated at D without having to involve any higher layer protocols, as [96, Eq. (9)]

$$
\begin{aligned}
\hat{p}_{nc} &= G(L_e(\Pi_R[\mathbf{u}_{\oplus}]),\, L_e(\Pi_R[\mathbf{u}_R]),\, \mathcal{G}) \\
&= G(L_e(\mathbf{u}_{\oplus}),\, L_e(\mathbf{u}_R),\, \mathcal{G}) \\
&= \frac{1}{|\mathcal{G}|} \sum_{\forall_g \in \mathcal{G}} \Pr(u_{\oplus}(g) = 1) \Pr(u_R(g) = 0) + \Pr(u_{\oplus}(g) = 0) \Pr(u_R(g) = 1) \\
&= \frac{1}{|\mathcal{G}|} \sum_{\forall_g \in \mathcal{G}} \frac{e^{L_e(u_{\oplus}(g))}}{\left(1 + e^{L_e(u_{\oplus}(g))}\right)} \frac{1}{\left(1 + e^{L_e(u_R(g))}\right)} + \frac{1}{\left(1 + e^{L_e(u_{\oplus}(g))}\right)} \frac{e^{L_e(u_R(g))}}{\left(1 + e^{L_e(u_R(g))}\right)} \\
&= \frac{1}{|\mathcal{G}|} \sum_{\forall_g \in \mathcal{G}} \frac{e^{L_e(u_{\oplus}(g))} + e^{L_e(u_R(g))}}{\left(1 + e^{L_e(u_{\oplus}(g))}\right)\left(1 + e^{L_e(u_R(g))}\right)}
\end{aligned} \tag{49}
$$

where $\hat{p}_{nc}$ is the estimated value of the probability p_{nc}, and the set $\mathcal{G}$ is defined as

$$
\mathcal{G} = \{g : |L_e(u_{\oplus}(g))| \geq T\} \tag{50}
$$

with T representing a threshold value. However, since the SD links suffer from block fading, we modified [96, eq. (9)]. **Algorithm 1** summarizes the JANCC decoding process.

The out-most "for-loop" in **Algorithm 1** is mainly to exchange the $extrinsic$ information between the decoders C_R^{-1} and $SCCC_j^{-1}$ specified by the identifier $\mathcal{F}$. To achieve a precise estimation of p_{nc}, we refer to [96] to introduce a threshold value T to eliminate some unreliable positions of the sequence $L_e(\mathbf{u}_{\oplus})$. However, unlike the assumption of the AWGN channels in [96], all the links here are assumed to suffer from block fading. Therefore, in the second out-most "for-loop", the value of T decreases (i.e., $T - \epsilon$, where $\epsilon = 0.05$ in this chapter) during every iterative operation of the loop until a sufficiently large number of $L_e(u_{\oplus}(g))$ in the sequence $L_e(\mathbf{u}_{\oplus})$ is guaranteed (three-quarters of the entire sequence-length at least in this chapter). The sequence $L_e(\mathbf{u}_{\oplus})$ will not be punctured if the value of T has already decreased at most n times ($n = 10$ in this chapter).

When the second out-most "for-loop" is completed, the estimation of correlation p_{nc} is performed using (49) where the $extrinsic$ information produced by the decoder C_R^{-1} is utilized. The intermediate $a\ priori$ LLR sequence $L_a(\mathbf{u}_{\oplus})$ is then produced using the LLR-updating function $f_c(\cdot)$. In the following "for-loop", the $a\ priori$ information to be provided to each specified decoder $SCCC_j^{-1}$ is calculated by performing a boxplus operation with the updated intermediate $a\ priori$ information, and the iter-

Algorithm 1: Decoding process of JANCC

Pre-defined: iterations I, interval ϵ, ratio ρ, threshold $T^{(0)}$, times n
Input: $L_e(\mathbf{u}_j),\ \forall_j \in \mathcal{F}$
Initialization: $\hat{p}_{nc} = 0.25$
for 1 **to** I **do**
  $L_e(\mathbf{u}_\oplus) = \sum_{\forall_j \in \mathcal{F}} \boxplus L_e(\mathbf{u}_j)$;
  for $l = 1$ **to** n **do**
    Find $\forall_q$ such that $|L_e(u_\oplus(q))| > T^{(l-1)}$;
    Store $\forall_q$ to set $\mathcal{Q}$;
    if $|\mathcal{Q}| \geq \rho \cdot \#L_e(\mathbf{u}_\oplus)$ **then**
      Exit **for**;
    end
    $T^{(l)} = T^{(l-1)} - \epsilon$;
    if $T^{(l)} \leq 0$ **then**
      Store all the indices of $L_e(\mathbf{u}_\oplus)$ to set $\mathcal{Q}$;
      Exit **for**;
    end
  end
  $L_a(\Pi_R[\mathbf{u}_R]) = f_c\left(L_e(\Pi_R[\mathbf{u}_\oplus]), \hat{p}_{nc}\right)$;
  Calculate $L_e(\Pi_R[\mathbf{u}_R])$ by C_R^{-1};
  $\hat{p}_{nc} = G(L_e(\Pi_R[\mathbf{u}_\oplus]),\ L_e(\Pi_R[\mathbf{u}_R]),\ \mathcal{Q})$;
  $L_a(\mathbf{u}_\oplus) = \Pi_R^{-1}[f_c\left(L_e(\Pi_R[\mathbf{u}_R]), \hat{p}_{nc}\right)]$;
  for *all* $j \in \mathcal{F}$ **do**
    Calculate $L_a(\mathbf{u}_j)$ by boxplus operation;
    Feed $L_a(\mathbf{u}_j)$ to $SCCC_j^{-1}$;
    Calculate $L_e(\mathbf{u}_j)$ by $SCCC_j^{-1}$ with I iterations;
  end
end
Calculate $\bar{\mathbf{u}}_j,\ \forall_j \in \mathcal{F}$;

ative decoding process is performed in each specified $SCCC_j^{-1}$ utilizing the updated $a\ priori$ information.

4.3 Numerical results

Table 5. Parameters used in simulations.

Variable	Value
Length of information sequence K	1024 bits
C_S	$(1, 5/7)_8$
C_R	$(1, 5/7)_8$
Code rate (K/M)	1/2
Decoding algorithm	log-MAP
Interval ϵ	0.05
Ratio ρ	3/4
Threshold $T^{(0)}$	3
Global iteration (GI) I	1
Local iteration (LI)	10
Loops between GI and LI	10
Interleavers	Random
Γ_{RD}	20 dB

Here, we provide the results of the simulations conducted to evaluate the JANCC-aided e-MARC scheme. The number of the re-transmission is a parameter and is set at 1 in the simulations, and the other parameters assumed in the simulations are summarized in TABLE 5. The text-based procedure of the decoding process can be referred in Section 2.4.

We use the e-MARC scheme with the DDEX strategy as an example. Furthermore, two other alternative orthogonal MARC systems are also provided in the simulations for comparison. One is the SDF-MARC scheme with the IR strategy, and the other is the SDF-MARC scheme with DDEX. The outage probability of the SDF-MARC system is numerically calculated using Monte Carlo methods, where we generated a sufficient number of random fading coefficients (h_{iR}, h_{iD} and h_{RD}) and measured the probability that the conditions provided in [33, Eqs. (4)-(6)] are not satisfied.

The structure for the three MARC systems are assumed to be symmetric in geometric gain where all the SR links have the same average SNR (Γ_{iR} = constant $\forall_i$) and all the SD links as well (Γ_{iR} = constant $\forall_i$). Finally, we define FER as the number of the information sequences that cannot be correctly decoded at D, even with the help of R, divided by the total number of the sequences transmitted by all the source nodes.

Fig. 28 demonstrates the FER performance with three source nodes, where $\Gamma_{iR} =$

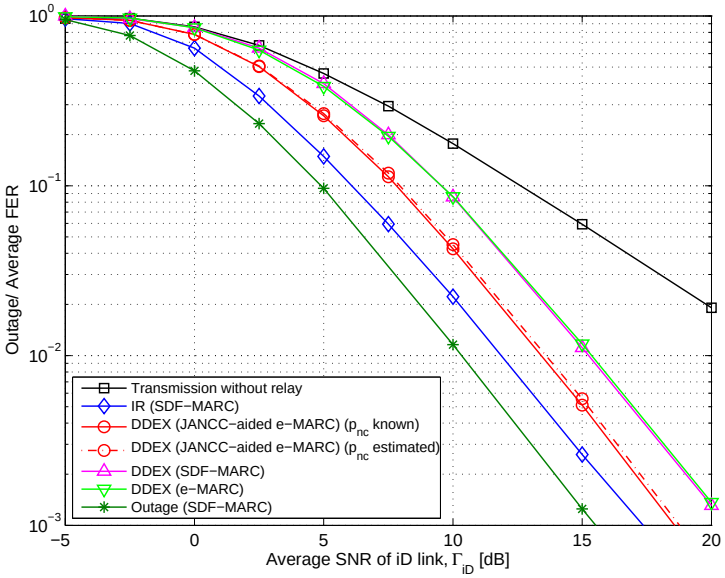

Fig 28. FER performance when $\Gamma_{iR} = \Gamma_{iD} + 0.5$ dB, $\Gamma_{RD} = 20$ dB, and the number of source nodes $N = 3$, [94] (© 2014 IEEE).

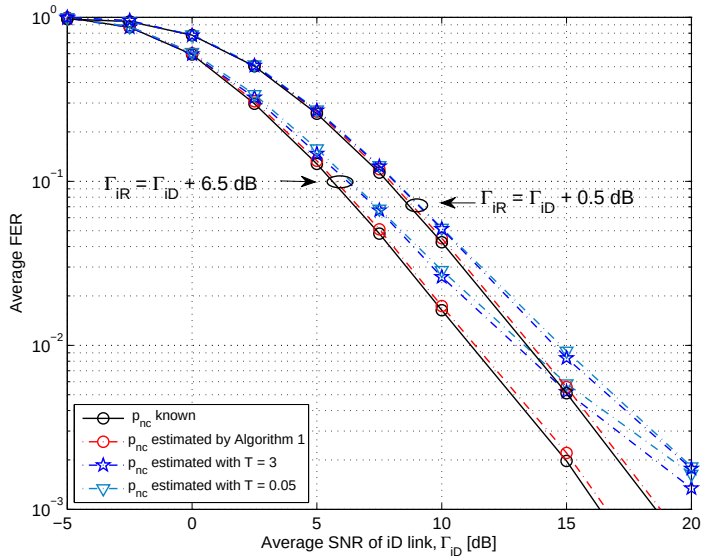

Fig 29. Estimation of p_{nc} using $\mathrm{Algorithm\ 1}$ and using [96, eq. (9)] with fixed threshold T values, respectively.

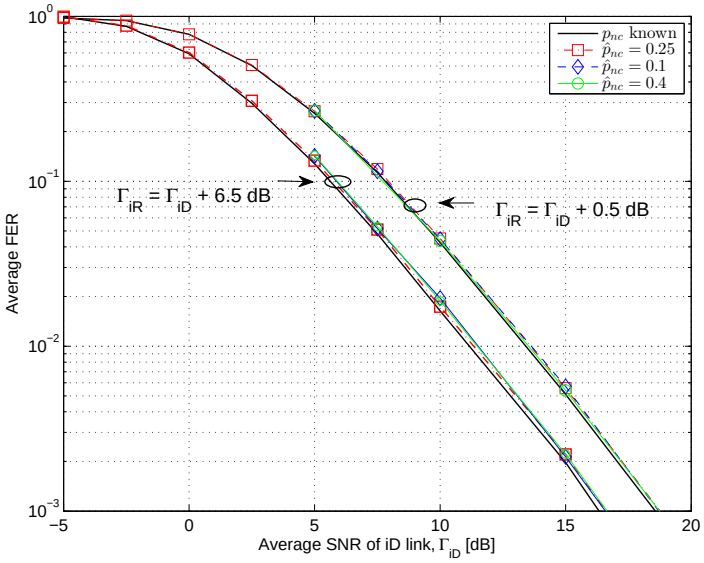

Fig 30. Estimation of p_{nc} using $\mathbf{Algorithm\ 1}$ with different initial $\hat{p}_{nc}$ settings.

$\Gamma_{iD} + 0.5$ dB. First, it can be observed that, with the DDEX strategy, the e-MARC scheme is worse than the SDF-MARC scheme as the number of the source nodes is increased. This is because XOR coding is always performed at the relay in e-MARC, by which the XOR-coded sequence may be corrupted by unnecessary erroneous estimates and thus the performance is degraded.

Next, we investigate the effect of the detection strategy applied at R with the SDF-MARC scheme. For the DDEX with the SDF-MARC scheme, as can be observed in Fig. 28, there is roughly a 3-dB loss in average Γ_{iD} at FER = 10^{-3} compared with the IR with the SDF-MARC scheme. The loss is due to the fact that DDEX only extracts the estimates of the information sequences output from the different detector. However, with the aid of the JANCC technique, the loss can be reduced to only 1.5 dB by efficiently exploiting the erroneous estimates of the transmitted source information received at R.

Furthermore, it can also be observed in Fig. 28 that by employing the proposed JANCC decoding algorithm (see $\mathbf{Algorithm\ 1}$), the FER performance of JANCC with the estimated $\hat{p}_{nc}$ is very close to the FER curve with correlation p_{nc} being known at D. Fig. 29 shows the results of the FER performance estimated by $\mathbf{Algorithm\ 1}$ and by [96, eq. (9)] with the fixed values of the threshold T, respectively, while Fig. 30

evaluates the initial $\hat{p}_{nc}$ settings in $\mathbf{Algorithm\ 1}$. It can be observed from Fig. 29 that neither a large or small fixed value of T can accurately estimate the correlation p_{nc}, while from Fig. 30 similar results are obtained for other values of $\hat{p}_{nc}$ initially set in $\mathbf{Algorithm\ 1}$. In fact, these observations, together with the application of low-complexity DDEX at R, makes the DDEX with the JANCC-aided e-MARC scheme practical in exchange for a 1.5-dB loss in average Γ_{iD}, and a significant reduction in power consumption can be achieved due to the low computational complexity required.

4.3.1 *Impact of SR link quality*

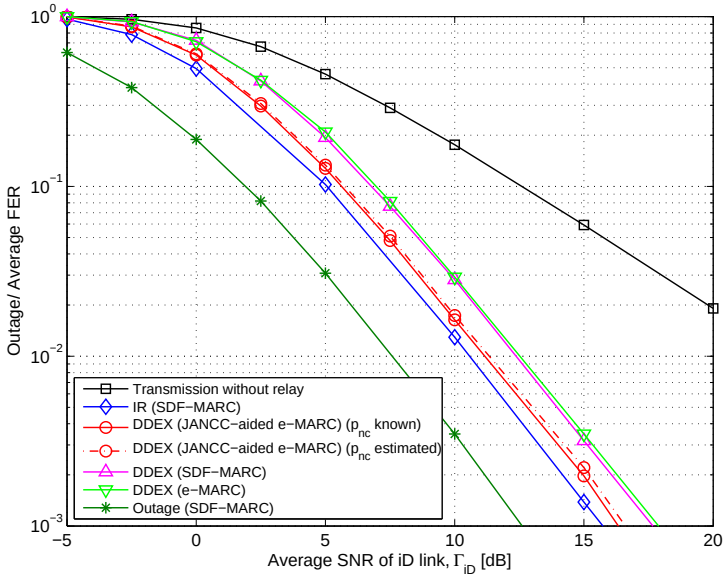

Fig 31. FER performance when $\Gamma_{iR} = \Gamma_{iD} + 6.5$ dB, $\Gamma_{RD} = 20$ dB, and the number of source nodes $N = 3$, [94] (© 2014 IEEE).

To consider the impact of the quality of the SR links on the FER performances of the three MARC systems, another scenario was tested, where $\Gamma_{iR} = \Gamma_{iD} + 6.5$ dB. It can be clearly observed in Fig. 31 that the gap in FER between the DDEX and IR strategies with SDF-MARC is reduced, because the better quality of the SR links achieves the higher accuracy of the sequences $\widetilde{\mathbf{u}}_i$ obtained at R, even by using the DDEX strategy. With the aid of JANCC, the DDEX with the e-MARC scheme can achieve 1-dB gain over the DDEX with the SDF-MARC scheme at FER = 10^{-3}, and only 0.5 dB away from the IR with SDF-MARC scheme. However, the DDEX with the e-MARC scheme is roughly 3.5 dB away from the outage probability of SDF-MARC [33] even with the aid of JANCC. This observation indicatively means that the optimal code design for the SR links is left as a future study, once the quality of the SR links is good.

4.3.2 Computational complexity evaluation

We also make a comparison between the two systems in terms of computational complexity: one is the IR with the SDF-MARC scheme, and the other is the DDEX with a JANCC-aided e-MARC scheme. The main difference between the two schemes is due mainly to the detection strategy applied at R, so we calculate the number of addition (ADD), multiplication (MUL) and comparison (COMP) operations needed to obtain one estimated information sequence $\widetilde{\mathbf{u}}_i$, where all the operations are on real numbers.

It is assumed $\widetilde{\mathbf{u}}_i$ is obtained by performing the IR strategy on the received vector $\mathbf{y}_{iR}$, where the log-MAP algorithm is used on the inner and outer codes with memory lengths m_1 and m_2, respectively. The number of operations needed per bit in the log-MAP decoding algorithm is provided in [108, Section 4.1]. Since the lengths of sequences decoded by the inner and outer decoders are M and K bits, respectively, the required number of operations per sequence of each constituent code is approximately M and K times higher, respectively.

However, with using the DDEX strategy, only one complex multiplication per bit, equivalent to two ADDs and four MULs, is required by the differential detection, Thus, $2M$ ADDs and $4M$ MULs in total are required in the detection of M-bit $\mathbf{y}_{iR}$. The sequence $\widetilde{\mathbf{u}}_i$ is simply extracted from the output of the differential detector, and thus, no operations are required.

The total computational costs for performing the IR and DDEX strategies are summarized in Table 6. With the parameters $m_1 = 1$, $m_2 = 2$, $K/M = 1/2$ and $I = 10$ iterations set in this chapter, the complexity of the IR strategy is at least 200 times higher than DDEX, which leads to significant power and memory saving for computation at R.

Table 6. Computational complexity comparison, [94] (© 2014 IEEE).

Operation	IR	DDEX
COMP	$[(5 \cdot 2^{m_1} - 2) \cdot M + (5 \cdot 2^{m_2} - 2) \cdot K] \cdot I$	0
ADD	$[(15 \cdot 2^{m_1} + 9) \cdot M + (15 \cdot 2^{m_2} + 11) \cdot K] \cdot I$	$2 \cdot M$
MUL	$(8 \cdot M + 8 \cdot K) \cdot I$	$4 \cdot M$
Look-up table	$[(5 \cdot 2^{m_1} - 2) \cdot M + (5 \cdot 2^{m_2} - 2) \cdot K] \cdot I$	0

4.3.3 Average goodput

To identify the probability for recovering the information sequence correctly at D with the SDF-MARC scheme and with the JANCC-aided e-MARC scheme, we also evaluate the average goodput of the three MARC systems used in the simulations. Tables 7 and 8 summarize all the combinations for the cases that require a re-transmission request for the SDF-MARC and JANCC-aided e-MARC schemes, respectively. The achievable goodput is defined as the number of correctly decoded information sequences at D totalling over all the source nodes, and the average goodput is calculated by averaging the achievable goodput under all the combinations according to the corresponding occurrence probabilities of those cases.

Table 7. Achievable goodput for SDF-MARC, [94] (© 2014 IEEE).

D sends request	X	✓	✓	✓	✓	✓	✓	✓	✓	✓
R forwarding	X	X	X	X	X	✓	✓	✓	✓	✓
Correctly decoded msgs at D	N	$N-1$	$\cdots$	1	0	N	$N-1$	$\cdots$	1	0
Achievable goodput	1	$\frac{N-1}{N}$	$\cdots$	$\frac{1}{N}$	0	$\frac{N}{N+1}$	$\frac{N-1}{N+1}$	$\cdots$	$\frac{1}{N+1}$	0

Table 8. Achievable goodput for JANCC-aided e-MARC, [94] (© 2014 IEEE).

D sends request	X	✓	✓	✓	✓	✓
R forwarding	X	✓	✓	✓	✓	✓
Correctly decoded msgs at D	N	N	$N-1$	$\cdots$	1	0
Achievable goodput	1	$\frac{N}{N+1}$	$\frac{N-1}{N+1}$	$\cdots$	$\frac{1}{N+1}$	0

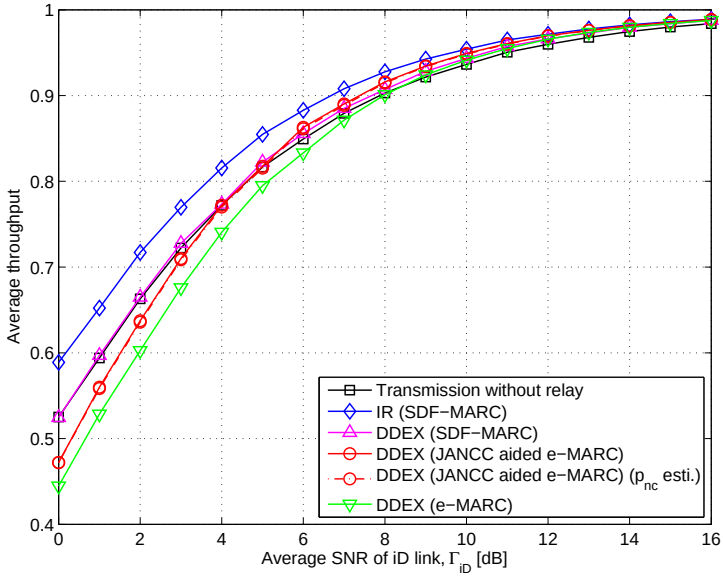

Fig 32. Average goodput when $\Gamma_{iR} = \Gamma_{iD} + 0.5$ dB, $\Gamma_{RD} = 20$ dB, and the number of source nodes $N = 3$, [94] (© 2014 IEEE).

Fig. 32 shows the average goodput efficiencies of all the systems for $\Gamma_{iR} = \Gamma_{iD} + 0.5$ dB. The average goodput of the JANCC-aided e-MARC scheme is even lower than the point-to-point transmission in the low SD SNR regime, which indicates even with the aid of the JANCC technique, the e-MARC system for the recovery of the information sequence at D is limited when the SR link quality is poor. The probability of $\widetilde{\mathbf{u}}_j$, $\forall_j \in \mathcal{F}$ after the detection of DDEX containing a large amount of errors is relatively high when the quality of the SR links is poor, and thus, the correlation between $\mathbf{u}_{\oplus}$ and $\mathbf{u}_R$ degrades if any one of the sequences $\widetilde{\mathbf{u}}_j$ contains a large amount of errors, which decreases the correction capability of JANCC decoding.

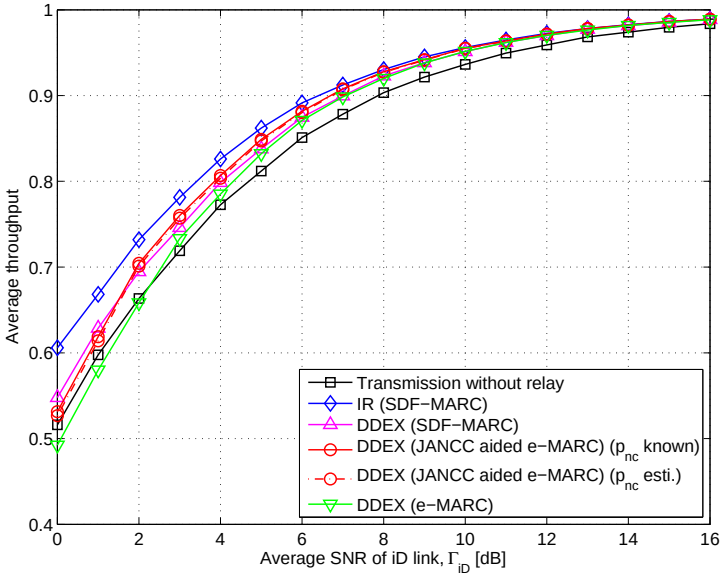

Fig 33. Average goodput when $\Gamma_{iR} = \Gamma_{iD} + 6.5$ dB, $\Gamma_{RD} = 20$ dB, and the number of source nodes $N = 3$, [94] (© 2014 IEEE).

As the quality of the SR links improves, as shown in Fig. 32 and Fig. 33, the performance of the JANCC-aided e-MARC scheme is apparently improved and outperforms the performance of scheme SDF-MARC scheme in terms of the average goodput efficiency as DDEX is applied. Furthermore, the average goodput of the DDEX with the JANCC-aided e-MARC scheme asymptotically approaches to that of the IR with the SDF-MARC scheme, as shown in Fig. 33.

4.4 Conclusion

This chapter has investigated the developed energy-efficient orthogonal MARC system. A low-complexity and non-coherent detection DDEX strategy was applied at the relay R to reduce the energy consumption. The proposed JANCC and its corresponding decoding techniques were employed to exploit the erroneous estimates output from DDEX. A vector is constructed in the JANCC technique to identify the indices of the source nodes whose information sequences are decoded in error at the destination D. The relay R performs network coding only on the estimates specified by the vector upon receiving the re-transmission request, which aims to avoid unnecessary erroneous

estimates being network coded. The proposed JANCC decoding algorithm estimated and exploited the correlation p_{nc} to update the $extrinsic$ LLR sequences during the iterative decoding process. In the case of the system setup assumed in this chapter, computational complexity of the DDEX is at least 200 times lower than the iterative decoding of the SCCC performed at R, in exchange for only a $0.5 - 1.5$ dB loss in the FER performance. However, a significant reduction in power consumption can be achieved due to low computational complexity required and the elimination of channel estimation. Furthermore, large latency incurred by the iterative decoding performed at the relay can be eliminated. Hence, the DDEX with the JANCC-aided e-MARC scheme is suitable for the relaying systems where the availability of the resources is limited, or to be used in real-time systems.

5 Conclusions and future studies

A thorough analysis of the DF-based MARC system based on the idea of lossy-forwarding has been provided in this thesis, where we aim to improve the performance of the MARC system with a relay subject to resources or/and time constraints by efficiently exploiting the erroneous estimates obtained at the relay.

A simple DF-based lossy-forwarding MARC system model, named e-MARC, has been proposed in Chapter 2 with its corresponding JNCC scheme. Network correlation in the e-MARC scheme has been utilized to exploit the forwarded erroneous estimates sent from the relay at the destination. Numerical results has shown that the erroneous estimates were helpful for the reconstruction of the information sequences sent via SD links, especially when the estimates contain only a few errors. As a result, by using very simple detection at the relay, it has been found that the proposed e-MARC system obtained roughly $0.2 - 0.4$ dB and $0.7 - 2.2$ dB gain from the SDF-MARC in AWGN and fading scenarios, respectively.

Chapter 3 theoretically derived the outage probability for the e-MARC system with two source nodes, and the derived outage probability was independent of signaling schemes. Comparisons with NC-MARC and SDF-MARC were also made. It was found through simulations that when one of the source nodes is far away from both the relay and the destination, the e-MARC system was superior to SDF-MARC in terms of outage performance. The impact of source correlation and network correlation on the outage probability of e-MARC was investigated. It was observed that for the case two source nodes are highly correlated, the outage performance can still be improved by exploiting the source correlation as long as one of the SD links is reliable. However, to improve the outage performance by exploiting the network correlation, the RD link and at least one of the SD links have to be reliable.

Chapter 4 proposed a JANCC technique to aid the e-MARC system with more source nodes. With using an identifier vector re-transmitted from the destination to the relay via a feedback channel, instead of all the estimates, only the specified estimates was/were network-coded and forwarded to the destination. This avoided the network correlation being corrupted by unspecified erroneous estimates in the XOR-coding process, and thus the network correlation can be exploited more effectively at the destination. Computer simulations demonstrated that JANCC-aided e-MARC is su-

perior to e-MARC in terms of FER and goodput efficiency. In the case of the system setup assumed in this thesis, the computational complexity of the DDEX strategy is at least 200 times lower than the iterative decoding of the SCCC (i.e., the IR strategy) performed at R, in exchange for only a $0.5-1.5$ dB loss in the FER performance. However, a significant reduction in power consumption can be achieved due to low computational complexity required and the elimination of channel estimation. Furthermore, large latency incurred by the iterative decoding process can be eliminated. Hence, the DDEX with JANCC-aided e-MARC scheme is quite useful for cooperative communications in resource-constrained wireless networks.

Several interesting topics based on this thesis can be further explored. We list several possible topics in the following as future studies:

– More sophisticated coding and modulation schemes could possibly be used for the practical realization of the e-MARC system. For example, Denoise-and-Forward strategy [110] and Joint-over-Antenna [111] detection could be applied at the relay and destination, respectively, for multi-access transmission with high order modulation.

– A derivation of the theoretical outage probability of SDF-MARC.

– The theoretical outage probability of the JANCC-aided e-MARC system could also possibly to be investigated, where the re-transmission is assumed to suffer from shadowing. Shadowing variation could be modeled by a time-correlated log-Normal random process.

– The average goodput of the JANCC-aided e-MARC system is inefficient when the SR link quality is poor, but it is highly possible that this could be improved by a well designed protocol for the coordination between R and D. For example, before the re-transmission, the error probabilities of the SR links, $\mathcal{P} = \{p_i\}_{i=1}^{N}$, could be estimated at R and forwarded to D. The set $\mathcal{F}$ could be updated by removing the indices of the sources whose estimates may contain a large number of errors at R.

– The average length of the identifier vector can be reduced if the vector could be designed in the form of variable length. The utilization of the identifier vector with a variable length could be more meaningful for a large number of sources contained in

the network, such as the MARC scenario considered in ANCC or GANCC [49, 50].

– The (network) correlation could be more efficiently utilized during the iterative decoding of LDPC with BP algorithm, since the process of updating the LLR sequence is inherent in the message passing process [112, 113].

References

1. Chin WH, Fan Z & Haines R (2014) Emerging technologies and research challenges for 5G wireless networks. IEEE Wireless Communications 21(2): 106–112.
2. Nakamura T, Nagata S, Benjebbour A, Kishiyama Y, Hai T, Xiaodong S, Ning Y & Nan L (2013) Trends in small cell enhancements in LTE advanced. IEEE Communications Magazine 51(2): 98–105.
3. Foschini G & Gans M (1998) On limits of wireless communications in a fading environment when using multiple antennas. Wireless Personal Communications, Kluwer Academic Publishers 6: pp. 311–335.
4. Paulraj A, Nabar R & Gore D (2003) Introduction to space-time wireless communications. Cambridge University Press, London, U.K.
5. Laneman J, Tse D & Wornell GW (2004) Cooperative diversity in wireless networks: Efficient protocols and outage behavior. IEEE Transactions on Information Theory 50(12): 3062–3080.
6. Jayaweera S (2004) An energy-efficient virtual MIMO architecture based on V-BLAST processing for distributed wireless sensor networks. In: Proceedings of the IEEE Communications Society Conference on Sensor and Ad Hoc Communications and Networks, pp. 299–308.
7. van der Meulen EC (1968) Transmission of informatin in a T-terminal discrete memoryless channel, PhD. dissertation. University of California, Berkeley.
8. van der Meulen EC (1971) Three-terminal communication channels. Advances in applied Probability 3: 120–154.
9. van der Meulen EC (1977) A survey of multiway channel in information theory: 1961-1976. IEEE Transactions on Information Theory IT-23(1): 1–37.
10. Cover T & Gamal A (1979) Capacity theorems for the relay channel. IEEE Transactions on Information Theory 25(5): 572–584.
11. Standards Committee L (2003) Part 11: Wireless LAN medium access control (MAC) and physical layer (PHY) specifications. IEEE-SA Standards Board.
12. Group IRT (May 2007) The p802.16j Baseline Document for Draft Standard for Local and Metropolitan Area Networks, 802.16j-06/026r4,.
13. (Mar. 2010) Further advancements for E-UTRA; Physical layer aspects. Sophia-Antipolis, France, 3GPP TR 36.814 V9.0.0, Release 9.
14. Chong P, Adachi F, Hamalainen S & Leung V (2007) Technologies in multihop cellular networks. IEEE Communications Magazine 45(9): 64–65.
15. Laneman J & Wornell GW (2003) Distributed space-time-coded protocols for exploiting cooperative diversity in wireless networks. IEEE Transactions on Information Theory 49(10): 2415–2425.
16. Sendonaris A, Erkip E & Aazhang B (2003) User cooperation diversity. part II. implementation aspects and performance analysis. IEEE Transactions on Communications 51(11): 1939–1948.
17. Boujemaa H (2012) Bit error probability of cooperative MC-CDMA systems using decode and forward relaying. European Transactions on Telecommunications 23(1): 25–35.
18. Vaze R & Heath R (2011) On the capacity and diversity-multiplexing tradeoff of the two-

way relay channel. IEEE Transactions on Information Theory 57(7): 4219–4234.
19. Kramer G & van Wijngaarden A (2000) On the white Gaussian multiple-access relay channel. In: Proceedings of the IEEE International Symposium on Information Theory, pp. 40–.
20. Akyildiz I, Su W, Sankarasubramaniam Y & Cayirci E (2002) A survey on sensor networks. IEEE Communications Magazine 40(8): 102–114.
21. Mirza'ee M, Salari S & Piltan A (2011) Single and multiple relay selection schemes with optimum relay factors in wireless sensor networks. In: Proceedings of the Iranian Conference on Electrical Engineering, pp. 1–1.
22. Ding L, Melodia T, Batalama S & Matyjas J (2010) Distributed routing, relay selection, and spectrum allocation in cognitive and cooperative ad hoc networks. In: Proceedings of the IEEE Communications Society Conference on Sensor Mesh and Ad Hoc Communications and Networks, pp. 1–9.
23. Wei Y, Yu F & Song M (2010) Distributed optimal relay selection in wireless cooperative networks with finite-state Markov channels. IEEE Transactions on Vehicular Technology 59(5): 2149–2158.
24. Eghbali H, Muhaidat S, Hejazi S & Ding Y (2013) Relay selection strategies for single-carrier frequency-domain equalization multi-relay cooperative networks. IEEE Transactions on Wireless Communications 12(5): 2034–2045.
25. Michalopoulos D, Suraweera H, Karagiannidis G & Schober R (2012) Amplify-and-forward relay selection with outdated channel estimates. IEEE Transactions on Communications 60(5): 1278–1290.
26. Laneman J & Wornell GW (2002) Distributed space-time coded protocols for exploiting cooperative diversity in wireless networks. In: Proceedings of the IEEE Global Telecommunications Conference, volume 1, pp. 77–81 vol.1.
27. Nosratinia A, Hunter T & Hedayat A (2004) Cooperative communication in wireless networks. IEEE Communications Magazine 42(10): 74–80.
28. Lin S & Daniel J Costello J (2004) Error control coding. Prentice Hall .
29. Woldegebreal D & Karl H (2007) Multiple-access relay channel with network coding and non-ideal source-relay channels. In: Proceedings of the International Symposium on Wireless Communication Systems, pp. 732–736.
30. Yang S & Koetter R (2007) Network coding over a noisy relay : a belief propagation approach. In: Proceedings of the IEEE International Symposium on Information Theory, pp. 801–804.
31. Mohamad A, Visoz R & Berthet AO (2013) Outage analysis of various cooperative strategies for the multiple access multiple relay channel. In: Proceedings of the International Symposium on Personal Indoor and Mobile Radio Communications, pp. 1321–1326.
32. Mohamad A, Visoz R & Berthet A (2013) Outage achievable rate analysis for the non orthogonal multiple access multiple relay channel. In: Proceedings of the IEEE Wireless Communications and Networking Conference Workshops, pp. 160–165.
33. Iscan O & Hausl C (2011) Iterative network and channel decoding for the relay channel with multiple sources. In: Proceedings of the IEEE Vehicular Technology Conference, pp. 1–5.
34. Hatefi A, Visoz R & Berthet A (2012) Near outage limit joint network coding and decoding for the semi-orthogonal multiple-access relay channel. In: Proceedings of the International Symposium on Network Coding, pp. 13–18.

35. Simoens S, Vidal J & Munoz O (2006) Compress-and-forward cooperative relaying in MIMO-OFDM systems. In: Proceedings of the IEEE 7th Workshop on Signal Processing Advances in Wireless Communications, pp. 1–5.
36. Dabora R & Servetto S (2007) Estimate-and-forward relaying for the Gaussian relay channel with coded modulation. In: Proceedings of the IEEE International Symposium on Information Theory, pp. 1046–1050.
37. Ahlswede R, Cai N, Li SY & Yeung R (2000) Network information flow. IEEE Transactions on Information Theory 46(4): 1204–1216.
38. Katti S, Rahul H, Hu W, Katabi D, Medard M & Crowcroft J (2008) XORs in the air: Practical wireless network coding. IEEE/ACM Transactions on Networking 16(3): 497–510.
39. Wu Y, Chou P & Kung SY (2005) Minimum-energy multicast in mobile ad hoc networks using network coding. IEEE Transactions on Communications 53(11): 1906–1918.
40. Li SY, Yeung R & Cai N (2003) Linear network coding. IEEE Transactions on Information Theory 49(2): 371–381.
41. Fragouli C, Boudec JY & Widmer J (2006) Network coding: an instant primer. ACM SIGCOMM Computer Communication 36(1): 63–68.
42. Ho T, Koetter R, Medard M, Karger D & Effros M (2003) The benefits of coding over routing in a randomized setting. In: Proceedings of the IEEE International Symposium on Information Theory, pp. 442–.
43. Kaiqian O, Yinlong X, Guanjun M & Yulin Z (2009) A peer-to-peer content distribution system based on combined network coding. In: Proceedings of the 2nd IEEE International Conference on Broadband Network Multimedia Technology, pp. 687–692.
44. Lu L, Liew SC & Zhang S (2011) Optimal decoding algorithm for asynchronous physical-layer network coding. In: Proceedings of IEEE International Conference on Communications, pp. 1–6.
45. Yang Q & Liew S (2014) Asynchronous convolutional-coded physical-layer network coding. IEEE Transactions on Wireless Communications PP(99): 1–1.
46. Wu X, Zhao C & You X (2011) On the bcjr algorithm for asynchronous physical-layer network coding. In: Proceedings of International Conference on Wireless Communications and Signal Processing, pp. 1–4.
47. Larsson P & Johansson N (2006) Multi-user ARQ. In: Proceedings of the IEEE 63rd Vehicular Technology Conference, volume 4, pp. 2052–2057.
48. Berger C, Zhou S, Wen Y, Willett P & Pattipati K (2008) Optimizing joint erasure- and error-correction coding for wireless packet transmissions. IEEE Transactions on Wireless Communications 7(11): 4586–4595.
49. Bao X & Li J (2008) Adaptive network coded cooperation (ANCC) for wireless relay networks: matching code-on-graph with network-on-graph. IEEE Transactions on Wireless Communications 7(2): 574–583.
50. Bao X & Li J (2011) Generalized adaptive network coded cooperation (GANCC): A unified framework for network coding and channel coding. IEEE Transactions on Communications 59(11): 2934–2938.
51. Hausl C, Schreckenbach F & Oikonomidis I (2005) Iterative network and channel decoding on a tanner graph. In: Proceedings of the Allerton Conference on Communications, Control and Computation.
52. Hausl C & Dupraz P (2006) Joint network-channel coding for the multiple-access relay

channel. In: Proceedings of the IEEE Communications Society on Sensor and Ad Hoc Communications and Networks, volume 3, pp. 817 –822.
53. Hausl C & Hagenauer J (2006) Iterative network and channel decoding for the two-way relay channel. In: Proceedings of the IEEE International Conference on Communications, volume 4, pp. 1568–1573.
54. Valenti M & Zhao B (2003) Distributed turbo codes: towards the capacity of the relay channel. In: Proceedings of the IEEE 58th Vehicular Technology Conference, volume 1, pp. 322–326 Vol.1.
55. Zhao B & Valenti M (2003) Distributed turbo coded diversity for relay channel. Electronics Letters 39(10): 786–787.
56. Duyck D, Capirone D, Boutros J & Moeneclaey M (2010) Analysis and construction of full-diversity joint network-LDPC codes for cooperative communications. EURASIP Journal on Wireless Communication Networks .
57. Duyck D, Capirone D, Heindlmaier M & Moeneclaey M (2011) Towards full-diversity joint network-channel coding for large networks. In: Proceedings of the 11th European Wireless Conference 2011, pp. 1–8.
58. MacKay D & Neal R (1997) Near Shannon limit performance of low density parity check codes. Electronics Letters 33(6): 457–458.
59. Zhang S, Liew SC, Q Z, Lu L & Wang H (2011) Non-memoryless analog network coding in two-way relay channel. In: Proceedings of the IEEE International Conference on Communications, pp. 1–6.
60. Berrou C & Glavieux A (1996) Near optimum error correcting coding and decoding: turbo-codes. IEEE Transactions on Communications 44(10): 1261–1271.
61. Bahl L, Cocke J, Jelinek F & Raviv J (1974) Optimal decoding of linear codes for minimizing symbol error rate. IEEE Transactions on Information Theory, 20(2): 284–287.
62. MacKay D (1999) Good error-correcting codes based on very sparse matrices. IEEE Transactions on Information Theory 45(2): 399–431.
63. Zhang Y & Zhang Z (2013) Joint network-channel coding with rateless code over multiple access relay system. IEEE Transactions on Wireless Communications 12(1): 320–332.
64. Li Y, Song G & Wang L (2009) Design of joint network-low density parity check codes based on the EXIT charts. IEEE Communications Letters 13(8): 600 –602.
65. Tang S, Cheng J, Sun C & Miura R (2009) Joint channel and network decoding for XOR-based relay in multi-access channel. IEICE Transactions on Communications E92-B(11): 3470–3477.
66. Xu X, Flanagan M, Koller C & Goertz N (2008) A shared-relay cooperative diversity scheme based on joint channel and network coding. In: Proceedings of the International Symposium on Information Theory and Its Applications, pp. 1 –6.
67. Hernaez M, Crespo P & Del Ser J (2013) On the design of a novel joint network-channel coding scheme for the multiple access relay channel. IEEE Journal on Selected Areas in Communications 31(8): 1368–1378.
68. Fang W, Hu C, Sun Z & Hou S (2012) Improved joint network-channel coding for the multiple-access relay channel. In: Proceedings of the International ICST Conference on Communications and Networking, pp. 722–726.
69. Hatefi A, Visoz R & Berthet A (2011) Full diversity distributed coding for the multiple access half-duplex relay channel. In: Proceedings of the International Symposium on Network Coding, pp. 1 –6.

70. Ding Y & Li G (2012) Multiple-access relay channel with direct network coding. In: Proceedings of the 2012 IEEE 14th International Conference on Communication Technology, pp. 1113–1117.
71. Pan H & Chen C (2012) Single-relay selections with amplify forwarding and network coding in two-way relay channels. In: Proceedings of the 2012 International Conference on Computer Science Service System, pp. 1232–1235.
72. Popovski P & Yomo H (2007) Physical network coding in two-way wireless relay channels. In: Proceedings of the IEEE International Conference on Communications, pp. 707–712.
73. Zhu Y, Wu X & Zhu T (2013) Hybrid af and df with network coding for wireless two way relay networks. In: Proceedings of the IEEE Wireless Communications and Networking Conference, pp. 2428–2433.
74. Zeitler G, Koetter R, Bauch G & Widmer J (2008) Design of network coding functions in multihop relay networks. In: Proceedings of the International Symposium on Turbo Codes and Related Topics, pp. 249–254.
75. Zeitler G, Koetter R, Bauch G & Widmer J (2009) On quantizer design for soft values in the multiple-access relay channel. In: Proceedings of the IEEE International Conference on Communications, pp. 1–5.
76. Schwandter S & Matz G (2010) A practical forwarding scheme for wireless relay channels based on the quantization of log-likelihood ratios. In: Proceedings of the IEEE International Conference on Acoustics Speech and Signal Processing, pp. 2502–2505.
77. Zeitler G, Bauch G & Widmer J (2012) Quantize-and-forward schemes for the orthogonal multiple-access relay channel. IEEE Transactions on Communications 60(4): 1148–1158.
78. Dietl G, Sciora M, Zeitler G, Bauch G & Widmer J (2011) A quantize-and-forward scheme for future wireless relay networks. In: IEEE Vehicular Technology Conference (VTC Fall), pp. 1–4.
79. Sneesens H & Vandendorpe L (2005) Soft decode and forward improves cooperative communications. In: Proceedings of the IEEE International Workshop on Computational Advances in Multi-Sensor Adaptive Processing, pp. 157–160.
80. Sneessens H & Vandendorpe L (2005) Soft decode and forward improves cooperative communications. In: Proceedings of the IEE International Conference on 3G and Beyond, pp. 1–4.
81. Sneessens H, Louveaux J & Vandendorpe L (2008) Turbo-coded decode-and-forward strategy resilient to relay errors. In: Proceedings of the IEEE International Conference on Acoustics, Speech and Signal Processing, pp. 3213–3216.
82. Gamal A & Kim Y (2011) Network Information theory. Cambridge University Press.
83. Khojastepour M, Sabharwal A & Aazhang B (2003) On capacity of Gaussian 'cheap' relay channel. In: Proceedings of the IEEE Global Telecommunications Conference, volume 3, pp. 1776–1780 vol.3.
84. Lu PS, Tervo V, Anwar K & Matsumoto T (2011) Low-complexity strategies for multiple access relaying. In: Proceedings of the IEEE Vehicular Technology Conference, pp. 1–6.
85. Lu PS & Matsumoto T (2011) Energy-efficient techniques allowing intra-link errors for block-fading multiple access relaying. In: Proceedings of the IEEE International Symposium on Personal Indoor and Mobile Radio Communications, pp. 1687–1691.
86. Anwar K & Matsumoto T (2012) Accumulator-assisted distributed turbo codes for relay systems exploiting source-relay correlation. IEEE Communications Letters 16(7): 1114 –1117.

87. Ten Brink S (2001) Convergence behavior of iteratively decoded parallel concatenated codes. IEEE Transactions on Communications 49(10): 1727–1737.
88. Brannstrom F, Rasmussen L & Grant A (2005) Convergence analysis and optimal scheduling for multiple concatenated codes. IEEE Transactions on Information Theory 51(9): 3354 – 3364.
89. Lu PS, Zhou X & Matsumoto T (2014) Outage probabilities of orthogonal multiple-access relaying techniques with imperfect source-relay links. IEEE Transactions on Wireless Communications, to be published.
90. Cheng M, Anwar K & Matsumoto T (2013) Outage probability of a relay strategy allowing intra-link errors utilizing Slepian-Wolf theorem. EURASIP Journal on Advances in Signal Processing 34.
91. Zhou X, Lu PS, Anwar K & Matsumoto T (2014) Correlated sources transmission in orthogonal multiple access relay channel: Theoretical analysis and performance evaluation. IEEE Transactions on Wireless Communications 13(3): 1424–1435.
92. Slepian D & Wolf J (1973) Noiseless coding of correlated information sources. IEEE Transactions on Information Theory 19(4): 471–480.
93. Zhou X, Cheng M, He X & Matsumoto T (2014) Exact and approximated outage probability analyses for decode-and-forward relaying system allowing intra-link errors. IEEE Transactions on Wireless Communications, to be published.
94. Lu PS, Zhou X, Anwar K & Matsumoto T (2014) Joint adaptive network-channel coding for energy-efficient multiple-access relaying. IEEE Transactions on Vehicular Technology 63(5): 2298–2305.
95. Garcia-Frias J (2001) Compression of correlated binary sources using turbo codes. IEEE Communications Letters 5(10): 417 –419.
96. Garcia-Frias J & Zhao Y (2005) Near-Shannon/Slepian-Wolf performance for unknown correlated sources over AWGN channels. IEEE Transactions on Communications 53(4): 555–559.
97. ten Brink S & Kramer G (2003) Design of repeat-accumulate codes for iterative detection and decoding. IEEE Transactions on Signal Processing 51(11): 2764 – 2772.
98. Anwar K & Matsumoto T (2012) Spatially concatenated codes with turbo equalization for correlated sources. IEEE Transactions on Signal Processing 60(10): 5572–5577.
99. Hagenauer J, Offer E & Papke L (1996) Iterative decoding of binary block and convolutional codes. IEEE Transactions on Information Theory 42(2): 429 –445.
100. ten Brink S (2001) Design of concatenated coding schemes based on iterativedecoding convergence. Ph.D. thesis, University of Stuttgart,published at Shaker, Aachen, Germany .
101. Sankaranarayanan L, Kramer G & Mandayam NB (2004) Hierarchical sensor networks: capacity bounds and cooperative strategies using the multiple-access relay channel model. In: Proceedings of the IEEE Communications Society Conference on Sensor and Ad Hoc Communications and Networks, pp. 191–199.
102. Cover TM & Thomas JA (2006) Elements of Information Theory, 2nd Edition. USA: John Wiley & Sons, Inc.
103. Tian C, Chen J, Diggavi S & Shamai S (2014) Optimality and approximate optimality of source-channel separation in networks. IEEE Transactions on Information Theory 60(2): 904–918.
104. Murin Y, Dabora R & Gunduz D (2013) Source-channel coding theorems for the multiple-access relay channel. IEEE Transactions on Information Theory 59(9): 5446–5465.

105. McEliece RJ (2002) The Theory of Information and Coding, 2nd Edition. Cambridge University Press.
106. Shampine L (2008) Matlab program for quadrature in 2D. Applied Mathematics and Computation 202(1): 266–274.
107. Maral G & Bousquet M (2009) Satellite Communications systems. John Wiley & Sons, Inc.
108. Robertson P, Villebrun E & Hoeher P (1995) A comparison of optimal and sub-optimal MAP decoding algorithms operating in the log domain. In: Proceedings of the IEEE International Conference on Communications, pp. 1009–1013.
109. Chatzigeorgiou I, Wassell I & Carrasco R (2008) On the frame error rate of transmission schemes on quasi-static fading channels. In: Proceedings of the 42nd Annual Conference on Information Sciences and Systems, pp. 577–581.
110. Koike-Akino T, Popovski P & Tarokh V (2009) Optimized constellations for two-way wireless relaying with physical network coding. IEEE Journal on Selected Areas in Communications, 27(5): 773–787.
111. Karjalainen J, Veselinovic N, Kansanen K & Matsumoto T (2007) Iterative frequency domain joint-over-antenna detection in multiuser mimo. IEEE Transactions on Wireless Communications 6(10): 3620–3631.
112. Tian T, Garcia-Frias J & Zhong W (2003) Compression of correlated sources using ldpc codes. In: Proceedings of the Data Compression Conference, pp. 450–.
113. Garcia-Frias J & Liu K (2008) Design of near-optimum quantum error-correcting codes based on generator and parity-check matrices of ldgm codes. In: Proceedings of the 42nd Annual Conference on Information Sciences and Systems, pp. 562–567.

Appendix 1 Derivation of (9)

Let us consider a very simple model of a block fading channel

$$y = hx + n \tag{51}$$

where the BPSK symbol $x \in \{+1, -1\}$, complex channel coefficient $h = h_R + jh_i$, and noise $n = n_R + jn_i$ is a complex AWGN with variance σ^2 per dimension (i.e., var(n_R) = var(n_i) = σ^2). Then, the destination performs coherent detection on the received signal y obtain the signal z, as

$$\begin{aligned} z &= \Re\left\{\frac{h^* y}{|h|^2}\right\} \\ &= x + \Re\left\{\frac{h^* n}{|h|^2}\right\} \end{aligned} \tag{52}$$

The variance of the signal after coherent detection becomes

$$\begin{aligned} \text{var}(z) &= \text{var}\left(\Re\left\{\frac{h^* n}{|h|^2}\right\}\right) \\ &= \text{var}\left(\Re\left\{\frac{(h_R - jh_i)(n_R + jn_i)}{|h|^2}\right\}\right) \\ &= \text{var}\left(\frac{h_R n_R + h_i n_i}{|h|^2}\right) \\ &= \text{var}\left(\frac{h_R n_R}{|h|^2}\right) + \text{var}\left(\frac{h_i n_i}{|h|^2}\right) \\ &= \frac{{h_R}^2}{\left({h_R}^2 + {h_i}^2\right)^2}\text{var}(n_R) + \frac{{h_i}^2}{\left({h_R}^2 + {h_i}^2\right)^2}\text{var}(n_i) \\ &= \frac{{h_R}^2}{\left({h_R}^2 + {h_i}^2\right)^2}\text{var}(n_R) + \frac{{h_i}^2}{\left({h_R}^2 + {h_i}^2\right)^2}\text{var}(n_i) \\ &= \frac{1}{|h|^2}\sigma^2 \\ &= {\sigma_z}^2 \end{aligned} \tag{53}$$

After that, we convert the detected signal $z \sim \mathcal{N}(0, {\sigma_z}^2)$ to its corresponding soft

channel values $L(z|x)$, as

$$\begin{aligned} L(z|x) &= \ln \frac{\Pr(z|x=+1)}{\Pr(z|x=-1)} \\ &= \ln \frac{\frac{1}{\sqrt{2\pi}\sigma_z} \cdot \exp^{\frac{-(z-1)^2}{2\sigma_z^2}}}{\frac{1}{\sqrt{2\pi}\sigma_z} \cdot \exp^{\frac{-(z+1)^2}{2\sigma_z^2}}} \\ &= \frac{-(z-1)^2 + (z+1)^2}{2\sigma_z^2} \\ &= \frac{4z}{2\sigma_z^2} \\ &= \frac{4z}{2\frac{1}{|h|^2}\sigma^2} \\ &= \frac{2\Re\{h^* y\}}{\sigma^2} \end{aligned} \tag{54}$$

Appendix 2 Derivation of (19a)-(19d)

We start the derivation of the results of (19a)-(19d) with the general equivalent system model of e-MARC shown in Fig. 34, where source nodes A and B are assumed to be correlated. Variables e_A, e_B, e_R and e_s are i.i.d. binary random variables with $\Pr(e_A = 1) = p_A$, $\Pr(e_B = 1) = p_B$, $\Pr(e_R = 1) = p_R$ and $\Pr(e_s = 1) = p_s$, respectively. According to the definition, the mutual information $I(\mathbf{u}_R; \hat{\mathbf{u}}_R)$ is

$$I(\mathbf{u}_R; \hat{\mathbf{u}}_R) = H(\hat{\mathbf{u}}_R) - H(\hat{\mathbf{u}}_R|\mathbf{u}_R). \tag{55}$$

Then, given the model shown in Fig. 34, $I(\mathbf{u}_R; \hat{\mathbf{u}}_R)$ can be further expressed as follows

$$\begin{aligned} I(\mathbf{u}_R; \hat{\mathbf{u}}_R) &= H(\underbrace{\mathbf{u}_A \oplus e_A}_{\widetilde{\mathbf{u}}_A} \oplus \underbrace{\mathbf{u}_B \oplus e_B}_{\widetilde{\mathbf{u}}_B} \oplus e_R) - H_b(p_R) \\ &= H(\underbrace{\mathbf{u}_A \oplus e_A}_{\widetilde{\mathbf{u}}_A} \oplus \underbrace{\mathbf{u}_A \oplus e_s \oplus e_B}_{\widetilde{\mathbf{u}}_B} \oplus e_R) - H_b(p_R) \\ &= H(e_A \oplus e_B \oplus e_R \oplus e_s) - H_b(p_R) \\ &= H_b(p_A * p_B * p_R * p_s) - H_b(p_R), \end{aligned} \tag{56}$$

where the operation $\alpha * \beta$ is defined as $\alpha(1-\beta) + \beta(1-\alpha)$, and $H_b(\cdot)$ denotes the binary entropy function [102]. For the sake of notation simplicity, we defined μ as $\mu = H(\hat{\mathbf{u}}_R) = H_b(p_A * p_B * p_R * p_s)$. Then, by using the chain rule, the joint entropy

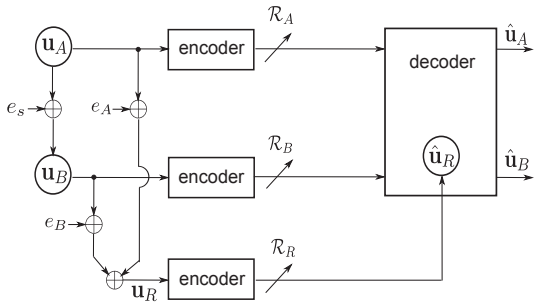

Fig 34. Generalized equivalent model of e-MARC, where source correlation is taken into account, [89] (© 2015 IEEE).

$H(\mathbf{u}_A, \mathbf{u}_B, \mathbf{u}_R, \hat{\mathbf{u}}_R)$ can be represented as

$$H(\mathbf{u}_A, \mathbf{u}_B, \mathbf{u}_R, \hat{\mathbf{u}}_R) = H(\mathbf{u}_A, \mathbf{u}_B) + H(\mathbf{u}_R|\mathbf{u}_A, \mathbf{u}_B) + H(\hat{\mathbf{u}}_R|\mathbf{u}_A, \mathbf{u}_B, \mathbf{u}_R) \quad (57a)$$
$$= H(\hat{\mathbf{u}}_R) + H(\mathbf{u}_A, \mathbf{u}_B|\hat{\mathbf{u}}_R) + H(\mathbf{u}_R|\mathbf{u}_A, \mathbf{u}_B, \hat{\mathbf{u}}_R). \quad (57b)$$

Hence, the conditional entropy $H(\mathbf{u}_A, \mathbf{u}_B|\hat{\mathbf{u}}_R)$ is expressed with the combination of (57a) and (57b), as

$$\begin{aligned} H(\mathbf{u}_A, \mathbf{u}_B|\hat{\mathbf{u}}_R) = {} & H(\mathbf{u}_A, \mathbf{u}_B) + H(\mathbf{u}_R|\mathbf{u}_A, \mathbf{u}_B) \\ & + H(\hat{\mathbf{u}}_R|\mathbf{u}_A, \mathbf{u}_B, \mathbf{u}_R) - H(\hat{\mathbf{u}}_R) \\ & - H(\mathbf{u}_R|\mathbf{u}_A, \mathbf{u}_B, \hat{\mathbf{u}}_R). \end{aligned} \quad (58)$$

Also, the conditional mutual information $I(\mathbf{u}_R; \hat{\mathbf{u}}_R|\mathbf{u}_A, \mathbf{u}_B)$ can be expressed by the chain rule, as

$$\begin{aligned} I(\mathbf{u}_R; \hat{\mathbf{u}}_R|\mathbf{u}_A, \mathbf{u}_B) &= H(\mathbf{u}_R|\mathbf{u}_A, \mathbf{u}_B) - H(\mathbf{u}_R|\mathbf{u}_A, \mathbf{u}_B, \hat{\mathbf{u}}_R) \\ &= H(\hat{\mathbf{u}}_R|\mathbf{u}_A, \mathbf{u}_B) - H(\hat{\mathbf{u}}_R|\mathbf{u}_A, \mathbf{u}_B, \mathbf{u}_R). \end{aligned} \quad (59)$$

By substituting $H(\mathbf{u}_R|\mathbf{u}_A, \mathbf{u}_B)$ of (59) into (58), $H(\mathbf{u}_A, \mathbf{u}_B|\hat{\mathbf{u}}_R)$ can be rewritten as

$$H(\mathbf{u}_A, \mathbf{u}_B|\hat{\mathbf{u}}_R) = H(\mathbf{u}_A, \mathbf{u}_B) + H(\hat{\mathbf{u}}_R|\mathbf{u}_A, \mathbf{u}_B) - H(\hat{\mathbf{u}}_R) \quad (60)$$

where the conditional entropy $H(\hat{\mathbf{u}}_R|\mathbf{u}_A, \mathbf{u}_B)$ is calculated as

$$\begin{aligned} H(\hat{\mathbf{u}}_R|\mathbf{u}_A, \mathbf{u}_B) &= H(\mathbf{u}_A \oplus e_A \oplus \mathbf{u}_B \oplus e_B \oplus e_R|\mathbf{u}_A, \mathbf{u}_B) \\ &= H(e_A \oplus e_B \oplus e_R). \end{aligned} \quad (61)$$

Therefore, $H(\mathbf{u}_A, \mathbf{u}_B|\hat{\mathbf{u}}_R)$ shown in the third inequality of (18) can be obtained by substituting (61) into (60), as

$$H(\mathbf{u}_A, \mathbf{u}_B|\hat{\mathbf{u}}_R) = H(\mathbf{u}_A, \mathbf{u}_B) + H(e_A \oplus e_B \oplus e_R) - H(\hat{\mathbf{u}}_R)$$
$$= 1 + H_b(p_s) + H_b(p_A * p_B * p_R) - \mu. \tag{62}$$

Again, let $\delta_s = H_b(p_s) + H_b(p_A * p_B * p_R) - \mu$ for simplicity. Since the conditional entropy $H(\mathbf{u}_A, \mathbf{u}_B|\hat{\mathbf{u}}_R)$ in (62) can also alternatively be expressed by the chain rule, as

$$H(\mathbf{u}_A, \mathbf{u}_B|\hat{\mathbf{u}}_R) = H(\mathbf{u}_B|\mathbf{u}_A, \hat{\mathbf{u}}_R) + H(\mathbf{u}_A|\hat{\mathbf{u}}_R) \tag{63a}$$
$$= H(\mathbf{u}_A|\mathbf{u}_B, \hat{\mathbf{u}}_R) + H(\mathbf{u}_B|\hat{\mathbf{u}}_R). \tag{63b}$$

Since the sequence $\hat{\mathbf{u}}_R$ is composed of $\mathbf{u}_A$, the conditional entropy $H(\mathbf{u}_A|\hat{\mathbf{u}}_R)$ in (63a) can be calculated as

$$H(\mathbf{u}_A|\hat{\mathbf{u}}_R) = H(\mathbf{u}_A|\mathbf{u}_A \oplus e_A \oplus \mathbf{u}_B \oplus e_B \oplus e_R)$$
$$= H(e_A \oplus \mathbf{u}_A \oplus e_s \oplus e_B \oplus e_R)$$
$$= 1. \tag{64}$$

Therefore, we can obtain $H(\mathbf{u}_B|\mathbf{u}_A, \hat{\mathbf{u}}_R)$, shown in the second inequality of (18), by substituting (62) and (64) into (63a), as

$$H(\mathbf{u}_B|\mathbf{u}_A, \hat{\mathbf{u}}_R) = \underbrace{H(\mathbf{u}_A, \mathbf{u}_B|\hat{\mathbf{u}}_R)}_{1+\delta_s} - \underbrace{H(\mathbf{u}_A|\hat{\mathbf{u}}_R)}_{1}$$
$$= \delta_s. \tag{65}$$

The conditional entropy $H(\mathbf{u}_A|\mathbf{u}_B, \hat{\mathbf{u}}_R)$ shown in the first inequality of (18) is also calculated in the same way, and the result is

$$H(\mathbf{u}_A|\mathbf{u}_B, \hat{\mathbf{u}}_R) = \delta_s. \tag{66}$$

A set of inequalities is obtained by combining (56), (62), (65) and (66), as

$$\begin{aligned} \mathcal{R}_A &\geq \delta_s, \\ \mathcal{R}_B &\geq \delta_s, \\ \mathcal{R}_A + \mathcal{R}_B &\geq 1 + \delta_s, \\ \mathcal{R}_R &\geq \mu - H_b(p_R). \end{aligned} \tag{67}$$

For the case that the two source nodes are uncorrelated (i.e., $p_s = 0.5$), $\mu = 1$ and $\delta_s = \delta = H_b(p_A * p_B * p_R)$, which leads (67) into (19a)-(19d).

Appendix 3 Explanation for (23) and (29)

The signaling chains $\mathcal{E}_S$ and $\mathcal{E}_R$ shown in Fig. 35 can be viewed as joint source-channel encoders, where $\mathbf{u}_i$ and $\mathbf{u}_R$ are the K-bit length i.i.d. binary information sequences generated from the source node i for $i \in \{A, B\}$ and relay R, respectively. Here $\mathbf{x}_i = \mathcal{E}_S(\mathbf{u}_i) = \{x_i(m)\}_{m=1}^{M}$ and $\mathbf{x}_R = \mathcal{E}_R(\mathbf{u}_R) = \{x_R(m)\}_{m=1}^{M}$ are M-length symbol sequences. For the sake of simplicity, modulation is not shown in Fig. 35. The transmissions from i and from R to the destination D are orthogonal since time-sharing is assumed in this thesis. According to [82, Section 14.1], the source-channel separation holds for the orthogonal multiple access channel. Thus, we apply the separation theorem to find the sufficient and necessary conditions for reliable transmissions for $\mathbf{u}_i$. By the separation theorem, the encoding processes of $\mathcal{E}_S$ and $\mathcal{E}_R$ are respectively treated as a combination of source coding and channel coding, as shown in Fig. 35. Here $\mathbf{b}_i$ and $\mathbf{b}_R$ are L-bit length i.i.d. sequences after the source coding of the encoders $\mathcal{E}_S$ and $\mathcal{E}_R$, respectively. Then, we define the source coding rates $\mathcal{R}_i$ and $\mathcal{R}_R$, channel coding rates

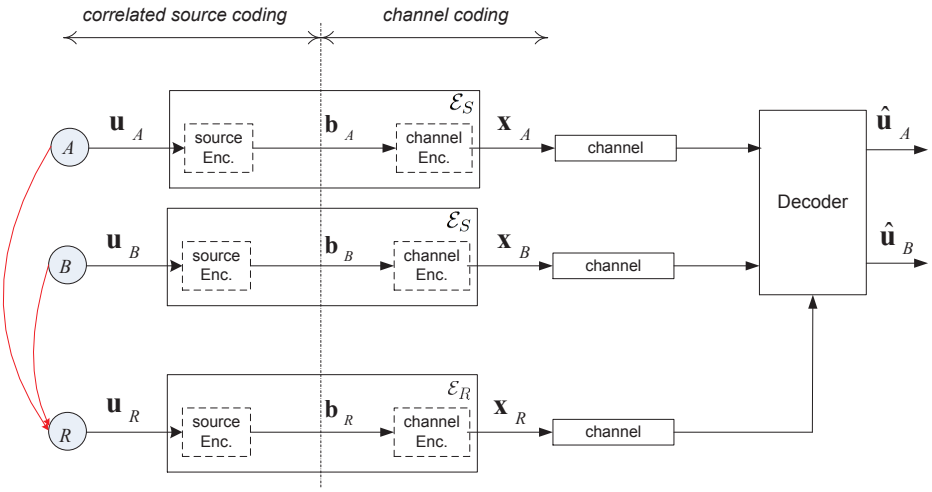

Fig 35. Source-channel separation is used to analyze the conditions for the recovery of $\mathbf{u}_i$.

$\mathcal{R}_{ch_i}$ and $\mathcal{R}_{ch_R}$, and end-to-end rates $\mathcal{R}_{ci}$ of $\mathcal{E}_S$ and $\mathcal{R}_{cR}$ of $\mathcal{E}_R$ as follows

$$\begin{aligned}
&\mathcal{R}_i = \mathcal{R}_R = L/K, \\
&\mathcal{R}_{ch_i} = \mathcal{R}_{ch_R} = L/M, \\
&\mathcal{R}_{ci} = \mathcal{R}_{cR} = K/M,
\end{aligned} \tag{68}$$

To make sure the sequence $\mathbf{u}_i$ can be recovered at the destination, the source coding rates $\mathcal{R}_i$ and $\mathcal{R}_R$ have to satisfy the inequalities shown in (19). Moreover, according to the channel coding theorem [102, Section 8.7], the channel coding rates $\mathcal{R}_{ch_i}$ and $\mathcal{R}_{ch_R}$ must satisfy the following inequality

$$\mathcal{R}_{ch_i} = \mathcal{R}_i \mathcal{R}_{ci} \leq C(\gamma_{_{iD}}); \qquad \mathcal{R}_{ch_R} = \mathcal{R}_R \mathcal{R}_{cR} \leq C(\gamma_{_{RD}}), \tag{69}$$

and equalities in (69) hold by assuming a capacity-achieving code is used in the iD and RD links.

Appendix 4 Divisions of integrals (33) and (34)

As shown in (28) and (30), the values of $\hat{p}_i(\gamma_{iR})$ and $\hat{p}_R(\gamma_{RD})$ become zero as the SNR γ_{iR} and γ_{RD} exceed the threshold value, and thus, the domain of the integral shown in (35) can be divided into eight intervals according to the threshold value γ_A^*, γ_B^* and γ_R^*, as

$$\begin{aligned}\Pr(\varepsilon_1) &= \Im[g_1; V] = \sum_{j=1}^{8} \Im[g_1; V_j] \\ \Pr(\varepsilon_2) &= \Im[g_2; V] = \sum_{j=1}^{8} \Im[g_2; V_j],\end{aligned} \tag{70}$$

where

$$\begin{aligned}V_1 &= \{(\gamma_{AR}, \gamma_{BR}, \gamma_{RD}) : \gamma_{AR} \in \mathbb{A}^+, \gamma_{BR} \in \mathbb{B}^+, \gamma_{RD} \in \mathbb{C}^+\} \\ V_2 &= \{(\gamma_{AR}, \gamma_{BR}, \gamma_{RD}) : \gamma_{AR} \in \mathbb{A}^+, \gamma_{BR} \in \mathbb{B}^-, \gamma_{RD} \in \mathbb{C}^+\} \\ V_3 &= \{(\gamma_{AR}, \gamma_{BR}, \gamma_{RD}) : \gamma_{AR} \in \mathbb{A}^-, \gamma_{BR} \in \mathbb{B}^+, \gamma_{RD} \in \mathbb{C}^+\} \\ V_4 &= \{(\gamma_{AR}, \gamma_{BR}, \gamma_{RD}) : \gamma_{AR} \in \mathbb{A}^-, \gamma_{BR} \in \mathbb{B}^-, \gamma_{RD} \in \mathbb{C}^+\} \\ V_5 &= \{(\gamma_{AR}, \gamma_{BR}, \gamma_{RD}) : \gamma_{AR} \in \mathbb{A}^+, \gamma_{BR} \in \mathbb{B}^+, \gamma_{RD} \in \mathbb{C}^-\} \\ V_6 &= \{(\gamma_{AR}, \gamma_{BR}, \gamma_{RD}) : \gamma_{AR} \in \mathbb{A}^+, \gamma_{BR} \in \mathbb{B}^-, \gamma_{RD} \in \mathbb{C}^-\} \\ V_7 &= \{(\gamma_{AR}, \gamma_{BR}, \gamma_{RD}) : \gamma_{AR} \in \mathbb{A}^-, \gamma_{BR} \in \mathbb{B}^+, \gamma_{RD} \in \mathbb{C}^-\} \\ V_8 &= \{(\gamma_{AR}, \gamma_{BR}, \gamma_{RD}) : \gamma_{AR} \in \mathbb{A}^-, \gamma_{BR} \in \mathbb{B}^-, \gamma_{RD} \in \mathbb{C}^-\}.\end{aligned} \tag{71}$$

Here, the sets $\mathbb{A}^-$, $\mathbb{A}^+$, $\mathbb{B}^-$, $\mathbb{B}^+$, $\mathbb{C}^-$ and $\mathbb{C}^+$ are defined as

$$\begin{aligned}\mathbb{A}^- &= [0, \gamma_A^*), \quad \mathbb{A}^+ = [\gamma_A^*, \infty) \\ \mathbb{B}^- &= [0, \gamma_B^*), \quad \mathbb{B}^+ = [\gamma_B^*, \infty) \\ \mathbb{C}^- &= [0, \gamma_R^*), \quad \mathbb{C}^+ = [\gamma_R^*, \infty).\end{aligned} \tag{72}$$

The integrals of (33) and (34) with respect to each interval listed in (71) are expressed in (73) and (74), respectively. The arguments $\hat{\delta}_j$ and $\hat{\omega}_j$ corresponding to each interval in (73) and (74) are summarized in Table 9.

Table 9. Arguments of functions $f_A^{-1}(\cdot)$ and $f_B^{-1}(\cdot)$ in (73) and (74), [89] (© 2015 IEEE).

$\hat{\delta}_1$	$H_b(0 * 0 * 0)$
$\hat{\delta}_2$	$H_b(0 * \tilde{p}_B(\gamma_{BR}) * 0)$
$\hat{\delta}_3$	$H_b(\tilde{p}_A(\gamma_{AR}) * 0 * 0)$
$\hat{\delta}_4$	$H_b(\tilde{p}_A(\gamma_{AR}) * \tilde{p}_B(\gamma_{BR}) * 0)$
$\hat{\delta}_5$	$H_b(0 * 0 * \tilde{p}_R(\gamma_{RD}))$
$\hat{\delta}_6$	$H_b(0 * \tilde{p}_B(\gamma_{BR}) * \tilde{p}_R(\gamma_{RD}))$
$\hat{\delta}_7$	$H_b(\tilde{p}_A(\gamma_{AR}) * 0 * \tilde{p}_R(\gamma_{RD}))$
$\hat{\delta}_8$	$H_b(\tilde{p}_A(\gamma_{AR}) * \tilde{p}_B(\gamma_{BR}) * \tilde{p}_R(\gamma_{RD}))$
$\hat{\omega}_1$	$\hat{\delta}_1 + 1 - f_A(\gamma_{AD})$
$\hat{\omega}_2$	$\hat{\delta}_2 + 1 - f_A(\gamma_{AD})$
$\hat{\omega}_3$	$\hat{\delta}_3 + 1 - f_A(\gamma_{AD})$
$\hat{\omega}_4$	$\hat{\delta}_4 + 1 - f_A(\gamma_{AD})$
$\hat{\omega}_5$	$\hat{\delta}_5 + 1 - f_A(\gamma_{AD})$
$\hat{\omega}_6$	$\hat{\delta}_6 + 1 - f_A(\gamma_{AD})$
$\hat{\omega}_7$	$\hat{\delta}_7 + 1 - f_A(\gamma_{AD})$
$\hat{\omega}_8$	$\hat{\delta}_8 + 1 - f_A(\gamma_{AD})$

$$\mathfrak{I}[g_1;V_1] = \frac{1}{\Gamma_{AD}} \exp\left(-\frac{\gamma_R^*}{\Gamma_{RD}} - \frac{\gamma_A^*}{\Gamma_{AR}} - \frac{\gamma_B^*}{\Gamma_{BR}}\right) \int_{f_A^{-1}(\hat{\delta}_1)}^{f_A^{-1}(1)} \exp\left(\frac{-f_B^{-1}(\hat{\omega}_1)}{\Gamma_{BD}} - \frac{\gamma_{AD}}{\Gamma_{AD}}\right) d\gamma_{AD}$$

$$\mathfrak{I}[g_1;V_2] = \frac{1}{\Gamma_{AD}\Gamma_{BR}} \exp\left(-\frac{\gamma_R^*}{\Gamma_{RD}} - \frac{\gamma_A^*}{\Gamma_{AR}}\right) \int_0^{\gamma_B^*} \int_{f_A^{-1}(\hat{\delta}_2)}^{f_A^{-1}(1)} \exp\left(\frac{-f_B^{-1}(\hat{\omega}_2)}{\Gamma_{BD}} - \frac{\gamma_{AD}}{\Gamma_{AD}} - \frac{\gamma_{BR}}{\Gamma_{BR}}\right) d\gamma_{AD}\, d\gamma_{BR}$$

$$\mathfrak{I}[g_1;V_3] = \frac{1}{\Gamma_{AD}\Gamma_{AR}} \exp\left(-\frac{\gamma_R^*}{\Gamma_{RD}} - \frac{\gamma_B^*}{\Gamma_{BR}}\right) \int_0^{\gamma_A^*} \int_{f_A^{-1}(\hat{\delta}_3)}^{f_A^{-1}(1)} \exp\left(\frac{-f_B^{-1}(\hat{\omega}_3)}{\Gamma_{BD}} - \frac{\gamma_{AD}}{\Gamma_{AD}} - \frac{\gamma_{AR}}{\Gamma_{AR}}\right) d\gamma_{AD}\, d\gamma_{AR}$$

$$\mathfrak{I}[g_1;V_4] = \frac{1}{\Gamma_{AD}\Gamma_{AR}\Gamma_{BR}} \exp\left(-\frac{\gamma_R^*}{\Gamma_{RD}}\right)$$
$$\cdot \int_0^{\gamma_B^*} \int_0^{\gamma_A^*} \int_{f_A^{-1}(\hat{\delta}_4)}^{f_A^{-1}(1)} \exp\left(\frac{-f_B^{-1}(\hat{\omega}_4)}{\Gamma_{BD}} - \frac{\gamma_{AD}}{\Gamma_{AD}} - \frac{\gamma_{AR}}{\Gamma_{AR}} - \frac{\gamma_{BR}}{\Gamma_{BR}}\right) d\gamma_{AD}\, d\gamma_{AR}\, d\gamma_{BR}$$

$$\mathfrak{I}[g_1;V_5] = \frac{1}{\Gamma_{AD}\Gamma_{RD}} \exp\left(-\frac{\gamma_A^*}{\Gamma_{AR}} - \frac{\gamma_B^*}{\Gamma_{BR}}\right) \int_0^{\gamma_R^*} \int_{f_A^{-1}(\hat{\delta}_5)}^{f_A^{-1}(1)} \exp\left(\frac{-f_B^{-1}(\hat{\omega}_5)}{\Gamma_{BD}} - \frac{\gamma_{AD}}{\Gamma_{AD}} - \frac{\gamma_{RD}}{\Gamma_{RD}}\right) d\gamma_{AD}\, d\gamma_{RD}$$

$$\mathfrak{I}[g_1;V_6] = \frac{1}{\Gamma_{AD}\Gamma_{RD}\Gamma_{BR}} \exp\left(-\frac{\gamma_A^*}{\Gamma_{AR}}\right)$$
$$\cdot \int_0^{\gamma_R^*} \int_0^{\gamma_B^*} \int_{f_A^{-1}(\hat{\delta}_6)}^{f_A^{-1}(1)} \exp\left(\frac{-f_B^{-1}(\hat{\omega}_6)}{\Gamma_{BD}} - \frac{\gamma_{AD}}{\Gamma_{AD}} - \frac{\gamma_{BR}}{\Gamma_{BR}} - \frac{\gamma_{RD}}{\Gamma_{RD}}\right) d\gamma_{AD}\, d\gamma_{BR}\, d\gamma_{RD}$$

$$\mathfrak{I}[g_1;V_7] = \frac{1}{\Gamma_{AD}\Gamma_{RD}\Gamma_{AR}} \exp\left(-\frac{\gamma_B^*}{\Gamma_{BR}}\right)$$
$$\cdot \int_0^{\gamma_R^*} \int_0^{\gamma_A^*} \int_{f_A^{-1}(\hat{\delta}_7)}^{f_A^{-1}(1)} \exp\left(\frac{-f_B^{-1}(\hat{\omega}_7)}{\Gamma_{BD}} - \frac{\gamma_{AD}}{\Gamma_{AD}} - \frac{\gamma_{AR}}{\Gamma_{AR}} - \frac{\gamma_{RD}}{\Gamma_{RD}}\right) d\gamma_{AD}\, d\gamma_{AR}\, d\gamma_{RD}$$

$$\mathfrak{I}[g_1;V_8] = \frac{1}{\Gamma_{AD}\Gamma_{RD}\Gamma_{AR}\Gamma_{BR}}$$
$$\cdot \int_0^{\gamma_R^*} \int_0^{\gamma_B^*} \int_0^{\gamma_A^*} \int_{f_A^{-1}(\hat{\delta}_8)}^{f_A^{-1}(1)} \exp\left(\frac{-f_B^{-1}(\hat{\omega}_8)}{\Gamma_{BD}} - \frac{\gamma_{AD}}{\Gamma_{AD}} - \frac{\gamma_{AR}}{\Gamma_{AR}} - \frac{\gamma_{BR}}{\Gamma_{BR}} - \frac{\gamma_{RD}}{\Gamma_{RD}}\right) d\gamma_{AD}\, d\gamma_{AR}\, d\gamma_{BR}\, d\gamma_{RD} \tag{73}$$

$$\mathfrak{I}[g_2;V_1] = \exp\left(\frac{-f_A^{-1}(1)}{\Gamma_{AD}} - \frac{\gamma_R^*}{\Gamma_{RD}} - \frac{\gamma_A^*}{\Gamma_{AR}} - \frac{\gamma_B^*}{\Gamma_{BR}}\right)$$

$$\mathfrak{I}[g_2;V_2] = \frac{1}{\Gamma_{BR}} \exp\left(\frac{-f_A^{-1}(1)}{\Gamma_{AD}} - \frac{\gamma_R^*}{\Gamma_{RD}} - \frac{\gamma_A^*}{\Gamma_{AR}}\right) \int_0^{\gamma_B^*} \exp\left(\frac{-f_B^{-1}(\hat{\delta}_2)}{\Gamma_{BD}} - \frac{\gamma_{BR}}{\Gamma_{BR}}\right) d\gamma_{BR}$$

$$\mathfrak{I}[g_2;V_3] = \frac{1}{\Gamma_{AR}} \exp\left(\frac{-f_A^{-1}(1)}{\Gamma_{AD}} - \frac{\gamma_R^*}{\Gamma_{RD}} - \frac{\gamma_B^*}{\Gamma_{BR}}\right) \int_0^{\gamma_A^*} \exp\left(\frac{-f_B^{-1}(\hat{\delta}_3)}{\Gamma_{BD}} - \frac{\gamma_{AR}}{\Gamma_{AR}}\right) d\gamma_{AR}$$

$$\mathfrak{I}[g_2;V_4] = \frac{1}{\Gamma_{AR}\Gamma_{BR}} \exp\left(\frac{-f_A^{-1}(1)}{\Gamma_{AD}} - \frac{\gamma_R^*}{\Gamma_{RD}}\right) \int_0^{\gamma_B^*} \int_0^{\gamma_A^*} \exp\left(\frac{-f_B^{-1}(\hat{\delta}_4)}{\Gamma_{BD}} - \frac{\gamma_{AR}}{\Gamma_{AR}} - \frac{\gamma_{BR}}{\Gamma_{BR}}\right) d\gamma_{AR}\, d\gamma_{BR}$$

$$\mathfrak{I}[g_2;V_5] = \frac{1}{\Gamma_{RD}} \exp\left(\frac{-f_A^{-1}(1)}{\Gamma_{AD}} - \frac{\gamma_A^*}{\Gamma_{AR}} - \frac{\gamma_B^*}{\Gamma_{BR}}\right) \int_0^{\gamma_R^*} \exp\left(\frac{-f_B^{-1}(\hat{\delta}_5)}{\Gamma_{BD}} - \frac{\gamma_{RD}}{\Gamma_{RD}}\right) d\gamma_{RD}$$

$$\mathfrak{I}[g_2;V_6] = \frac{1}{\Gamma_{RD}\Gamma_{BR}} \exp\left(\frac{-f_A^{-1}(1)}{\Gamma_{AD}} - \frac{\gamma_A^*}{\Gamma_{AR}}\right) \int_0^{\gamma_R^*} \int_0^{\gamma_B^*} \exp\left(\frac{-f_B^{-1}(\hat{\delta}_6)}{\Gamma_{BD}} - \frac{\gamma_{BR}}{\Gamma_{BR}} - \frac{\gamma_{RD}}{\Gamma_{RD}}\right) d\gamma_{BR}\, d\gamma_{RD}$$

$$\mathfrak{I}[g_2;V_7] = \frac{1}{\Gamma_{RD}\Gamma_{AR}} \exp\left(\frac{-f_A^{-1}(1)}{\Gamma_{AD}} - \frac{\gamma_B^*}{\Gamma_{BR}}\right) \int_0^{\gamma_R^*} \int_0^{\gamma_A^*} \exp\left(\frac{-f_B^{-1}(\hat{\delta}_7)}{\Gamma_{BD}} - \frac{\gamma_{AR}}{\Gamma_{AR}} - \frac{\gamma_{RD}}{\Gamma_{RD}}\right) d\gamma_{AR}\, d\gamma_{RD}$$

$$\mathfrak{I}[g_2;V_8] = \frac{1}{\Gamma_{RD}\Gamma_{AR}\Gamma_{BR}} \exp\left(\frac{-f_A^{-1}(1)}{\Gamma_{AD}}\right)$$
$$\cdot \int_0^{\gamma_R^*} \int_0^{\gamma_B^*} \int_0^{\gamma_A^*} \exp\left(\frac{-f_B^{-1}(\hat{\delta}_8)}{\Gamma_{BD}} - \frac{\gamma_{AR}}{\Gamma_{AR}} - \frac{\gamma_{BR}}{\Gamma_{BR}} - \frac{\gamma_{RD}}{\Gamma_{RD}}\right) d\gamma_{AR}\, d\gamma_{BR}\, d\gamma_{RD} \tag{74}$$

Appendix 5 Superiority/inferiority of e-MARC related to SDF-MARC in Asymmetric/Symmetric scenarios

As mentioned in Section 3.2.2, the SDF-MARC and e-MARC systems belong to different categories of MARC (SDF-MARC is "address-based", while e-MARC is "non-address-based"). Here we try to provide more details to better understand how the e-MARC and SDF-MARC systems behave in asymmetric and symmetric topologies, let us consider **Case A** and **Case B** shown in the Fig. 36 in the following.

In **Case A** shown in Fig. 36, the information estimates sent via the BR and BD links both contain errors with high probability. The erroneous $\widetilde{\mathbf{u}}_B$, instead of being discarded by the SDF-MARC system, can still be utilized in the e-MARC system at the destination, which contributes to the improvement of the outage performance. Hence, the proposed e-MARC system is superior to the SDF-MARC system in **Case A**. However, we cannot exactly evaluate how much better the proposed e-MARC system is than the SDF-MARC system, because as mentioned above, there is no explicit mathematical expressions to calculate the theoretical outage probability of the SDF-MARC system.

On the contrary, in **Case B** shown in Fig. 36, the information estimates sent via the AR and BD links both contain errors with high probability. Correctly decoded $\widetilde{\mathbf{u}}_B$ is guaranteed in the SDF-MARC system to help recover the information sequence sent via the BD link. However, network coding is always performed in the proposed e-MARC system, which results in the correctly decoded $\widetilde{\mathbf{u}}_B$ being corrupted by the erroneous

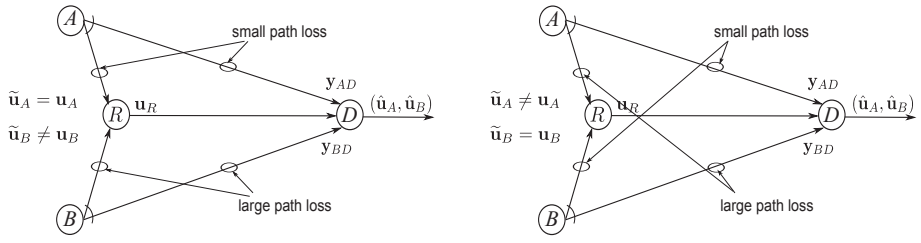

Case A **Case B**

Fig 36. $\mathbf{u}_R = \widetilde{\mathbf{u}}_A \oplus \widetilde{\mathbf{u}}_B$ in e-MARC for both case; while $\mathbf{u}_R = \widetilde{\mathbf{u}}_A$ and $\mathbf{u}_R = \widetilde{\mathbf{u}}_B$ in SDF-MARC for Case A and Case B, respectively.

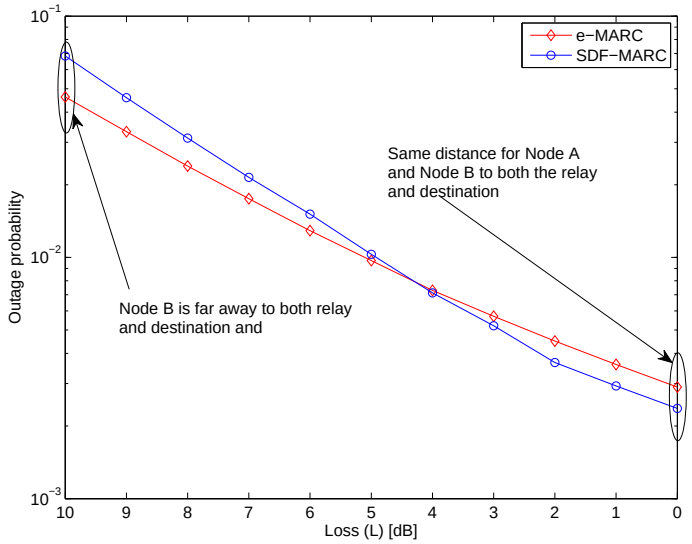

Fig 37. Outage probabilities of e-MARC and SDF-MARC are shown as functions of loss L, where Γ_{AD} and Δ are fixed to 10 dB and 3 dB, respectively.

$\widetilde{\mathbf{u}}_A$ in the network-coding process, and the erroneous XOR-ed sequence degrades the outage performance. Therefore, the proposed e-MARC system is inferior to the SDF-MARC system in **Case B**. Nevertheless, we cannot exactly evaluate how worse the proposed e-MARC is than SDF-MARC.

For the Asymmetric scenario where the loss L = 10 dB, **Case A** is most likely to occur since node B is far away from both the relay and destination, and hence it is reasonable for the proposed e-MARC system to be advantageous, shown in Fig. 37. As the node B gradually moves close to both the relay and destination (i.e. L from 10 dB to 0 dB), the probability that **Case A** occurs decreases while the probability that **Case B** occurs increases. According to simulation results shown in Fig. 37, SDF-MARC outperforms e-MARC as the value of L is less than 4 dB.

The explanation mentioned above for the superiority/inferiority of e-MARC related to SDF-MARC in the Asymmetric/Symmetric scenarios is only text-based, not based on mathematical analyses. In addition, deriving explicit mathematical expression of the outage probability with SDF-MARC is out of the scope of this thesis. Therefore, we do not include the explanation in the main body of the thesis.